UNIVERSITÀ DEGLI STUDI DI PADOVA

Dipartimento di
Agronomia Animali Alimenti Risorse Naturali e Ambiente

Corso di Laurea Magistrale in
Scienze e Tecnologie per l'Ambiente e il Territorio

QUANTIFICATION OF HISTORICAL CARBON STORAGE IN THE SOIL OF A TEMPERATE RAINFOREST IN SOUTHERN SOUTH AMERICA

Quantificazione dell'accumulo di carbonio nel suolo di una foresta pluviale temperata del Sud America

Laureanda
Ilaria Folie
1129819

Relatore
Prof. Andrea Pitacco
Correlatore
Prof. Jorge Francisco Perez-Quezada
Dr.ssa Eva Niedermeyer

ANNO ACCADEMICO 2017/2018

Contents

1 Abstract

Carbon-dense forests are defined by the high capacity to store carbon in the biomass of various layers aboveground and belowground. This phenomenon is associated mainly with humid and relatively cold climatic conditions. Typically, temperate forests are found in this kind of environment, which may allow the storage of large quantity of carbon in the soil.

Temperate forests store globally less carbon in comparison with boreal and tropical forests, with most of the total carbon stored in the soil, due the particular condition in which they are developed.

The fallowing study was conducted in 2017 in 2017 on Chiloé Island, in Southern Chile. The alternation of different types of ecosystems after the last glaciation, such as wetlands (wet climate) and forests (dry climate), may conferred to the soil peculiar properties. In this last Era, however, the climate on the Island permitted the development of a type of vegetation dominated by forest, known as the northern Patagonian old-growth temperate rainforest.

Therefore, this study focused on estimating the storage of carbon in the soil, with qualitative (n-alkane biomarker) and quantitative (TOC, GC-MS) analyses, in order to discriminate what kind of vegetation dominated this area in the past and consequently, discover the possible carbon content stored in soil that contributed each ecosystem.

The high concentration of long n-alkane chains (nC27-nC31 homologues) in the leaf waxes, which are typical of dry environments, provides positive results about the prevalence of the forest ecosystem over that of peatlands.

3 Riassunto esteso

Le foreste primarie sono caratteristiche per la loro elevata capacità di sequestrare il carbonio e trasformarlo in sostanza organica (biomassa) sia in superficie, che negli strati sotto superficiali.
Il grado di conservazione della sostanza organica dipende da diversi fattori climatici, in particolare da temperatura e umidità. La sostanza organica si conserva più efficientemente in condizioni fredde e umide, condizioni tipiche delle foreste temperate. Questo tipo di ecosistema, infatti, è in grado di stoccare elevate quantità di carbonio. A livello globale, le foreste temperate sequestrano minori quantità di carbonio rispetto a quelle boreali e tropicali, ma sono in grado di immagazzinarne la maggior parte nel suolo, creando quindi una cospicua e durevole riserva.
Lo studio presentato in questo elaborato è stato realizzato con profili di suolo prelevati nella foresta temperata dell'isola di Chiloé, situata lungo la costa del Cile meridionale. Precedenti studi hanno messo in evidenza un'alternanza di differenti tipologie di vegetazione (foreste e paludi) susseguitesi dopo l'ultima glaciazione. Le condizioni climatiche verificatesi nell'ultimo millennio, invece, hanno permesso lo sviluppo e la crescita di una foresta temperata primaria tipica della Patagonia settentrionale.
L'obiettivo di questa ricerca è quello di analizzare i campioni di suolo al fine di identificarne e valutarne la quantità di carbonio stoccata e il tipo di vegetazione responsabile dello stoccaggio nel corso dei millenni. Per lo svolgimento della ricerca sono state utilizzate tecniche sia di tipo qualitativo (biomarcatori lipidici e gas cromatografia) che quantitativo (analisi del carbonio organico totale (TOC) e spettrometria di massa).
Lo studio ha prodotto risultati che hanno mostrato la prevalenza di un ecosistema di tipo forestale rispetto a quello palustre. L'abbondanza di lunghe catene carboniose (omologhi nC27-nC31) che compongono le cere delle foglie di queste piante, sono indice, infatti, di un ambiente prevalentemente terrestre.

4 Introduction

4.1 Carbon and Carbon Cycle

Life on Earth is balanced on natural cycles, which involves four different spheres: biosphere, hydrosphere, lithosphere, and atmosphere. This four elements are strictly connected and they host all the biogeochemical processes and elements of the Earth.

As carbon (C) is one of the most ubiquitous components in biological compounds and minerals, its cycle is a fundamental contributor and regulator to the Earth's system It is present in all known life forms, making up to 50% of the dry weight of living things (Ussiri et al, 2017).

Carbon is naturally found in different physical states and compounds, depending on its physico-chemical and allotropic properties and on the environmental conditions. It can be found as elemental carbon, and as inorganic or organic compounds.

Elemental C is usually found in soil and sediments as a product of an incomplete combustion of organic matter (charcoal, graphite) and as geological sources from the occur f other processes (coal, diamond) (Schumacher, 2002).

Inorganic C is mostly present as a gas like CO_2 and CH_4, or in mineral form such as carbonates; the two most commons are calcite ($CaCO_3$) and dolomite [$CaMg(CO_3)_2$]. These rocks are originated in absence of biological activity or they could be formed by fossilized organic matter,for instance, by ancient seashells.

The *Organic C* in the soil is originated by the growth and dead of living organisms suchplants and animals, and their decomposition. Different degradation states of the matter, from freshly deposited litter (leaves, stems, branches) to highly decomposed forms, such as hummus and humic acids (Schumacher, 2002).

Carbon can also be found in unnatural states through the addition of anthropogenic inputs. Most of them are derived-organic compounds (volatile organic compound (VOC), chlorofluorocarbon (CFC), polycyclic aromatic hydrocarbons (PAHs**)**, polychlorinated biphenyl (PCB), halogenated compounds, pesticides, etc.) products originated by human activities, such as contaminants from oil spills, industries, urban waste, traffic, livestock's, tanneries, wood production, deforestation,

agricultural and food processes. These types of molecules are detrimental artificial substances introduced into the environment, capable of alter the balanced of the ecosystem and to modify the life-compatible quantities and concentrations naturally present in these environments.

These various carbon compounds react, move and change state through different steps and interactions between living organisms and the biogeochemical spheres in a complex process called **carbon cycle** (Fig. 1). This cycle is characterized from continuous exchanges of energy and matter, through fluxes which determine places where carbon accumulates (called pools, stocks or reservoirs), or it is released and absorbed from another one. These destinations are commonly defined as *sinks* (storage of C) and *sources* (loss of C).

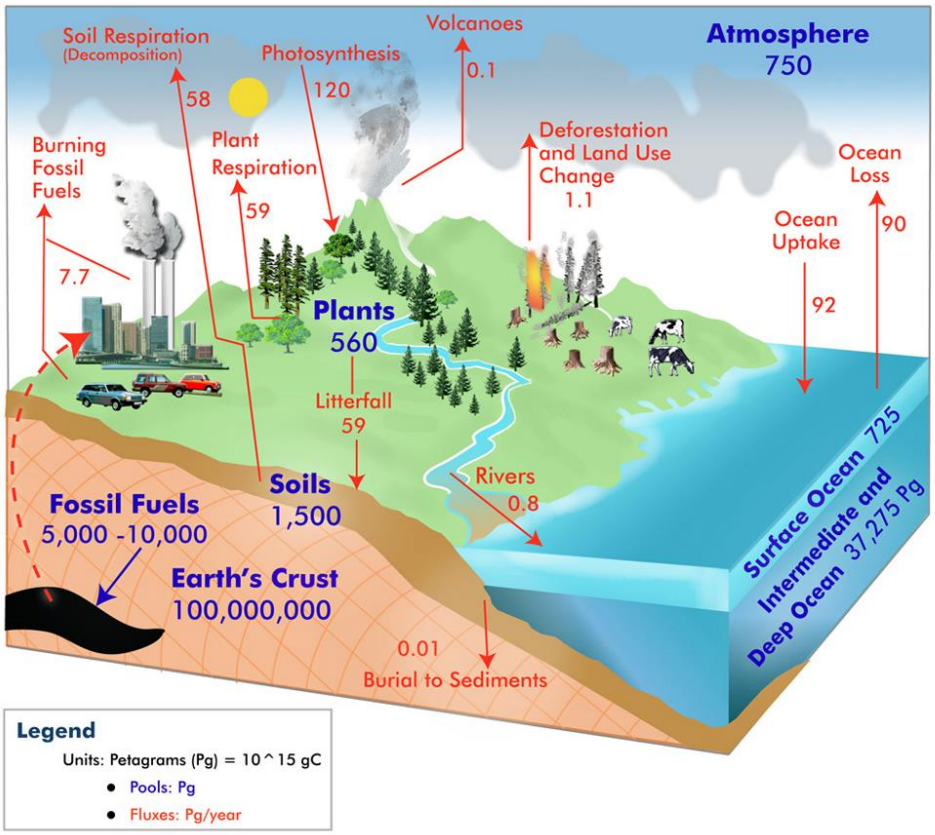

Fig. 1*: The Global Carbon Budget,* Ussiri et al. 2017)

Carbon is present in the atmosphere mostly in form of carbon dioxide (CO_2), the most oxidant state of carbon, with a minor concentration of methan (CH_4) and other compounds. CO_2 in the atmosphere is fundamental because it contributes to the greenhouse effec , which allows

maintenance of an Earth surface temperature that will favor life. Currently, its stock in the atmosphere is around 750 PgC (concentration of ~400 ppm). A sudden increase (from 560 PgC,~280ppm) began over 200 years ago, when the industrial age started (Falkowski et al., 2000). Various predictions anticipate that this concentration will continue to rise with future climate change and the continuous anthropogenic input of CO_2 into the atmosphere, causing greenhouse effect intensification and consequently, a rise in temperatures on Earth's surface.

CO_2 is transferred from atmosphere to the biosphere and geosphere pools through the plant's activity.

Photosynthesis is the chemical process by which plants use inorganic carbon (CO_2) and sunlight to convert nutrients into organic compounds and carbohydrates, producing biomass and releasing oxygen (Gorte, 2009)

$$6\ CO_2 + 6\ H_2O + \text{solar energy} \rightarrow C_6H_{12}O_6 + 6\ O_2$$

Leaves, roots, limbs, and stems are composed of carbon in different quantities depending on the plant species, age, environmental conditions, growth pattern (Gorte, 2009). Thus, different species of plants are able to sequester CO_2 from the atmosphere in various amounts. For example, woody stems produced by trees have the greatest ability to store carbon, because of the density of wood and the large size of trees (University of New Hampshire-UNH, 2014). Therefore, the plant system is a form of carbon sink, which can collectively stores about 560 PgC; with photosynthesis, carbon is removed about ~120PgC/year from the atmosphere and is transferred into the terrestrial and biosphere. However, there are many processes in which plants are losing carbon: *respiration* of living biomass, where a portion of the CO_2 previously captured (almost 50%) is released back into the atmosphere as a product of metabolism (UNH, 2014); tree mortality, microbial decomposition of litter; oxidation and mineralization of soil carbon; degradation and disturbance, such as land use change, fires, withdraw of fossil fuel. All these processes drive carbon as a source.

The intensity of these carbon losses is related to time scale diurnal-seasonal factors and climatic and environmental variables (Malhi, Baldocchi, & Jarvis, 1999). The plant can store carbon throughout their life (decades or thousands of years), when they die, fall to the ground, forming the litterfall and the organic matter in the soil (SOM). Their tissues can rapidly decay (leaves, small roots, and stems) or persist longer (wood, large roots, and branches). Until their decomposition,

they store carbon as organic matter (OM). As decomposition begins, a variety of microorganisms in the soil (bacteria, fungi), breakdown the plant and C through the respiration process, which generates a rate of~60 PgC/y as flux in the atmosphere, known as *soil respiration* (UNH, 2014).

Also oceans store huge amount of carbon, but this stay mainly in form of dissolved inorganic carbon (DOM) at high depths, which is stored for long periods of time (~38000 PgC). On the surface resides a small amount of carbon (~1000 PgC): CO_2 is absorbed and located as air bubbles on the ocean surface. These bubbles are entering then into the water through the diffusion phenomena and dissolve into the water, forming carbonic acid (H_2CO_3). For its frequent and continuous exchanges with the atmosphere, carbon has a smaller residence time in the superficial layers of the ocean. Contrary, when the carbonic acid dissolves, it forms hydrogen ion (H^+) and carbonate ion (CO_3^-). The latter one composes carbonates through reactions with minerals and other components and organisms, forming shells and rocks during the time, which deposit to the bottom of oceans. As opposed to terrestrial vegetation, biological processes and storage of carbon in marine plants are reduced because of their high breakdown rate (UNH, 2014).

All the mentioned carbon pools are in constant flux, ranging from few years to millennia, with large exchanges of fluxes and rapid reservoir turnover. However, the greatest carbon pool is found in the Earth's crust and mantle (lithosphere) with an amount of ~100 000 000 PgC. This reservoir has a much slower turnover rate, with a range of millions of years (geological time)(Ussiri et al., 2017). Carbon in lithosphere derives from sedimentary and silicate rocks, agglomerates of calcium carbonate, dolomites, shells, skeletons of marine organisms, hardening of mud and limestone. Carbon in this shape could be reintroduced into the cycle with weathering erosion (rain, wind, snow, river, vulcan activity, etc), which forms soil particles and minerals that are transported in the atmosphere, biosphere, and hydrosphere to restart the cycle again (UNH, 2014; Ussiri et al., 2017).

In modern times, a human carbon input is also necessary to be considered in this natural process. Copious amounts of CO_2 comes from anthropogenic activities, such as fossil fuel combustion, land cover change, deforestation, transport, and human settlements, which are substantially influencing the cycle and introducing carbon into the atmosphere. This amount reaches more or less the ~7PgC; though it may seems to be a small quantity in comparison of other carbon emissions and stocks on Earth, it is sufficient enough to create a disequilibrium in the carbon cycle that was once regulated and controlled by natural flows between sinks and sources. The storage of carbon in vegetation, accumulated then as fossil fuels (coal, oil, natural gasses) for millions of

years are now being released too quickly back into the atmosphere, compared to the natural time scale that occurred before anthropogenic influences causing a disruption in the natural cycle of carbon

There is, therefore, a high risk which is causing a disturbance in what was a functional balance of the carbon cycle prior to human influences, which has previously regulated life on earth for millions of years.

4.2 Carbon storage in soil Earth ecosystem

Carbon cycle is characterized by exchanges of fluxes and reservoirs, which are balanced between them (Ussiri et al.l, 2017). This balance is identify as “dynamic equilibrium”, because the carbon itself is moving among comparts, but it is in equilibrium as the system try to keep it in balance, and the net fluxes of inputs and outputs compensate each other. When the inputs to the reservoirs exceed outputs the amount of storage increases, and vice versa (UNH, 2014; Ussiri et al., 2017)

Quantify fluxes and storage of carbon in the terrestrial biosphere is not easy, because of the complex biology underlying carbon storage, the variety and heterogeneity of vegetation and soil, and in addition also the effects of human activities and the land cover change and management (Ussiri et al., 2017). These inputs could bring an imbalance between sectors.

Soil sector is a habitat which contains all variety of life and ranges in size from small niches to entire landscapes. Soil compart is essential to sustain the primary production in an ecosystem, through the formation of organic matter (Appendix 1). Organic matter is composed of different organic compounds: from a relatively fresh vascular plant and microbial biomass to refractory components, which are accumulating slowly over thousands of years (Trumbore, 1993). Soil sector is important also for the nutrient cycling, climate control, determination of chemical, physical and biological properties of the environment, support of plants and animals life. In soil occur the decomposition of SOM and the transformation and storage of nutrients (Brevik et al., 2015). Carbon has an abundant stock that resides in soil (~1500 PgC) (UNH, 2014; Trumbore, 1993) and every different kind of ecosystem or landscape which it sustains, holds different capacity to store carbon, depending on many environmental and climate factors (Appendix 2).

4.2.1 Forest ecosystems

One of the highest carbon net sinks in the world is forest ecosystem. Forests, covering about 4.1 billion hectares of land area globally (Dixon et al., 1995; Lal, 2005), ~30% of the land surface (Fig. 2A)(Bonan, 2008). Forest biomes (Appendix 3) are the main reserves for terrestrial carbon on Earth. They are one of the major components of Gross Primary Production- GPP (Malhi, Baldocchi,

& Jarvis, 1999) and contribute ~50% of terrestrial Net Primary Production - NPP (Bonan, 2008). GPP represent the total uptake of CO_2 by photosynthesis (Baker et al. 2016) and NPP is defined as the difference between GPP and autotrophic respiration (R_a) (Aragao, 2014).

More of being an important carbon sink in the Earth system, forest biome is also fundamental since it provides ecological, economic and social services. It offers protection for biodiversity, and soil resources, sustaining of the hydrologic cycle, provision of food, medicinal, wood products, and recreational uses for the various human needs.

Carbon is stored in different amounts in the different forest type: boreal, tropical and temperate forest (Fig. 2B). Temperate forests generally store less carbon (6-14% of the total C pool) (Pan et al., 2011), in comparison with boreal (23-49%) and tropical (17-60%) forests (Malhi et al. 1999, IPCC 2001, Gorte 2009). This is more related to the area that each forest type cover in the world than to the amount of C stored per hectare.

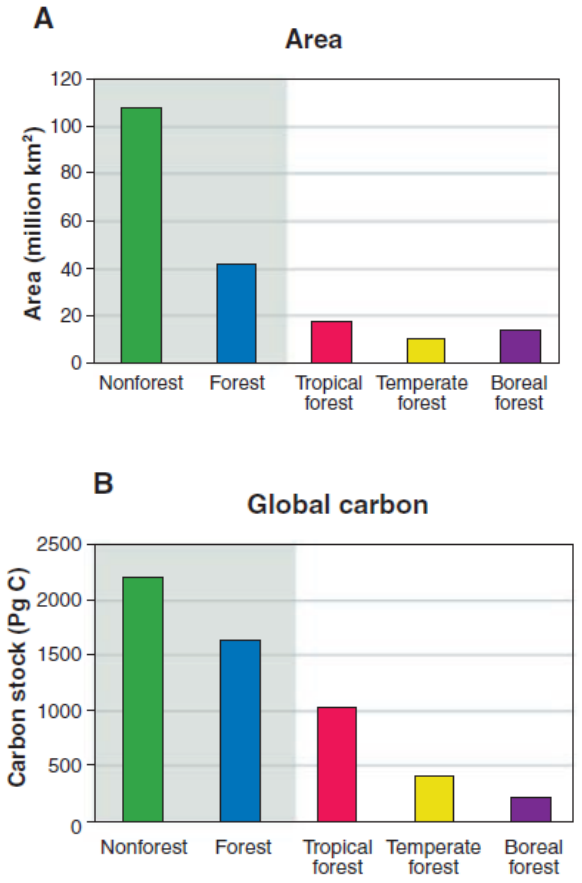

Fig. 2: *A) Geographic extent (km ^{2}) and B). Total (plant nd soil) C stock (PgC) of non forest and forest (tropical, temperate and boreal) biomes (Bonan, 2008)*

It is estimated that boreal forests, which cover 1135 million ha (Pan et al. 2011), store the largest amount of carbon in their soils (about 84%), compared to other ecosystems in the world (Gorte, 2009). This figure is due to the low degradation rate of the organic matter in the soil, caused by the cold and anoxic conditions, which allow the accumulation of a huge quantity of carbon (Gorte, 2009). Contrariwise, tropical forests (1392 million ha) (Pan etal. 2011), store the largest amount of carbon in their aboveground vegetation (44 Mg C ha^{-1}) but a modest amount in their soil (45-50%) (Gorte 2009, IPCC 2001), due to the high decomposition rates in zones with humid and warm conditions (Gorte, 2009). Temperate forests store an amount of carbon between 100-300 Mg C ha^{-1}, depending on the site (Mahli et al., 1994, Dixon

et al. 1994, IGBP-DIS, 1999, IPCC 2001), and about 62% of the total carbon is stored in the soil. They have higher mean biomass density per hectare (270 Mg C ha^{-1}in comparison with boreal forests (83 Mg C ha^{-1}) (Houghton et al., 2009) and store more carbon in the soil (147 Mg C ha^{-1}) compared to tropical forests (122 Mg C ha^{-1}) (IGBP-DIS, 1999; IPCC 2001), due also to the slow organic matter decomposition process.

4.2.1.1 Temperate forest

Temperate forests cover a global area of about 1038 million ha (Pan et al., 2001). This ecosystem is characterized by relatively cold temperatures, ranging from -30°C to 30°C with mean annual temperatures of 5-10°C. Humidity and precipitation are high ranging from 50-200cm yr^{-1}, and its climate is characterized by warm, mild summers and cool, or cold winters (Lal, et al. 2012). Though not as diverse as tropical forests, temperate forests host a wide variety of vegetation and plant species such as: temperate coniferous, broadleaf evergreen or deciduous trees, shrubs, herbs, mosses, and lichens. As the biodiversity varies considerably within the region, it serves as a useful indicator of site-specific climate (Lal, et al. 2012).

Typically, temperate forest soil is defined by high fertility containing high amounts of organic matter. The net primary production in this biome is significant, making the environment suitable to support a considerable amount of biomass production. In contrast with tropical rainforest, temperate forest store more carbon in the soil (about 100 MgC $ha^{-1,}$ and often more) than in biomass and it has slower decomposition rates than that of tropics (Lal, et al. 2012). The high capacity to store carbon and the suitable conditions for the conservation of organic matter, lead this biome to have an important role in the global carbon cycle (Lal, et al. 2012; IPCC, 2014). Despite the minor global vegetation cover of this biome compared to the other forests, it contains ~50% of the worlds plant biomass, and~10% of its terrestrial carbon (Bonan, 2008). Furthermore, it acts as an important global carbon sink, as its absorption rate was measured at ~0.8Pg yr^{-1}in the last decade, 35% of global carbon storage in intact forests and 65% of the global net forest carbon sink (Pan et al., 2001; IPCC, 2014).

4.2.2 Peatland ecosystem

A significant carbon reservoir on Earth is also peatland ecosystems. Although they occupy only the 3% of the world surface (400 million ha) (Joosen et al. 2002, Parish etal. 2008), they have an extraordinary capacity for storing carbon (Fig. 4). Indeed, peatland is the most efficient carbon storage of all terrestrial environment: it contains more carbon per ha than other ecosystems on mineral soil. More than one third of carbon earth stock is sequestered by this system (400-600 Gt), making peatlands the top long-term carbon storage in the terrestrial biosphere.

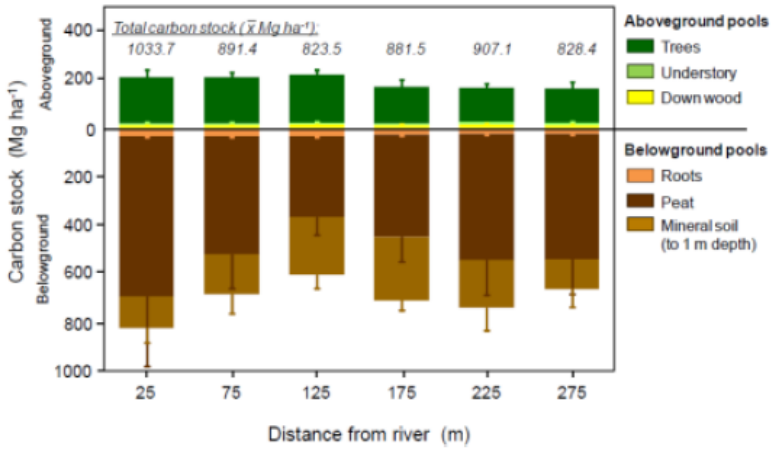

Fig. 4: *Carbon storage by peatland system (VITRI)*

Peatlands are wetlands characterized by the accumulation of peat, dead and decaying plant material under permanent water saturation environments (Parish et al., 2008). The anaerobic condition prevents the enzyme phenol oxidase from eliminating phenolic compounds (Freeman, Ostle, & Kang, 2001). In this circumstance, the activities of decomposing organisms are inhibited, leading to a decreased rate of decay of dead organic material and consequently, to the accumulation of peat (Freeman et al., 2001; Joosen & Clarke, 2002). Because of their slow decay rates, peatlands are considered systems with a positive balance between the Net Primary Production (NNP) and decomposition rate (Loisel et al., 2010; Tolonen et al. 1992, Clymo 1984). However, this delicate balance could be easily disturbed and can become a potent and dangerous source of CO_2, CH_4 and N_2O, due to human interventions and the diffuse land degradation and land use change. Therefore, peatlands are one of the most threatened ecosystems in the world.

About 14-20% of peatlands are used for agriculture, and undefined peat swamp forests are transforming through drainage and burning into cultivated and harvested plots (IPCC, 2007).

Thus, natural ecosystems could be at the same time sink or source of carbon, depending on the process (natural or anthropogenic) wherein are involved (Gorte, 2009). Human interventions are typically fast and violent, producing discrepancy among the balance of the natural environmental dynamics. The change does not permit the ecosystem to adapt itself immediately, because of the high rate and speed of variation. Carbon sequestration, inversely, is a long and slow process, which takes hundreds or thousands of years to occur and it involves delicate dynamics in the environment. The break of this equilibrium could lead to consequences that are unexpected, unpredictable, and hard to manage.

Therefore, it is important to understand and investigate these natural mechanisms, their development, and their possible external disturbances.

4.3 Chiloè Island

The Island of Chiloé (41”30’-43”30’ S Latitude) is the major Island of the Archipelago of Chiloé (Hajek et. al, 1975) and is situated in the Region de *Los Lagos* in Chile (~39- 42”s latitude). This region has been the object of several paleoclimate investigations, which made extensive and detailed records of Quaternary glaciation, and it is an important region for the study of interhemispheric comparison and reconstruction of glacial chronologies. The optimal climate permits the preservation of organic matter, making it suitable for radiocarbon and macrofossil dating even for non-glacial intervals (Porter, 1981).

The Island of Chiloé constitutes a unique situation of climatically and biogeographical interests. Indeed, its history has allowed it to maintain curious features and interest for the evaluation of the effects of the Pleistocene glaciations on the flora, on the climate and for the establishing patterns of the postglacial recolonization vegetation (Heusser et al., 1977).

The Island, in general, is characterized by a temperate rainy weather, with many variations. The mean annual precipitation ranges from 1,900 to 2,300 mm, sometimes receiving as much as 5,000 to 6,000 mm in some areas (Perez et al., 2003) and the annual mean temperature is about 9.6°C (Perez, et al. 2010).

The Chiloè’s region along the Pacific coast is defined by an Oceanic climate with smaller seasonal differences between the wettest and the driest months, and between the maximum and minimum monthly temperatures. The part in Andean Chiloé is identified by a more continental climate, represented by low winter temperatures and a wide temperature range (Di Castri et al., 1976).

The zone which comprises the Cordillera de la Costa (known locally as *Cordillera de Piuchué*) is characterized by wetter and colder climate conditions. The summit of this chain mountain is the highest peak on the Island and rises to 700-800 m, while the southern and Eastern part of the Island has low and undulating terrain, with elevations only up to 400 m. In this area, a Mediterranean climate is established with warmer and drier zones expressed mainly by greater summer dryness (Castri et al., 1976).

Because of its height (823 masl), the Cordillera de la Costa (Castri et al., 1976) would not have been glaciated, since it has constituted a barrier to the advance of glaciers. As a result, the Chiloé’s Island is considerate the boundary between the territory that was completely covered by glacier and was only partially covered by ice (Appendix 4)(Villagrán 1990).

The topography of the Island is therefore characterized by the colonization and post-glacial colonization vegetation. Indeed, the sectors of a low latitude of the north and coastal east of the Island were covered at least three times by glaciers during the Pleistocene (Heusseret al., 1977).
The ice flowed down from the western slope of the Cordillera de Los Andes (higher altitudes about 2,000 m) crossed and merged with the strait that separates the island from the mainland (Villagran et al, 1997). The glaciers advanced through the Island and reached the Pacific Ocean at the latitude of 42''40'S (Heusser et al., 1977).

Three major glacial drifts in the northern part of the Island can be recognized:
- The **Fuerte San Antonio Drift**. It is the oldest drift in the Ancud's region and is dated to be *hundreds of thousands of years old* (Villagran, 1988).
- The **Intermediate Drift.** Represents the middle unit and may have encountered more than one glaciation (Villagran, 1988). It contains many stratifications and various types of rock, including that of Andean. This drift has, however, been exposed to massive erosions over time which has made investigations into its history challenging. Date the interill wood is the best source of understanding, which attributes its age to more than *57,000* radiocarbon years old (Villagran, 1988).
- The **Llanquihue Drift**. Was named so because of its emplacement during the last glaciation, the Llanquihue Glaciation (Villagran. 1988). From their exhaustive radiocarbon chronology defined the timing of the local LGM between 34,300 and 18,000 cal yr BP. The Llanquihue drift overlies the other glacial layers and covers almost completely the eastern part of the Island (Villagran. 1988). This drift was subdivided into three components of different age (Porter, 1981), named Llanquihue I, II and Ill, listed by age from oldest to youngest. The first date is predicted older than the range of conventional radiocarbon dating, the second date is dated from the peat clasts in the till of 20,100 *+1-500* yr BP and the third date seems to have been deposited by a readvance of the Llanquihue glacier following an interval of recession when it withdrew to the eastern end of the Lago Llanquihue basin (Porter, 1981). It is predicted that it occurred around 14 500 yr BP, with a deglaciation after 13 000 yr BP, culminating about 11.000 yr B.P. when outlet glaciers of the Patagonian ice caps reached their present extent (Villagran, 1987).

As this island represents a boundary between glaciated and only partially glaciated in the last glaciation (Villagran, 1990), it uncovers many unique characteristics which are observable today.

For example the climate variations (rainfall occurring throughout the year, but also Mediterranean-type climate and regions with relatively drier summers), floristic composition, vegetation distribution, and forest successions of temperate old-growth evergreen rainforest (Valdivian, North-Patagonian, and Subantarctic forests) and soil's structure. (Villagran, 1988). In particular, the alternation of different types of ecosystems after the last glaciation, such as peatlands (wet climate) and forests (drier climate), conferred to the soil peculiar properties.

4.3.1 Chiloè native forest

Many authors consider that the Cordillera de la Costa as the main refuge of the forest during the Pleistocene (Skottsberg 1916, Looser 1935, Heusser 1972, 1982). Since the last glaciation, many floristic compositions have been changed in this territory. Furthermore, from paleontological records it could be possible that different patterns of late Quaternary forest succession occured, which can be recognized on the basis of changes in floristic composition (Heusser 1972):

- ***Valdivian forest***. This formation is distributed in sectors of low altitude in the northern part of the Island, until 250 masl. It is dominated mainly by species in temperate temperatures (Villagran, 1985), like *Aextoxicon, Eucryphius cordifolia, Gevuina avellana, Caldcluvia paniculata, Laurelia philippiana, Nothofagus* tipo-obliqua, and various taxa in the family of *Myrtaceae*. This type of forest typically grows on well-drained substrates and its soils have a brown-earth profile. The soils show a rapid incorporation of litter into the upper layers and are not very acidic (Castri et al., 1976)
- ***North-Patagonian forest.*** *It is* distributed on both slopes of the *Cordillera of Piuchué*, between altitudes of 250 and 450 m. It is characterized by *Myrtaceae* and *Laurelia philippiana, tipo-Myrceugenia, tipo-Amomyrtus Hydrangea, Pseudopanax laeteviren (Villagran, 1985), Nothofagus nitida, Tepualia stipularis, and Weinmannia trichosperma*. The soil of this landscape, of the valley floors and areas of impeded drainage, where Tepualia vegetation dominates, have a thick superlicial mat of acid humus or peat with only a moderate amount of downwashing of organic material into the mineral substrate (Castri et al., 1976)
- ***North-Patagonian-Sub-Antarctic forest***. It is distributed in the low altitude in the southern part of the Island and above 450 masl. On both sides of the Piuchué Range,

are presented discontinuous forest patches which alternate with sectors of Magellanic tundras dominated by conifers, *Nothofagus tipo-dombey, Weinmannia trichosperma, Podocarpus nubigena, Drimys winteri, Saxegothaea conspicua, Desfontainea spinose, Fitzroya/Pilgerodendron Escallonia, Maytenus magellanica, Tepualia stipularis* (Villagran, 1985). Of the conifers, several species of southern beech, and *Drimys winteri,* and cushion bogs of *Astelia pumila, Gaimardia australis,* and *Donatia fascicularis* (Villagran, 1985). In these uplands, peat formation occurs chiefly in hollows gleys and peaty gleys are widespread, and forest patches occur only on shallow superficial acid (mor) humus layers (Castri et al., 1976)

The archipelago of Chiloé represents a confluence region of very important floristic elements of the southern Chilean forests (Valdivian, north Patagonian and Subantarctic forests), which is an element of extraordinary biogeographical interest (Perez, 2003).

4.3.2 Chiloe's Island degradation

The rural landscape of Chiloé Island is characterized nowadays by a mosaic of remnant forest fragments, woodlands, peatlands and grazing pastures, due also to intense human activities. The clearcutting and burning of the *tepu* forest, the native forest which occupied earlier this area, is replaced now by a wetland environment dominated by *Sphagnum* sp. (Díaz et al. 2007, 2008, Cabezas et al. 2015), called *anthropogenic peatlands*.

Sphagnum-dominated ecosystems, locally named as "*mallines"* o "*pomponales*", from the *Mapuche* term *poñpoñ* (moss or sponge) (María F. Díaz et al., 2008), are characterized by a particular tissue structure, formed by big hydrophilic cells, which can absorb a huge quantity of water, accumulating up to 20 times its weight (Zegers et al. 2006, Iturraspe et al. 2000). Their leaves are small and composed of only a layer of these cells. This kind of tissue leads the variation of the water content in the plant during the different period of the year, depending on the evapotranspiration and the availability of water in the environment (Iturraspe et al. 2000). This property confers an important reservoir of water in the peat soil in the dry period.

These kind of peatlands may reach many meters of depth, do the accumulation of organic matter in hundreds or thousands of years. Above the peat soil lies a top layer formed by a continuous matrix of *Sphagnum* mosses. It forms an environment poor in nutrients (low concentration of nitrogen), with acidic, anoxic and colder conditions, which protect this zone from molds and bacteria, permit the peat to grow (María F. Díaz et al., 2008) and provide a difficult environment for the growth of different species. Furthermore, *Sphagnum* moss itself produce *sphagnol*, a complex phenolic compound which has antibiotic properties and inhibits the life of other plants, sequestering essential nutrients and suppressing microbial activity (Aerts, D. F. Whigham, & Verhoeven, 1999; Zegers et al., 2006). All these conditions result in the accumulation of the organic matter with a very low decomposition rate (Aerts et al. 1999, Clymo et al. 1998).

The slow decomposition of organic matter due the anoxia, permits a high accumulation of carbon in the soil, which allows species from the *Sphagnum* genus to be the main contributors that can incorporate carbon. This peculiarity is a positive vantage for the sequestration of the carbon from the atmosphere, but it is also dangerous for the release of carbon when this ecosystem is degraded, such as the most of these environs in the world.

The major cause of the degradation, threat, and overexploitation of the natural peatlands and forests in the Chiloé Island is the cutting of the forest, the drainage of peatlands, the fire for the industrial trees plantation, its use as energy and the commercial harvesting of the *Sphagnum* mosses. The main uses of *Sphagnum* mosses are in horticulture, fruit trees, orchids plantation, for the absorbent products and packaging material, and diverse uses as plant medicinal (María F. Díaz et al., 2008; Rochefort, 2000). It is extracted the acrotelm, the active upper soil layer, and once harvested it could regrow depending on the way of management, the availability of light and water, the distance to the water table and the air temperature (Gerold 1995, Clymo et al. 1998, Gunnarsson etal. 2004, Díaz et al. 2012).

Unfortunately, these activities lead a landscape with a poor drainage, with a sporadic accumulation of peat and the exclusive growth of *Sphagnum* mosses, almost the only species that is adapted to this flooded condition (Carmona et al., 2010; M. Francisca Díaz et al., 2007; María F. Díaz et al., 2008). All these processes cause the fall of the water table level to the depth of the most decomposed level, characterized by a high density and water retention, decreasing the water availability for the *Sphagnum* mosses up in the surface, whose has a weak capillarity uptake capability. Thus, it is unable to tap water during strong evaporative demand period, losing its

capacity of store water even with fluctuations through wet and dry periods, causing flooding during wet months and a waters evaporation increase during the warm months (Price, 1996; Zegers et al., 2006).

The conversion of forests into anthropogenic peatlands caused, besides of all the issues mentioned above, the loss of a high amount of carbon, and the increase in decomposition rate of organic matter. Hence, this may be triggering a positive feedback system over global warming, with the release of CO_2 into the atmosphere. Moreover, recent studies discovered that old-growth forests, like that one subject of our research, are not carbon neutral, as usually thought (Gower et al. 1996), but they can act efficiently in sequestering carbon like younger and more productive forests. This transformation then not only causes the loss of carbon store but cut also a possible important sink of carbon out.

After all, anthropogenic peatlands contain significant amounts of carbon (115 Mg C ha^{-1}) in the soil (Cabezas et al., 2015), therefore it is important to preserve both of these actual ecosystems, forests and peatlands, to avoid further losses of carbon and decomposition of organic matter. This should start by preserving these species-rich ecosystems. For those that are already degraded, there should be ecological restoration and a more sustainable method for the harvesting *Sphagnum* mosses and cutting of the forest trees.

4.4 Theoretical framework

4.4.1 Total Organic Carbon - TOC

The total organic carbon (TOC) amount in the soil is an important proxy which indicated the accumulation and distribution of total organic matter (OM) in the soil (Meyers et al., 2005).

TOC concentration is dependent on climate conditions, especially temperature, moisture, pH, precipitation and anaerobicity (Ronkainen, 2015; Zhou et al., 2005). In wet environments such as peatlands and bogs, organic matter is well preserved, under condition of limited oxygen and therefore, biodegradability is slowed (Meyers et al., 1993; Lallier-vergès at al., 1999). In drier and warmer environments, microbiological activity is enhanced and consequently, there is an increase in post-decomposition and a reduction of OM accumulation in soil, even if these climatic settings provide the conditions for a remarkable vegetative growth (Guifang et al.,2008).

OM is accumulated by plants during their life through the photosynthesis process. When the vegetation dies, it releases carbon into the atmosphere with a different rate depending on the ecosystem type. Thus, the amount of carbon sequestered from vegetation depends on the type of vegetation, mode of death, the rate of decomposition, environment, and history of the site. (Gorte, 2009)

Organic carbon (OC) is found in the upper soil layers and in the surface as partially decomposed vegetation (humus), roots and in decomposer organisms. OC is lost when the decomposition process begins (Gorte, 2009). OM is also found in the subsoil, but mostly comes from root input and in the form of dissolved organic matter (DOC) (Lorenz and Lal 2005). This occurs especially in temperate forest ecosystems, where a wet and humid environment is characteristic. DOC has different pathways, dynamics, and properties, which allow the movement and the shift of OM particles into deeper layers. These migrations are depending on the climate, vegetation, plant cover, living organisms in the area, soil texture, root systems and on bioturbation. Actually, the decrease of organic matter in the soil is a natural process explained by the different balance between the rate of accumulation and degradation of the organic matter.

Several studies suggest that soil OM in subsoil is more enriched in microbial-derived carbon compounds and depleted in energy rich-plant-derived carbon compare to the topsoil. This means that in the deeper layers the microbiological activity is higher in comparison to the surface (Rumpel et al., 2011). This is also confirmed from the decrease of the Carbon/Nitrogen (C/N) ratio, and the increase of the stable C and N isotope ratios with the depth, which indicates a high decomposing process in deep soil (Rumpel et al., 2011). Decomposition in soil is made principally from microorganisms and enzymes, which destabilize and disrupt the physical structure of OM, decomposing it with the loss of the significant amounts of soil OM, with a consequent release of CO_2 (Krull et al., 2003; Rumpel et al., 2011)

There are many methods to quantify total carbon, but at the same time, it is not possible to determine where the sources of C are coming from. In soil and sediments, the total carbon (TC) is measured by summing the amount of inorganic C (TIC) and TOC (Schumacher, 2002).

TC= TIC + TOC

All methods of measuring the TOC are based on the oxidation (thermal or chemical) of organic carbon with carbon dioxide (CO_2). This is detected and determined quantitatively trough CHN analyzers.

4.4.2 Geochemical biomarkers

In the last decade, the use and application of geochemical biomarkers have exponentially increased in ecological, environmental and paleoclimate research.

Biomarkers are organic molecules that can be traced to a particular source organism, a group of organisms or to a process. They can be used as a direct indicator of specific environmental, climate and vegetation condition changes, paleo-elevation and human impact changes, for past terrestrial and aquatic ecosystem reconstructions. Parameters that can be obtained with this method are lake surface temperature, hydrology, salinity, temperature, pH, vegetation type, organic soil matter input, and soil carbon storage.

Examples of biomarkers are bacterial and plants membrane lipids, N-C-H-isotope analysis, specific molecules, compound-specific isotopes, organisms. They are used differently in various research fields, such as clinical sciences, as indicators of the presence of a disease or response to treatment (Brennan et al., 2013; Van Bon et al., 2014), in toxicology, to analyze the effect of a toxic species in a biota (Clemente et al., 2014), in the forensic sciences, to furnish information about crimes (Concheri et al, 2001), in environmental sciences, as an indicator of possible pollution, signal or presence of a substance in an area (Tissot et al. , 2005).

Biomarkers have peculiar characteristics which allow them to conserve themselves throughout millennia:

- Biomarkes are studied through the *geochemical biomarker method*, which is based on organic geochemistry and the presupposition that carbon is one of the main constituents of all living organisms on Earth (Ronkainen, 2015a). Therefore, they are *easily dispersed* in the environment, simply to find and to observe them.
- Biomarkers are or form *strong organic compounds* with high stability and resistance against decomposition.
- Biomarkers *are preserved in biological and geological material*. Terrestrial plants are the major producers of biological components (root, resin grains, phytoclasts, leaf wax), but most of them are mineralized and transformed during the phase of transport or diagenesis. Only a little part of these is well conserved in geologic materials (sediment, soil, rock, coal, petroleum, waxes) (Hautevelle et al., 2006),

but even a small amount of organic matter that is well preserved can provide a wealth of information (Castañeda et al., 2011; Jansen et al., 2017). The modality of their conservation depends on their "packaging", their entrapment or their encapsulation in different matrixes. Examples are mineral matrix, shell, bones, rocks; biopolymer matrix, cell walls, leaves, insect cuticles, pollen grains, colloidal matrix, humic acids, and detrital debris (Eglinton et al., 2008). Some compounds could reach their matrix or may become adsorbed or dissolved within them, conserving themselves in this way.

Every kind of biomarker has a different history, with diverse modality of transport (i.e. by wind, rivers, sea and animals), different path and timing of sedimentation, from land to sedimentary basins, and different diagenesis (Hautevelle, et al., 2006), which characterize them and give them unique attributes.

4.4.2.1 Lipid wax n-alkane biomarkers

In geochemistry, the most important classes of macromolecules are carbohydrates, proteins, and lipids. These make up every organism on Earth, and they change in relation to the environment.

Taller plants, for example, are mostly composed by lignin and cellulose, the main components of the supportive and structural tissue of plants, but these are degradable and they may transform or degrade over time (Ronkainen, 2015, Killops et al., 2008). On the contrary, lipids are compounds that are quite stable and can be preserved in a relatively unaltered state (Pancost, Baas, & Geel, 2002).

Lipids are organic molecules that have scarce solubility in water but they are extractable from organisms through apolar solvent. They are substances such as fats, oils, wax, hormones, steroids, vitamins, phospholipids with no protein components on the cell wall (McMurry, 2008).

Plants are composed of two types of lipids: structural and deposit lipids. The first one has a protective function with impermeable action (mostly waxes), which form the membrane structure and the cell organelles (glyco and phospholipids). They are supporting the cell walls (phospholipid bilayer) and are employed to transport electrons and organic substrates. The second type has a deposit function in fruits and seeds (oils) with the important role of providing energy reserves.

They are formed by triglycerides, or rather esters derived from glycerol and three fatty acid molecules (McMurry, 2008).

Lipids in plants are mostly components parts that are in contact with the atmosphere in order to protect them. Therefore, they form cell walls, waxy components of leaf cuticles, stems, spores, pollen, resinous tissues, and petals.

This protective lipid stratum is called the cuticle, and it is composed of cutin, which is bound by a layer of wax: epicuticular and intracuticular waxes (Eglinton et al., 1967). The epicuticular structure is formed by waxy components, and cutin in terrestrial plant. This layer acts as a barrier against uncontrolled water evaporation, but also minimizes mechanical and chemical damage to leaf, cells and inhibits fungal, bacterial, parasites and insect attacks (Eglinton et al., 1967; Ronkainen, 2015). They also regulate albedo, wettability and excessive ultraviolet radiation, and are composed by aliphatic acyclic compounds, such as fatty acids, primary and secondary alcohols, alkanes, aldehydes and ketones (Ardenghi, et al., 2017; Eglinton et al., 1967).

The intracuticular structure is formed by waxes which prevent uncontrolled transpiration and are composed mostly of cyclic triterpenoids (Ardenghi et al., 2017; Ronkainen, 2015).

Next to the waxy layer, just outside the leaves (cuticle) on the inside, is a layer of pectin, followed by the cellulose cell wall.

Pectins are, therefore, structural components fulfilling important functions of protecting plants against withering and drought, and support growth and development of cells and cell walls (Yapo, 2011).

Cellulose is the most common organic polymer. It is a complex molecule, formed by many glucose molecules (300 to 3000 molecules) joined by glycosidic β(1→4) bonds. This strong arrangement forms the plant skeletal component and with hemicellulose, lignin and pectin confer to plants that allows for extraordinary structural and defensive properties. According to the species type and life stage, plants have different cellulose conformation, orientation, and biodegradability (Klemm et al., 2005).

Hence, among the different structures that make up leaves, surely the most resistant to diagenesis and degradation are waxes. They more faithfully maintain the properties and characteristics of the plant over time. Wax lipids, instead of carbohydrates (readily degradable components), for example, are the most studied biomarkers in paleogeological science (Pancost et al., 2002).

Lipid n-alkanes are hydrocarbons that are found in the cuticle of leaves and steams of terrestrial plants (Eglinton et al., 2008; Sachse et al., 2006, Gamarra et al., 2015). The have strong structure, composed by non-polar covalent bonds among their hydrogen atoms, which make them resist exchanges based on the environment. Moreover, their water insolubility, negligible volatility (for compounds with more than 20 carbon atoms), chemical inertness (Eglinton et al., 2008) and lack of functional groups, implies a high resistance to diagenesis and biodegradation. That may create an accumulation in soil and sediments (Ardenghi et al., 2017; Eglinton et al., 2008; Kahmen et al., 2013). As they preserve their primary structure over geological time, it makes them useful research proxies (Ardenghi et al., 2017; J. Nichols et al., 2010; Niedermeyer et al., 2016; Sachse et al., 2006). They originate from plant remains, and they can reflect original organisms, local vegetation cover and climate (Zheng et al., 2009). N –alkanes derive from different biological sources, and can be classified according to (based on) to the length of the carbon chain.

Recent studies (Eglinton et al., 2008; Ficken et al., 1998, 2000; Pancost et al., 2002, Li et al., 2016; Nichols et al., 2006) discovered that short carbon chain mainly derived from bacterial and algal input (C14-19 n-alkane chains) (Han and Calvin, 1969; Albro, 1976; Weete, 1976; Wakeham, 1990), mid carbon chain derived principally from submerged aquatic plants (C23-25 n-alkane chains), long C chains come mostly from terrestrial higher plants, tree, and shrubs (C27-31 n-alkane chains), and higher C chains (>n-C31 n-alkane chains) represent mostly input from grasses and herbs (Maffei, 1996).

For instance, various studies show how n-C23 and n-C25 are maximizing in *Sphagnum* sp. (Sachse et al. 2006). N-C27 are maximizing in alder, birch, willow, shrubs, sedges, *Fagus* sp., herbaceous taxa and in *Sphagnum* sp. too (Ficken et al., 1998; Sachse et al., 2006; Tarasov et al., 2013). N-C29 is common in *Alnus*, *Quercus, Carpinus* species, (Sachse et al., 2006) and *shrubs*. N-C31 in *Arctous, Vaccinium*, *Quercus ,Carpinus, Myrtus* species (Sachse et al., 2006, Tarasov et al., 2013). N-C33 in *Myrtus species*, *R. lanuginosum* and grasses in general(Sachse et al., 2006 Ficken et al., 1998)

There are, however, species that can grow within different environments, with variations in n-alkane distribution, such as *Sphagnum* species, which were found both in hollow areas of bogs (*Sp. recurvum, Sp. papillosum and Sp. cuspidatum*) with a maximum of C23 n-alkane chains (Xie et al., 2000), and in drier hummock tops (*Sp. magellanicum,* and *Sp. capillifolium*), with great abundance also of n-C31 homologues (Nichols et al., 2006)

Also deciduous and evergreen trees, angiosperm, and gymnosperm produce different amount of n-alkanes. In deciduous tree leaves, n-alkanes with nC25–nC31 carbon atoms and a strong odd over even carbon number predominance, are much more present rather than in coniferous tree needles (Maffei, 1996; Sachse et al., 2006). Since deciduous trees are producing more biomass each year and consequently, litter and organic matter accumulation (Sachse et al., 2006).

The distribution of n-alkanes is mostly dependent on the place where the species are grown. Two plants of the same species, therefore, could have different n-alkane patterns if they live in different places. For example, a previous study (Sachse et al., 2006) observed that the average chain length (ACL) of *Betula* species, changes along the European latitude. Precisely, mean ACL value increased towards the southern regions, assuming probably that southwards there is a longer vegetation period and a more potential incoming radiation. Thus, plants are producing longer n-alkane chains to protect their leaves from water loss.

4.4.2.1.1 Suppositions

It is supposed that long n-alkane chains in leaf waxes are synthesized from plants to protect from potential incoming radiation, evaporation and water loss (Eglinton et al., 2008; Gamarra et al., 2015). This phenomenon could be caused also by evaporative loss of shorter chain due to increases in evaporation.

Leaves waxes are produced from plants during the whole growing season, to protect every external part of the plant, and mainly the most sensitive ones (Li et al., 2016; Sachse et al., 2006). Indeed, researchers show that there are high productions of long n-alkane chains in inflorescences, which are the most critical organ in a plant to ensure their reproduction. Therefore, in grasses, whose boundary layer is in direct contact with atmospheric agents and is exposed to an intense evaporative demand, long n-alkane chain (C31-C33 homologues) are well abundant (Dietrich et al., 2014) to conserve as much water as possible to avoid desiccation of inflorescences (Gamarra, 2015).

Other parts of the plant that are not directly enrolled in evaporative processes are less enriched with long chains, and they may have other epithelial structures with different functions. Such as

roots, which are the less enriched long n-alkane chain parts, because the root tip is meant to be permeable to facilitate water and other substance uptake by the plant. Likewise, a water impermeable waxy layer in this structure would be counter-productive for the plant. So, every species, part and organs have their own function with their own structure. The more exposed and sensitive these components, the more they will be protected by thick waxy layers and long n-Alkane chains (Gamarra et al., 2015).

With these assumptions it is possible to discriminate between species there are diversified in short or long n-alkane chains enrichment. Therefore, with this kind of analysis, it is thinkable to discover the vegetation that live or has lived in an area, more or less resistant to drier or humid environments. This technique then, is well applicate to differentiate between vascular and no-vascular plants, such as mosses or trees, for example.

4.4.2.1.2 Ratios used to explain n-alkane distribution

Many studies have used different ratios to estimate the contribution of various species and their relative n-alkane abundance in the soil. For example, the **n-C23/n-C25** ratio is used for distinguishing among different *Sphagnum* species and computing their relative abundance (Andersson et al., 2011; Bingham et al., 2010). The corrected-model **n-C23/n-C29** n-alkane ratio is used to differentiate between inputs from *Sphagnum* and non-*Sphagnum* species (Nichols et al., 2006b). It is used n-C29, because it is quite rare in *Sphagnum* species and abundant in other plant species, but other homologue, for example n-C31, is abundant in both non-*Sphagnum* and *Sphagnum* species. The **C23/(C27 + C31)** ratio is used to describe the relative moisture in peat profile and to separate fen and bog phases in permafrost environments (Andersson et al., 2011). Various observations (Bingham et al., 2010; Ficken, et al., 2000a) illustrate that the latter ratio represents better inputs from *Sphagnum* and vascular plants, because the C23/C29 n-alkane ratio, in general, does not completely reflect the vegetation input and the moisture conditions in the profile (Andersson et al., 2011).

Mosses/Tree Ratio – MT

MT ratio - **C23/(C27+C29+C31) -** indicates the abundance of the distribution of short chains (n-C23 alkane homologues) representative of mosses (*Sphagnum* species), over long chains (n-C27, n-C29, n-C31 alkane chains), indicative of trees. This ratio estimates, therefore, the prevailing abundance of one kind of vegetation, which could be a *Sphagnum* mosses, on the other, a forest, for example.

Aquatic Ratio - P_{aq}

P_{aq} ratio reflects the abundance relative to submerged vascular macrophytes to terrestrial plants. It was described by Ficken et al. (2000) in lacustrine circumstances, and it expresses the relative proportion of mid-length chain length (n-C23, n-C25) to long-chain length (n-C29, n-C31):

P_{aq}=(C23 +C25)/(C23 +C25+C29+C31)

P_{aq} values >0.4 indicate the probably dominance of submerged and floating macrophytes; P_{aq} <0.4, instead, indicates dominance of vascular plants (Ficken et al., 2000).

Waxy ratio - P_{wax}

The ratio that reflects the relative proportions of waxy hydrocarbons derived from emergent macrophytes and terrestrial plants to total hydrocarbons is the **P_{wax}** (Guifang et al., 2008):

P_{wax}= (C27 + C29 + C31)/(C23+ C25 + C27 + C29 + C31)

High P_{wax} ratio suggests a strong input from vascular plants and dry conditions, while low P_{wax} values indicate Sphagnum domination and wetter conditions (Zheng et al., 2007; Andersson et al., 2011).

Carbon Preference Index - CPI

N-alkanes in this range of carbon chain (>C21), show predominantly strong odds over even carbon chain predominance (Eglinton et al., 1967; Kolattukudy, 1977; Li et al., 2016), rather than other carbon chains (alkanols, alkanoic, n-alcohols and n-fatty acids) which derived mainly from higher plant, but have typically an even carbon number preference. Even numbered n-alkanoic acids are precursors of the odd-numbered n-alkanes, after losing a single carbon. Therefore, this characteristic odd/even carbon-number distribution is a consequence of the universal polyketide (acetate, malonate) biosynthetic pathway. Biosynthetic reactions of this type give rise to the observed compound biases that are evident in extracts of representative vascular plant-surface waxes (Saliot et al., 1988). This preference of the carbon chain is represented by the carbon-number preference index **(CPI)** (Eglinton et al., 2008).

CPI is a measure of the alteration of organic matter, used as degradation proxy by quantifying the predominance of the carbon chains and furnishes an estimation of the continental/marine quality of the organic matter (Saliot et al., 1988)

CPI is an important parameter which describes the molecular distribution of long n-alkanes chains, with the relative proportion of even or odd-numbered chain lengths in biological and geological samples. Biomarkers from different origins have different CPI values. CPI > 1 means a predominance of odd over even chain lengths, indicating a terrestrial plant source (Bush et al., 2013). N-alkane from the cuticular waxes of higher plants have a strong odd/even predominance and give a CPI values >5. These results show larger differences between the chains, and vice versa (Rao et al., 2009). Low CPI values mean mature or degraded organic matter (J. Strauss et al., 2015).

N-Alkane from bacteria and algae, for example, show a weak odd-over-even predominance with low CPI values (Zhou, Xie, Meyers, & Zheng, 2005)

Average Chain Length - ACL

Average chain Length **(ACL)** is the weighted average of the various carbon chain lengths. Usually, it defines chain length of the C27 to C33 n-alkanes present in a geological sample (Bush et al., 2013). It is one of the main average chain length tools together with CPI, and both are indicative of the biogenic sources, alteration, and organic matter overprint (Ronkainen, 2015).

4.4.2.1.3 Limitation of n-alkane biomarker method

Even if the lipid biomarker method is rapid, easy to apply and brings immediate results with differentiation also of different sources, it has many limitations.

- Plants in general contain less than 2% of lipids as biomass. Thus, the plant lipid represents only a low percentage of the total OM (Eglinton et al., 2008; Ronkainen, 2015) and could not fully reflect the OM sources (Zheng et al., 2007).
- There is variability in the molecular composition of the plant-derived OM, caused by diverse sources (different species, plant parts, genetic assembly), develop in different settings, climate, and environmental conditions. Also, conservation, ontogenesis and/or degradation in soil could furnish different pathways in the soil, depending on external environmental factors, age and microbiological activity (Jansen et al., 2017).
- The airborne contribution might have considerable relevance, as it could cause the input of alien molecules, such as dust particles and aerosols, transported from large distances that may influence the local signal (Conte et al., 2002).
- The contribution of modern roots could obscure the sample signal, for this reason, the preparation phase is significant to provide a clean and reliable sample.
- It is important to also pay attention to the source of the scan chain. Every species maximizes the n-Alkane chains at a specific carbon number, but it is possible that a species contains a high abundance of more C, as *Sphagnum* sp. with both n-C23 and n-C31 abundant carbon chains. This is depending also on the condition in which the plant is growing (Sachse et al., 2006).

Hence, although recently a lot of research has been conducted on this molecular proxy method and it is still in development, limitations are present. Also available data on plant and soil chemical composition for different substance classes are still limited. Thus, sometimes it is helpful in paleoenvironmental studies and reconstructions to combine and cross-check with geolipid biomarker or other non-molecular methods and techniques, such as fossil pollen data, δD, δ13C, testate amoebae, rhizoliths (Jansen et al., 2017; Ronkainen, 2015).

4.4.2.1.4 Roots contribution

More recent studies (Huang et al., 2011; Huguet et al., 2012; Kuhn et al., 2010; Nichols et al., 2006; Nierop et al., 2005) show that roots represent >70% of global net primary productivity of total carbon plant-derived carbon and they improved the carbon storage in the soil (Rasse et al., 2005).

Roots are growing in plants with the function of catching water, minerals, and nutrients from various parts of the soil layers. The more plant growth in a humid environment with high water availability and high water table, the more its radical apparatus won't be developed deep in the soil. If the plant grows in an arid environment, with low water availability, it needs to develop a more extensive, deep root system, in order to access water for its growth which is present at greater depths in more arid climates. Examples of these ecosystems which foster deep root growth are desert regions i.e. desert biomes, which could host species with 68m root system depth such as *Acacia erioloba*, Kalahari, Botswana (Jennings, 1974). Differently, boreal forest ecosystem are reaching ~3,3 m rooting growing depth, and tundra biomes ~1m (Canadell et al., 1996).

Temperate forest biomes typically have maximum rooting depth of 3.7 m, but only 35% of the root biomass is growing below 0.3 m. That means that the most of the roots and their C contribution are allocated in the first 0.3-0.5 m.
Chiloé forest is characterized by a horizontally root system, developed mostly in the first 50 cm (Schulze et al., 1996). Hence, most of the root systems are allocated in these layers.

Root input, therefore, could be an issue when applied as molecular proxies because of two reasons:

1. *Occlusion of leaf wax lipid signal:* roots may contain different lipid composition, in quantity and quality in comparison to other plant organs (Jansen et al.2006; Martelanc et al. 2007). Nevertheless, root biomass contribution in soil (20-50% depending on the biome) is not necessarily proportionate to their n-alcan lipid input (Gamarra et al., 2015)

2. The *contribution of young root* input: they may overprinting the original signal input and disturb the chronology (Gocke et al., 2014; Lavrieu et al., 2012).

Root n-alkane input varies significantly among many factors, such as different site, plant species, biome, depth. Therefore, the real contribution of roots is quite difficult to measure and evaluate and this topic is still the center of scientific debate, without any founded conclusions (Gocke et al., 2013; Jansen et al., 2017, Lavrieux et al., 2012).

4.4.3 Gas Chromatography - Mass Spectrometry (GC-MS)

Chromatography is a technique used for the separation of the components of a mixture based on the division between phases. The underlying principle of chromatography is based on the separation through different affinity of the compounds between two phases:

- a fixed phase, or stationary phase, which can be a solid or a liquid supported on solid;
- a mobile, liquid or gaseous phase, which is continuously flowed on the stationary phase.

The stationary phase, consisting of a finely divided powder, made to increase the surface development, is contained within a thin tube (chromatographic column). The mixture which should be separate and placed on top of the chromatographic column and the mobile phase, also called eluent, is continuously flowed through the column, moving through the interstices of the mobile phase and filling them.

The Gas Chromatography (GC) is a technique used exclusively for analytical purposes that uses a gas (carrier gas) as a mobile phase. It transports the sample through the column. It is, therefore, used to analyze gaseous substances, but also liquid or solids, as long as they are volatile in the range 0-500 °C. In the GC there are no significant interactions between the molecules of the mixture to be analyzed and the mobile phase (a carrier gas, N2, He, Ar). The components of the mixture, in fact, are separated above all according to their different volatility: the more a component is volatile, the lower its retention time in the column, and the faster will be eluted. According to their different affinity for the stationary phase, the more a component is similar to the stationary phase, the higher its retention time will be.
The column is inserted in a thermostat (oven) that allows choosing the most suitable temperature for a given chromatographic analysis (constant temperature or variable by gradient). So, the liquid or solid compounds (<1 mg) is separated in their elemental components by the gas chromatograph. The detection of the signal is made by the mass spectrometry (MS). The signal produced by the detector is sent to a computer which records the chromatogram. With this coupled GC-MS system it is possible to obtain qualitative and quantitative determination of organic compounds in a variety of matrices. This technique provides molecular profiles of organic compounds which could be compared with standards molecules or mass spectra libraries. It is also possible to discover the composition of natural substances with the analysis of the presence of specific molecular biomarkers (Ronkainen 2015).

5 Research question

The interesting peculiarities of the forest of Chiloè Island and its soil and the incumbent threat of climate change and human activities in this area motivated us to investigate more in depth on this site.

The *aim* of this research was to quantify the amount of carbon sequestered by the different kinds of vegetation during the past. This estimation was done by using quantitative analysis (TOC measurement, MS) to evaluate carbon content in the soil profile, combined with qualitative analysis (n-alkane biomarkers, GC-MS) to estimate the contribution of vegetation types.

Investigate the past is necessary and very useful to act accordingly in the present, with the necessary and correct tools to ameliorate and amend the future.

6 Material and Methods

6.1 Study area

The study was carried out at the ***Senda Darwin Biological Station*** (***EBSD***, 42º53' S, 73º40' O) (Fig. 5), a private protected area located in the north of the Chiloé Island, 15 km east from Ancud. The EBSD covers more than 113 ha and is formed by forest, shrubs, peatlands and forest plantations. The study site is a 100-ha forest patch, dominated by native North-Patagonian rainforest species, with evergreen, mixed broad-leaved trees, reaching 25 m high, such as Coigue de Chiloé (*Nothofagus nitida),* Canelo *(Drimys winteri),* Tepú *(Tepualia stipularia),* Olivillo *(Aextoxicon punctatum),* Avellano *(Gevuina avellana),* Luma *(Amomyrtus luma),* Ulmo *(Eucryphia cordifolia),* Tiaca *(Caldcluvia paniculata),* Trevo *(Dasyphyllum diacanthoides*) and also narrow-leaf conifers, Mañío hembra (*Saxegothaea conspicua*) and Mañío macho (*Podocarpus nubigena*). Also the abundant cover of the native bamboo Quila (*Chusquea quila)* takes part to this floristic assemblage (Aravena et al., 2002; Villagran, 1985).

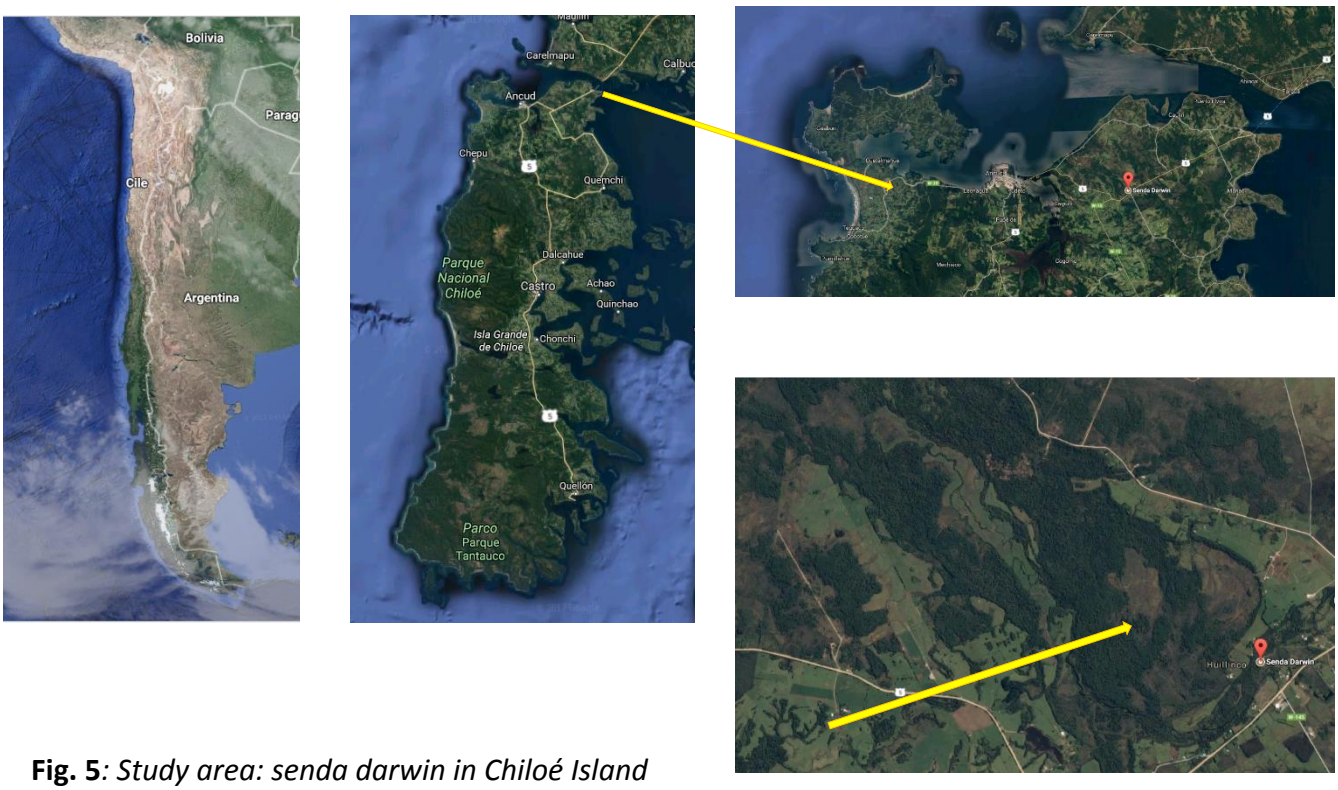

Fig. 5*: Study area: senda darwin in Chiloé Island*

The climate of the area is characterized by a temperate rainy weather, with oceanic influence (Aravena et al., 2002). The mean annual precipitation ranges from 1,900 to 2,300 mm, reaching even 6,000 mm in some areas (Perez et al., 2003). The annual mean temperature is about 9.6°C (Carmona et al., 2010) with maximum monthly temperatures in January (16°C) and minimum monthly temperatures in July-August (5 ºC) (Aravena et al., 2002).

A recent study (Perez-Quezada et al., u.n.) revealed that this forests store 211 Mg C ha^{-1} in tree biomass and 764 Mg ha^{-1} in soil (72% of total), which is significantly higher than the average in temperate forests.

6.2 Field Collection Samples

For this study, there were three cores collected from the forest of the Senda Darwin Station.

The drilling locations were established with a standard distance of approximately 100 m from each other (**Fig. 6**).

The study site area had a soil depth of approximately 50 cm, and at some points, it reached 1 m. At every extraction point, the soil was full of roots and branches, which presented challenges to the collection of the samples.

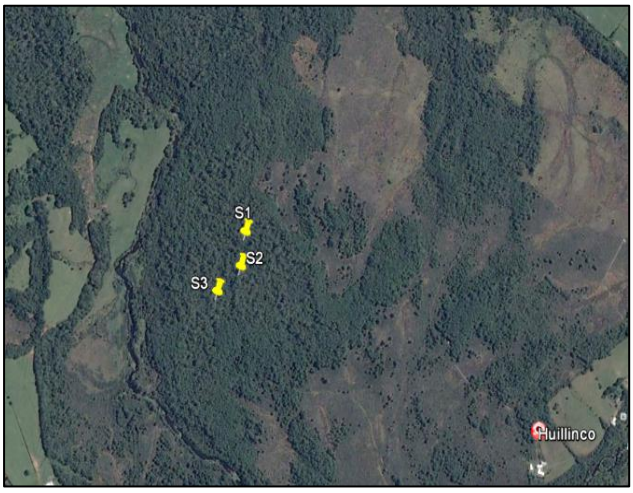

Fig. 6: *Three site area (above), soil core and Senda Darwin forest (below)*

The first two profiles (Core 1 and 2) were taken from inaccessible areas of the forest. The roots and lianas of the trees have made the transition crucial. The main trees found on this site were *canelo*, *coigue* and the *ulmo*. Core 3 was withdrawn from a moister area, where trunks of the trees rest lying horizontally and vertically on a carpet of moss and marsh plants. The first soil layers were only soft spongy moss.

The vegetation in the Senda Darwin area has developed a significant root system in the first layers of soil (0.5- 1m) due to the shallow depth of the soil, even though the trees have been observed to grow as high as 25 m.

The three soil cores were taken from a depth of 50 cm using a Russian peat core auger (Eijkelkamp, Giesbeek, Holand). For each sample point, three cores were collected to ensure there was enough material for analysis. Each soil core was then divided into 5 cm thick layers, resulting in 10 samples for each core (3x(10x3)= 90 samples in total). The samples were stored in plastic bags and transported to the Laboratory of Ecosystem Ecology, of the Agronomy Faculty of the University of Chile.

6.3 Laboratory Procedure

6.3.1 Physical Analysis

The sections of equal depth at each sampling point were placed together in aluminum tubes, weighted and dried in an oven at 40°C for 48 hours. Afterward, they were weighted again, coarsely ground, and stored in plastic tubes of 10 ml volume for further analyses. The core samples data were then gathered to estimate the water content, weight, volume and dry bulk density of each profile (Appendix 5).

The further analyses (TOC measurements and n-alkane biomarkers analyses) were performed at the Senckenberg Institute - a Research Centre of Climate and Biodiversity in Frankfurt am Main, in Germany.

6.3.2 Roots separation

Each sample was divided into different fractions, to separate the roots from the soil as much as possible.

Plant roots play an important role in terms of contribution to organic matter into subsoil horizons. With dissolved organic matter and bioturbation (biotic activity which rework the soil and creating conditions for the nutrient alteration and chemical and physical change of the sediment texture), root biomass (also litter and root exudates) are one of the main sources of carbon input in the soil.

Thus, to avoid misunderstandings between leaves/roots signal for this study, which could bring modern lipid n-alkane inputs to the soil sample, a method of precision root separation was carried out.

The largest root particles were separated with tweezers (Fraction O), the smaller particles using different size sieves: fraction A of >0.2 mm, fraction B of <0.063 mm, fraction C of >0.063 and 0.2 mm, and fraction D with the finest roots (Fig. 7).

Fraction O

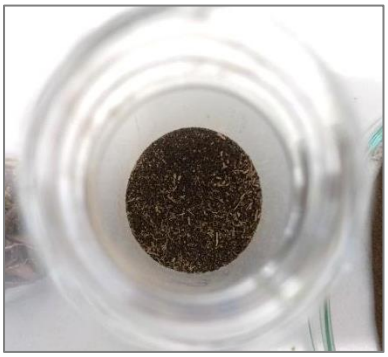

Fraction A

Fraction B

Fraction C

Fraction D

Fig. 7: *An example of each fraction*

The C fraction is derived from the amount of material that did not pass through the 0.063mm sieve and was filtered with filter paper in distilled water. The moist soil samples were frozen overnight. The next day, the C fraction was put in the freeze dryer ALPHA 1-2 LDplus to extract water from the frozen material. This process, known as sublimation, converts ice directly to vapor. This is possible because the material is put under vacuum conditions, at temperatures lower than -10°C. Through this process, a water soluble product can be obtained, which will have the same characteristics as the original product after addition of water. Thus, the compounds remain qualitatively and quantitatively unchanged. The C fraction samples were then put at -55°C ice condenser and 0.099 mbar vacuum.

Afterward, the dried samples were stored in separate beakers, and the different roots deposited on the filter paper were dried and separated in different containers (fraction D). The B fraction was the finest and cleanest of all the samples, and it was used for further analyses because of its purity. The processes of these operations were essential to process a clean, uncontaminated and sample, free of roots.

So, the finest fraction (<0.063mm) were used for the TOC measurements and then-alkane biomarker analyses.

6.3.3 TOC measurements

For the analyses of this study, the direct quantitation of TC was made through the destruction of organic matter present in the soil via heat at high temperatures. These analyses were performed with an analyzer Leco EC-12. This device does not distinguish between organic and inorganic carbon.

However, for the Chiloé forest soil, which contains a large amount of organic matter, the decarbonization process was not necessary, due to the execution of a test method done with hydrochloric acid, HCl (10%: 771 ml Distilled water, 240 ml HCl 37%). The method provides the application of many drops of HCl on the sample, and if it doesn't form bubbles and nothing was dissolved, it indicates that there was no presence of carbonates (HCl is a strong acid, that in contact with carbonates, it decomposes them).

The analyzer determines the TOC amount by the combustion of the sample material. During the sample material combustion in a high-temperature induction furnace at ~1000°, carbon is transformed into carbon dioxide. The carbon dioxide is trapped in a measuring cell where the gas concentration is determined by an infrared detector. TOC content is defined according to sample weight and is given in percentage of weight.

Once collected, the samples were stored at 4°C, and dried in the oven immediately followed by sealing them properly in storage containers. Before the effective measure of TOC, it is necessary to remove all the larger organic particles by physically pulling particles out or by sieving the samples, leading to a more accurate evaluation of the soil and sediment C amount.

Small portions from the finest size fraction (<0,063mm) of each sample were weighed (Appendix 5).

Under normal circumstances, carbon in soil should decrease with increasing depth due to the high ratio of organic matter accumulation in the first layers of soil and the increase of the degradation phenomena in the deepest layers. Taking this into account, it was taken a TOC values range of 10% (most superficial layer) to 1% (deepest layer), with the corresponding ideal sample and standard weight.

The detection limit of the Leco EC-12 is 0.001% and the precision is ± 0.004 at a sample weight of 0.5 g (Leco company brochure). Analyses were performed in the laboratory of the Riedberg Campus, Biocentre of the Goethe University in Frankfurt am Main.

6.3.4 N-Alkane Biomarker Analysis

Because of their abundance in the environment, their ease and rapid identification, extraction, isolation and purification and the minimal required quantity (<1g), n-alcane are widely used as proxy for many paleoenvironmental studies. In particular, there are often investigated with a geolipids method, an advantageous and useful technique.

From the soil samples with <0,063 mm size, was extracted the organic compounds and analyzed the n-alkanes composition.

6.3.4.1 Organic extraction

The extraction of organic matter from the soil sample was realized using the fast Pressurized Solvent Extraction method (PSE). To achieve it, it was handled the BUCHI SpeedExtractor E-914/E-916 in the Senckenberg Institute in Frankfurt am Main (Germany) (Fig. 8, Appendix 6).

Pressurized solvent extraction is an efficient way to extract organic compounds from various solid or semi-solid matrices at elevated temperatures and pressure. This is an optimization process which reduces time and solvent consumption, ensures high recoveries and avoids the cross-contamination between adjacent samples. A pre-treatment is required to reach a successful extraction. In particular, samples should be perfectly dry: wet samples reduce extraction efficiency and may cause blowback due to restricted flow through the sample bed and may cause interferences due to co-extractions.

Fig. 8: *BUCHI SpeedExtractor E-914/E916*

For the analysis was used the finest size fraction (<0,063mm) obtained from sieving, as the efficiency of the extraction is proportional to the surface area in contact with the solvent, the smaller the particles and the large the relative surface area, the more efficient is the extraction. However, very fine-meshed samples may form tightly compressed beds which restricted solvent

penetration and may impede solvent discharge. To avoid this, it is ideal to mix the sample dust with combusted sand (sample/sand 1:1). The cell preparation for extraction is done with the use of 20 ml cells, filled with 3 g of sand, sample/sand 1:1, and sand again, retaining a void approx. 1 cm in height between the sample bed and the upper filter (to ensure uniform flow and avoid samples clogging). Cells were closed with opportune glass fiber thimbles and paper filter, to reduce the sample loss upon transfer, and avoid clogging the samples and simplify the cleaning procedure.

The extraction cycle involves three steps: *heat up* step, where temperature and pressure are slowly increased until the default parameter setting; *hold* step, where parameters remain constant; *discharge* step, in which the extraction product is discharged via pressure compensation and collected in the vials at temperature and pressure of 76 °C and 100 bar.

The solvent has the major impact on the extraction result, this is important to choose a solvent which has similar polarity to that of the analytes. It had been arranged a process with 4 cycles with the use of dichloromethane (CH_2Cl_2) and methanol (CH_3OH) as solvents, in the proportion of DCM/MeOH 9:1 (duration: 1.5 h ca) (Appendix 6).

Before and after the extraction it was made a flush cycle with fresh solvent (100% Methanol, 2min) and gas (N_2, 1min) to clean up and to dry the cell, avoiding contamination of extract residues and remaining liquids from the last cycle to a subsequent run.

Total lipid extracts (TLE) were collected in 240ml vials with proper porous caps (Fig. 9). They were transferred in 40ml vials and dried under a flow of nitrogen in a Bio-tage Turbovap LV at 36°C and 10-15bar for 20-30 min. Dried samples were stored in the fridge at 4°C.

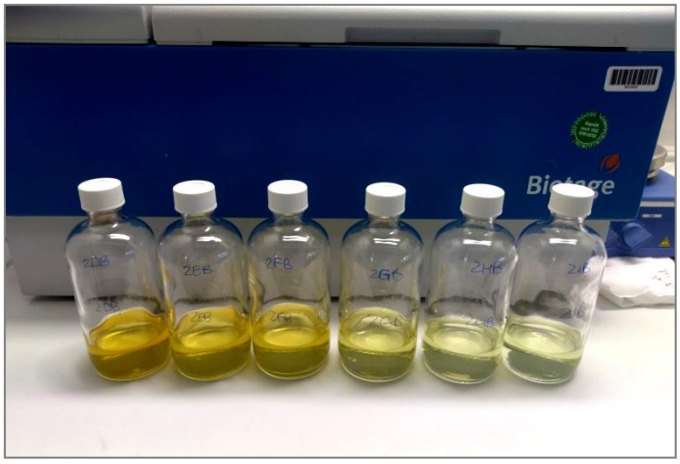

Fig. 9*: Total Liquid Extract – TLE- after organic extraction*

6.3.4.2 Fractionation

For the fractionation and purification, the dried samples were dissolved in hexane (HEX). Five fractionation were made with different solvents:

- Fraction A with hexane, HEX

for the separation of apolar compounds, polycyclic aromatics, aliphatic compounds (alkanes)

- Fraction B with hexane and dichloromethane, HEX:DCM (4:1)

for the separation of polar compounds: alcohols, aromatics, aldehydes, and ketones

- Fraction C with dichloromethane and acetone, DCM: C_3H_6O (9:1)

for the extraction of polar organic acids

- Fraction D with methanol, MeOH

for the extraction of hetero components

- Fraction E with Formic Acid in dichloromethane (2% in DCM)

for the extraction of fatty acids

Each fraction was dried with TurboVap and stored in the fridge. Only A fraction was used for the alkanes analyses, the other ones have been kept for any future studies.

6.3.5 GC-MS

For the GC-MS measurement, the apolar fraction (fraction A) containing n-alkanes was eluted using n-hexane as carrier gas and further purified using $AgNO_3$ coated silica-gel. n-Alkanes were analyzed by gas chromatography/mass spectrometry (GC/MS) using a ThermoScientific Trace GC Ultra – AS al/AS1310 - DSQII equipped with a HP-5MS SiO_2 column (30m x 0.25 nm x 0.25 mm). The GC oven was held at 70°C for 1 min, ramped at 10°C/min to 180°C (5 min hold), ramped at 3°C/min to 320°C (25 min hold). N-Alkanes were identified by comparing their retention time and mass spectrum to an external standard (n-C_7 to n-C_{40}; Supelco 49452-U1000ηg/µl, with a concentration of 25ηg/µl in (cyclo)hexane and quantified using peak areas calibrated against the corresponding standard peak (Appendix 7).

The profile of TOC and n-alkane analysis was graphically compared to investigate (Fig. 12) the carbon provision of each plant-type, hypothesizing that a high content of short-n-Alkane chains (C23-C25) are referable to a more humid environment, and, therefore, similar to a peatland ecosystem. On the contrary, an abundance of longer n-alkane chains is attributable to a drier environment, populated by more terrestrial and high plant vegetation.

7 Results

In the three soil profiles, different pattern could be observed in the amount of soil organic carbon (kg/m^2) from the surface to the deepest layers. In contrast, the percentage of TOC decreases proportionally with depth and bulk density trends show regular tendency along the depth in all three profiles (Figure 10).

Core 1 shows an irregular trend along the profile: it starts with an increase of OC content (0.31 kg/m^2) until 20 cm (2.90 kg/m^2). From 20 cm depth values stabilize roughly around value 2,9. On the other hand, %TOC has a regular downward trend from the surface (30.9%) to the deepest layer (4.5%).

Core 2 has a more regular pattern with a range between 1.4 and 2.9 kg/m^2. There is an increasing trend from the surface until 20 cm depth (2.9 kg/m^2), and a small decrease until the deeper layers (up to 1.44 kg/m^2). The percentage of TOC decreases regularly along the profile, obtaining results starting from 32.5% to 7.1% in depth.

Core 3 shows a mean content of C lower than the other two cores, with a minimum of 1.02 kg/m^2 at 15 cm depth, and a maximum of 2.2 kg/m^2 at 35 cm depth. The TOC content in this case also decreases proportionally and remains in the range between 30% and 9%, from the upper layer to the bottom.

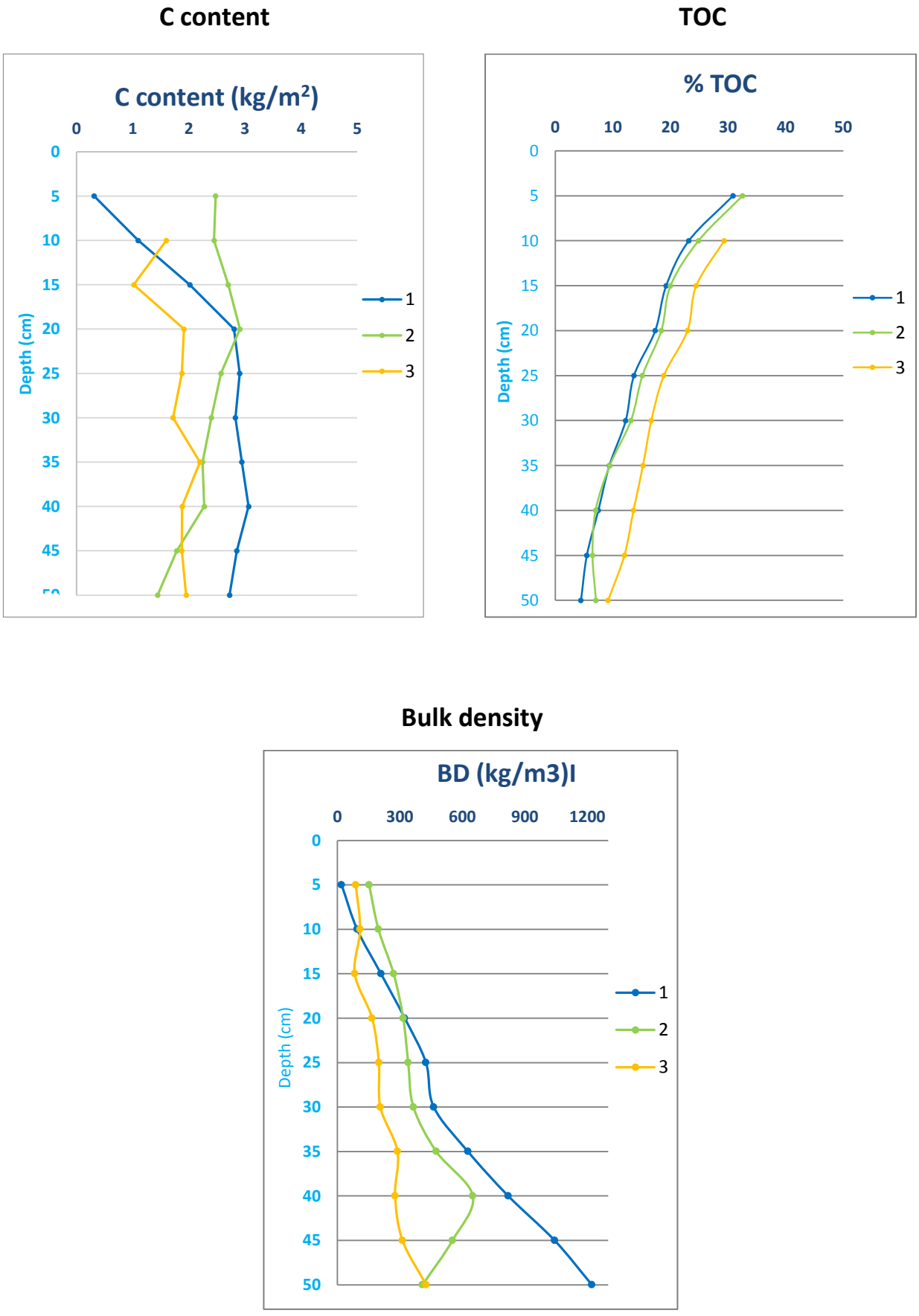

Figure 10: *Carbon content (kg/m2), Total Organic Carbon (%) and Bulk Density (kg/m3) along the depth in cores 1, 2, 3.* -TOC values come with an error of ±10%, due to linearity effects-.

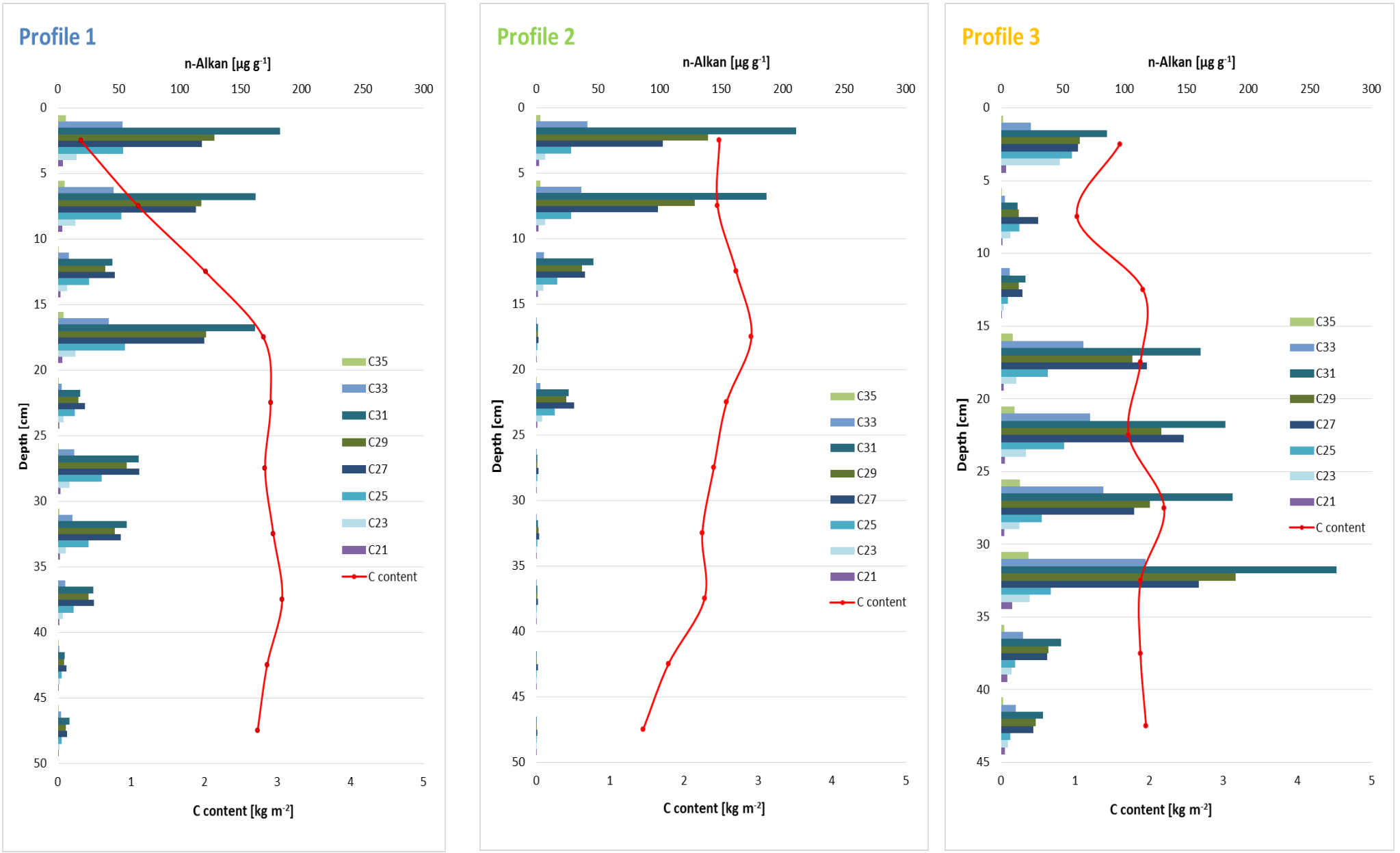

Figure 11: Comparison of C content (kg m^{-2}) and n-alkanes concentration (µg g^{-1}) in the three profiles

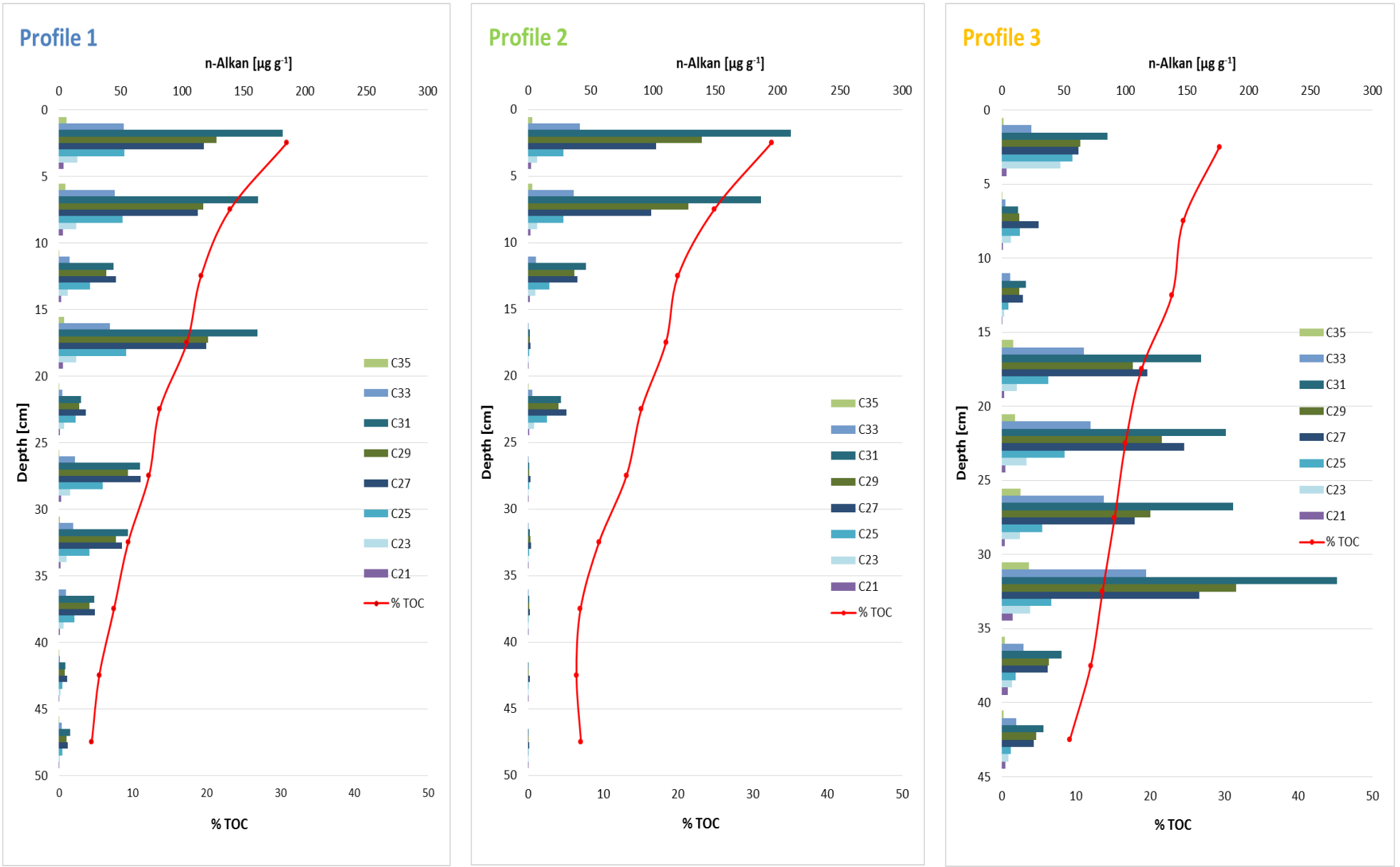

Figure 12: Comparison of TOC values(%) and n-alkanes concentration(µg g^{-1}) in the three profiles

In soil profiles 1 and 2, n-alkane concentrations are highest in the upper layers, and decrease with depth. This pattern is reflected in TOC values as well. However, core 3 display a very different pattern, with highest n-Alkanes concentration between 25 and 40 cm. OC content shows irregular patterns, as mentioned above, in line or not with the n-alkane concentration among the different study sites (Fig.11, 12).

Cores 1 and 2 show a highest concentration of n-Alkane in the first layers (<15cm), with concentrations mostly higher than 100 μg/g. As depth increases, the mean n-alkane concentration declines.

N-alkanes concentration in core 1 is significantly high in values. For the first 15 cm the most abundant n-alkane homologues are n-C27, n-C29, and n-C31, exceeded 100 μg/g. The C31 homologue for example reached a peak value of 180 μg/g. In deep layers, the quantity of n-Alkane decreases, remaining however these three chains the most preponderant. In this profile is noticeable the divergent trends between OC content and n-alkane concentration: in the upper layers there is a high concentration of n-alkane homologues, rather than a small, but increasing, content of OC at the same levels. When n-alkane concentration declines, OC content is reaching a regular trend.

In core 2, there is a high abundance of n-alkanes for the first 10 cm, especially with the carbon chains of C27, C29, and C31, with a maximum value of 210 μg/g for n-C31 homologue concentration. There is, however, a strong decrease in the concentration of n alkanes from 20 cm onwards (values of the order of just units/decimals). Both TOC and OC content trends are slowly decreasing along the depth.

Depth profile of n-alkane concentration in core 3 differs from those of cores 1 and 2, showing higher concentration of n-alkanes, with maximum values between 25 and 45 cm depth, which are surpassing 270 μg/g. In the deepest layers n-alkane concentrations is then lowering. Also for profile 3 the preponderant n-alkane homologue is the n-C31.

TOC values indicate a regular decreasing downward trend, even if n-alkane concentration is high in the middle layers. Accordingly with this concentration's pattern, OC content shows a possible linear relation with n-alkane trends.

As a result, from measurements of OC content, TOC and n-alkane concentration is it possible to detect similar patterns of TOC values, but different OC content and n-alkane concentration among the three profiles.

The diverse distributions of n-alkanes homologues through the profiles are expressed by different ratios that are choose to interpret these patterns (Fig.13, Appendix 18).

Also the ratio results illustrate the dissimilarity among the three study areas.

Paq ratio reflects the abundance of terrestrial plants (longer n-alkane chains) over the submerged vegetation (shorter n-alkane chains). It shows a mean values in a range between 0.1 and 0.5. Core 1 illustrates Paq values around 0.2 in the superficial layers and with depth values until 0.4 fluctuating between 0.2 and 0.4. Core 2 has an irregular but increasing pathway, from a low value in the superficial layer (0.1) to higher values reaching 0.6 in the deeper layer. Profile 3 starts with high values of almost 0.5, and decreasing rapidly to 0.1-0.2 with depth.

The **Pwax** ratio indicates the probably origin of waxy hydrocarbons in n-alkane homologues. It shows fluctuations between 0.7 and 0.9, with the exception of core 2, which has a decreasing trend and reaches 0.63 in the deepest layer and the superficial layer of profile 3 as well (0.63).

CPI observes the grade of degradation of organic matter, identifying the predominance of the n-alkane chains. CPI values in all samples show high values, with an average of 9. A decrease of values with the depth is perceivable mostly in the core 2, where a lower value is in the deeper zone (from 10 to 5); in the other specimens trends fluctuate between 7-10.

MT (Mosses/Tree) Ratio is chosen in order to study the distribution of short chains, which are indicative of mosses, versus long chain, which are indicative of trees. In the core analyses it shows a mean regular trend for all the samples in the middle zone, but a different situation happens for the superficial and deeper layers. Principally, in profile 2, values around 0.2 are reached in the deeper layers, unlike the average of the other cores (<0.1). Furthermore, core 3 delineates higher values in the superficial layers, reaching 0.4.

The **ACL** (fig.8) index expresses the average of the length n-alkane chains concentration. It represents a main value of 28.9 among all the profiles. Core 1 varies in a range between 28.7 and 29.2 along the whole profile. For profile 2 the trend is decreasing along the profile: superficial layers seemed to

contain longer chain compounds (max 29.4) compared to the deepest values, which show lower ACL values (27.8). Core 3 shows an irregular trend for the first 20 cm, then the fluctuation stabilizes around value 29.

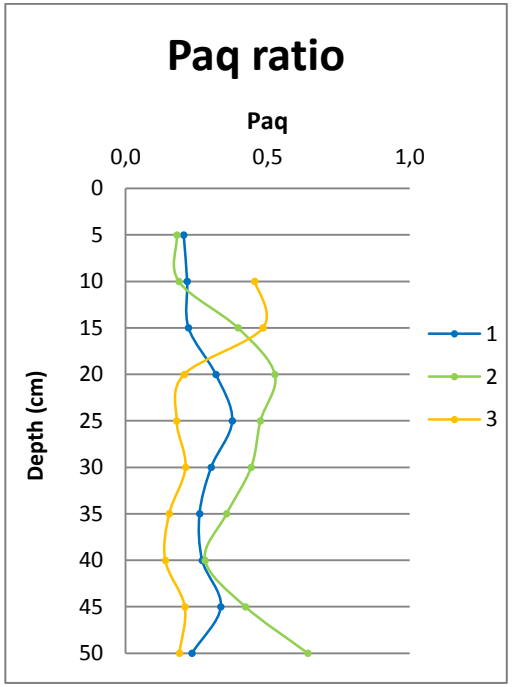

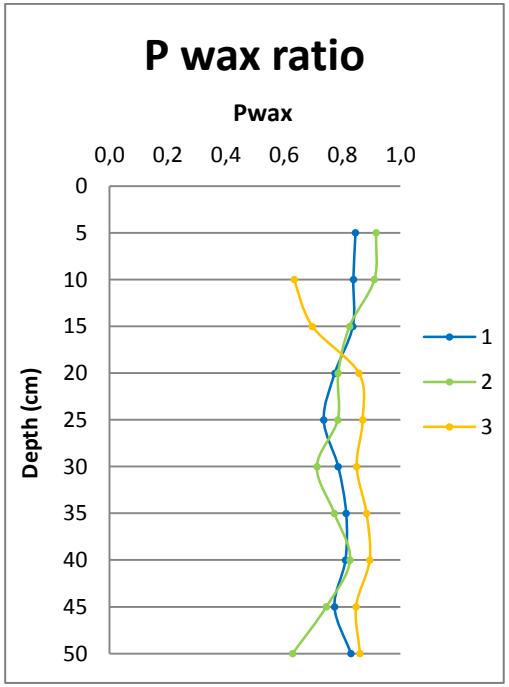

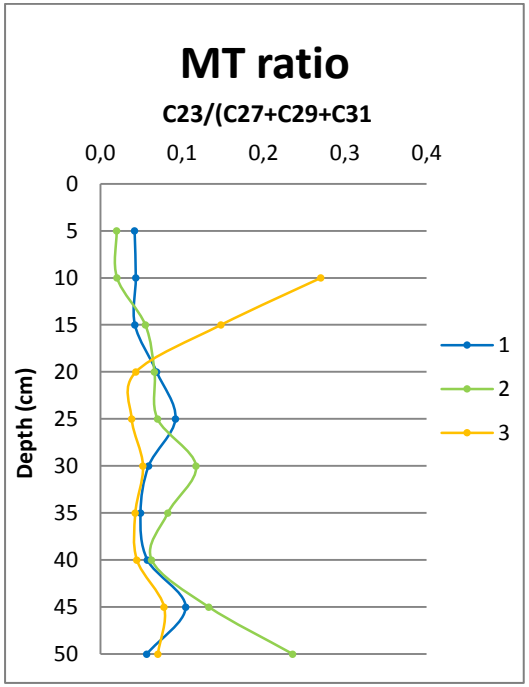

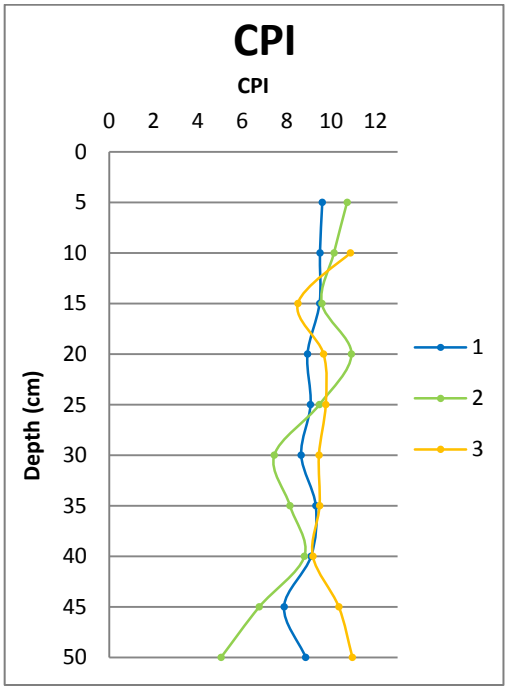

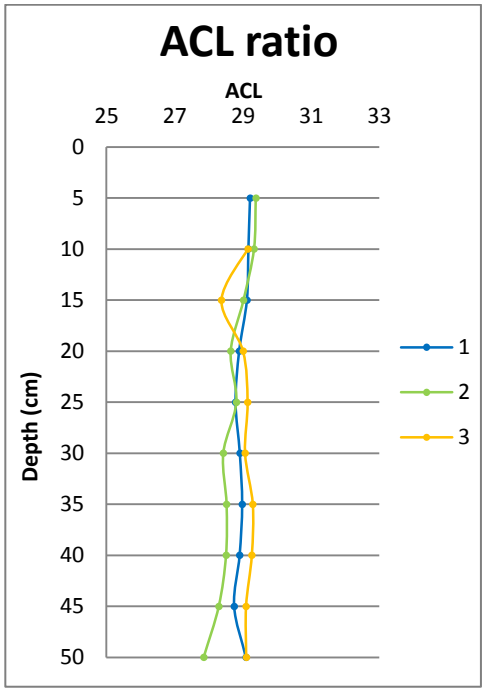

Fig 13: Ratios:
Paq, Pwax, MT,CPI ACL

8 Discussion

As it is visible from data in Fig. 11 and Fig. 12, the amount of C (kg/m^2) in the soil is generally increasing with depth, but the relative percentage of TOC decreases proportionally.

The C content trend could be related to the bulk density values, which in turn are depending mostly on soil texture and the organic matter content (Daddow et al., 1987). Generally, bulk density in the three profiles increased with depth. This may be possible due the soil compaction in the deeper layers, which caused a bulk volume reduction, and consequently, an increase of density section. Indeed, the C content trend seems to follow that one of the bulk density.

The opposite tendency of TOC may be due to the enrichment of C in the upper layers, in form of OC, derived from rest of vegetation, roots, shrubs, organisms, but with increased depth, the OC could be more decomposed or mineralized, decreasing in content.

In all the samples it is evident a relation among n-alkanes concentration and %TOC. TOC content and n-Alkanes concentration are decreasing with depth. It is appreciable that in all the samples for the first layers there is a highest concentration of n-Alkanes which is continuously decreasing. TOC decreases with depth and so does n-alkanes content. This could be plausible because n-alkanes are part of TOC.

For profiles 1 and 2, the trends are similar, but core 3 shows differences as it is visible an increase of the n-alkanes concentration around 25-40 cm depth. This divergent trend is probable due to the different environment where the profiles originate. The location of core 3 is attributable to a wet superficial environment, with mosses and high moisture content. Data of this profile show a mean concentration of OC content of 1.7 kgC/m^2 and %TOC of 18%. Cores 1 and 2 bring values of 2.35 – 2.32 kgC/m^2 and 14.3 – 15.40 %TOC respectively.

Core 3 shows also very high n-alkane concentration in the middle layers, which is completely different from patterns of profiles 1 and 2. As well as the natural high presence of n-alkane concentrations, this increase could be attributable to a high presence of roots in this profile section, or a possible contamination of the core during the sampling, due to the moist superficial layers.

In general, it could be expected that all three areas were characterized from terrestrial vegetation, interspersed by spot with a moister environment.

P_{aq} describes the relative abundance of short (C23 and C25) and long (C27 – C31) n-alkane chains. It is typically used as indicator of lacustrine versus terrestrial condition and indicates the different categories of vegetation in a particular area. In this study it may possible to applicate it for expressing higher plants (trees, grasses, shrubs) versus mosses (Sphagnum) presence.
While looking at core 1, the range of values (0.2-0.4) is more representative of higher plants. Core 2 shows values which conduct drier situation (terrestrial vegetation), reaching high values (0.65), and indicating a moister environment. Profile 3 shows an interesting tendency, starting with high values, and lowering abruptly to a 0.2-0.1 range. This trend could be explained by the environmental conditions in which the core was levied from a semi-swamp area with mosses underneath trees in forest. The superficial zone of mosses, peat and organic matter may have contaminated the subsequent layers with a large amount of C23 n-Alkane chain, or in the past, a sudden change in vegetation may have occurred, from dry period to wet conditions.

P_{wax} shows the relative contribution of waxy hydrocarbons from emerged macrophytes and terrestrial plants to the total hydrocarbons. P_{wax} is an index which compares the proportions of long-chain n- alkanes (n-C27+n-C29 +n-C31) to the sum of short and long chain n-alkanes (n-C23+ n-C25+ n-C27+ n-C29+ n-C31) (Ronkainen, 2015). It aims to show the relative proportion of waxy hydrocarbons over the total proportion of hydrocarbons. High P_{wax} ratio suggests a strong input from vascular plants and dry conditions, while low P_{wax} values indicate Sphagnum domination and wetter conditions (Andersson et al., 2011; Ronkainen, 2015; Zheng et al. 2007). In this case, high values of P_{wax}, indicate a relatively dry environment, but the peak of lower rates in according with the results of the other ratios, show moister conditions in the deeper layers of core 2 and in the first layer of core 3.

MT (Mosses/Trees) ratio indicates relative contribution of n-C23 alkane chain over long chains. Long chain n-Alkanes (C27, C29, and C31) maximize their abundance in woody and terrestrial species; in fact, these chains are related to vascular plant waxes. In particular, low values indicate a strong input of vascular plants over Sphagnum species. Relative low values are discovered in the middle layers with modest changes in the extreme parts of the profiles. Most noteworthy the value of core 2 increases more than in the other profiles, and core 3 shows higher values in the

upper layers, with a decrease in the deeper ones. This is justifiable from the study site of profile 3, in which there were present mosses on the surfaces layers.

CPI shows a strong odd-to-even carbon number predominance that could mean that these lipid chains come from the terrestrial plant, particularly from cuticular waxes. The general high values that are slowly decreasing among the profile may represent a less decomposed organic matter source. Contrary, the deeper layers of profile 2 decreased in values to around 6 or 5, indicating a more decomposed source of organic material.

To summarize a CPI value holds significance. Many factors influence it during times of microbial reworking and diagenesis, which are contingent on different rates of degradation and alteration under different climatic conditions on. For example, under a cold, dry climate, microbial degradation and diagenesis of organic matter are slowed, and may preserve a high CPI value, and consecutively a conservation of the organic matter too (Xie et al. 2007; Zhou, et al.,2005). In contrast, in a warm, wet climate, the microbial degradation and diagenesis accelerate and may result in lower CPI values (Zhou, et al., 2005).

It is notable how P_{aq} and CPI of sample 2 have an opposite tendency, representing a notable situation: the first layers, expressed with low P_{aq} values and high CPI values, indicating a drier situation rather than one in the deeper zone ones, which suggest that there were more humid conditions.

From the **ACL** results, it is possible to predict the average of the n-alkane chain along the profiles. In general, the average holds high values around 29, with differentiation in some points of the sundry profile depths, such as from 30cm onwards in core 2 (>28.5) and at 15 cm depth in core 3. Despite these small fluctuations, the ACL present data that are traceable to areas with a predominantly terrestrial type of vegetation with typical higher plants n-alkane chains, rather than shorter n-Alkane chains, attributable to a more humid and aquatic environment.

ACL doesn't show much variation between the three soil profiles, which is to be expected as they derive from spatially nearby locations.

9 Conclusions

Carbon quantification analysis revealed high organic carbon (OC) concentration and content in the soil, confirming findings from a previous study. The relationship observed between OC content and the lipid n-alkane distributions suggests a high concentration of both OC and long carbon chains. Notably, n-C31 homologue is detected as the most abundant lipid chain in all three profiles, which usually maximizes its concentration in terrestrial plants, such as trees and woody species. Therefore, these data allow us to suppose the dominance of forest vegetation in this area over time.

N-alkane distributions and ratios provide important information on the separation between vegetation types, but are not conclusive. In particular, the use of the P_{aq} ratio in these analyses did not provide answers on the types of ecosystems in the area, but gives information regarding the precise location and time where cores were withdrawn. In fact, this index does not tell whether or not there was a peat environment. That is expected from the higher P_{aq} value in upper layers of profile 3, where mosses are growing underneath trees within the forest at the study site. Consequently, it is possible to reach quite high P_{aq} values in upper layers, even if the surface is dominated by forest. Therefore, from the analyses, this proxy should not be used to determine forest versus peatland conditions at the study sites.

A better indicator for monitoring the presence of mosses in a specific area could be n-C23 homologues, in which n- are being produced predominately by *Sphagnum* species. This is the MT ratio, which discriminates the presence of mosses (no vascular plants) and terrestrial vegetation (vascular plants) in a specific spot. This, in fact, is confirmed exactly from the situation existent in study site 3. Here, the first soil layer is dominated by *Sphagnum* mosses, and the results illustrate higher ratio values rather the other sampling sites, where the first layers are characterized mostly by topsoil, roots and humus, and their ratio values stay lower. Remembering that high value of MT ratio indicate a predominance of n-C23 homologues, and consequently, the presence of mosses (wetter environment).

Furthermore, it is possible to observe that there is a high heterogeneity in the area. In fact, it can be detected that despite the proximity of the sampling sites, there are different trends both in the n-alkane homologues distributions, and also in terms of OC content, and consequently, of n-alkanes concentration. This opens the possibility for future studies relating, for example, to the

heterogeneity of an ecosystem or to the n-alkane homologue distributions of the current floristic vegetation in the area.

10 Comments

The study site forest can be considered a symbol of conservation and protection of biodiversity on Chiloé's Island. Without human influence, the forest thrived as soil and growing conditions were left to natural processes, but nowadays they are disappearing due to deforestation and detrimental human influences. Deforestation occurs for wood extraction, the creation of pastures and agricultural land, the creation of peatlands, and development of Sphagnum cultivation land which is high in commercial demand.

All these disturbances could have dire repercussions for the forest's biodiversity, but also for the global carbon cycle. In fact, further disruption is likely to cause a long-term disequilibrium in the global carbon cycle.

For these reasons, this island's vegetation must be conserved and protected. Fortunately, protections are already mandated in some areas, sites for this study for example. And thanks to the activity of the staff of *Senda Darwin Biological Station*, who is taking actions to preserve, reconstruct research and monitor human influence effects are being slowed. Additionally, they are educating the people, with guides, lectures, meetings at schools, universities, and privates institutes to bring awareness to their cause of conservation and preservation of this ecosystem.

It is essential to give the land back to inhabitants who wish to use its resources sustainably and not cause irreversible damage with intentions of preserving its long term well being. Younger generations will depend on it for years to come and it is crucial that the carbon cycle is maintained and systems are not unbalanced by detrimental human influences.

11 References

Aerts, R., D. F. Whigham, D. F., & Verhoeven, J. T. A. (1999). *Plant-Mediated Controls on Nutrient Cycling in Temperate Fens and Bogs. Ecology*, 80(7), 2170–2181.

Andersson, R. A., Kuhry, P., Meyers, P., Zebühr, Y., Crill, P., & Mörth, M. (2011). *Impacts of paleohydrological changes on n-alkane biomarker compositions of a Holocene peat sequence in the eastern European Russian Arctic. Organic Geochemistry*. 42(9), 1065–1075.

Aravena, J. C., Carmona, M. R., Pérez, C. A., & Armesto, J. J. (2002). *Changes in tree species richness, stand structure and soil properties in a successional chronosequence in northern Chiloé Island, Chile*. Revista Chilena de Historia Natural, 75(2), 339–360.

Ardenghi, N., Mulch, A., Pross, J., & Maria Niedermeyer, E. (2017). *Leaf wax n-alkane extraction: An optimised procedure*. Organic Geochemistry, 113, 283–292.

Baas, M., Pancost, R., Geel, B. Van, & Damste, J. S. S. (2000). *A comparative study of lipids in Sphagnum species*. Organic Chemestry, 31, 535–541.

Baker, A., Routh, J., & Roychoudhury, A. N. (2016). *Biomarker records of palaeoenvironmental variations in subtropical Southern Africa since the late Pleistocene* : *Evidences from a coastal peatland*, 451, 1–12.

Bingham, E. M., McClymont, E. L., Väliranta, M., Mauquoy, D., Roberts, Z., Chambers, F. M., & Evershed, R. P. (2010). *Conservative composition of n-alkane biomarkers in Sphagnum species: Implications for palaeoclimate reconstruction in ombrotrophic peat bogs*. Organic Geochemistry, 41(2), 214–220.

Bonan, G. B. (2008). *Forests and Climate Change : Forcings, Feebacks, and the Climate Benefits of Forests*. Science, 320(June), 1444–1450.

Bush, R. T., & McInerney, F. A. (2013). *Leaf wax n-alkane distributions in and across modern plants: Implications for paleoecology and chemotaxonomy.* Geochimica et Cosmochimica Acta, 117, 161–179.

Cabezas, J., Galleguillos, M., Valdés, A., Fuentes, J. P., Pérez, C., & Perez-Quezada, J. F. (2015). *Evaluation of impacts of management in an anthropogenic peatland using field and remote sensing data*. Ecosphere, 6(December), 1–24.

Canadell, J., Jackson, R. ., Ehleringer, J. R., Mooney, H. A., Sala, O. E., & Schulze, E. D. (1996). *Maximum rooting depth of vegetation types at the global scale.* Oecologia, 108, 583–584.

Carmona, M. R., Aravena, J. C., Bustamante-sánchez, M. A., Celis-Diez, J. L., Charrier, A., Díaz, I. A., & Armesto, J. J. (2010). *Estación Biológica Senda Darwin: Investigación ecológica de largo plazo en la interfase ciencia-sociedad*. Revista Chilena de Historia Natural, 83(1), 113–142.

Castañeda, I. S., & Schouten, S. (2011). *A review of molecular organic proxies for examining modern and ancient lacustrine environments*. Quaternary Science Reviews, 30(21–22), 2851–2891.

Castanha, C., & Trumbore, S. E. (2008). *Methods of Separating Soil Carbon Pools Affect the Chemistry and Turnover Time of Isolated Fractions*ì.

Centre for Sustainability and the Global Environment, Nelson Institute, University of Wisconsin-Madison. http://nelson.wisc.edu/sage/index.php

Clymo, R. S. (1984). *The Limits to Peat Bog Growth*. Philosophical Transactions of the Royal Society of London. Series B. Biological Sciences, 303(1117), 605–654.

Clymo, R. S., & Hayward, P. M. (1998). *The ecology of Spagnum. Sphagnum, the peatland carbon economy, and climate change*. British Bryological Society, 361–368.

Daddow L. & Warringto G.E. (1987): *Growth limiting soil bulk densities as influenced by soil texture*. Watershed systems development group, USDA Forest Service , Colorado.

Díaz, M. F., Bigelow, S., & Armesto, J. J. (2007). *Alteration of the hydrologic cycle due to forest clearing and its consequences for rainforest succession*. Forest Ecology and Management, 244(1–3), 32–40.

Díaz, M. F., Larraín, J., Zegers, G., & Tapia, C. (2008). *Caracterización florística e hidrológica de turberas de la Isla Grande de Chiloé, Chile*. Revista Chilena de Historia Natural, 81(4), 455–468.

Díaz, M. F., Tapia, C., Jiménez, P., & Bacigalupe, L. (2012). *Sphagnum magellanicum growth and productivity in Chilean anthropogenic peatlands*. Revista Chilena de Historia Natural, 85(4), 513–518.

Dixon RK, Brown S, Houghton RA, Solomon AM, Trexler MC,& Wisniewski J. (1994). *Carbon Pools and Flux of Global Forest Ecosystems*. Science 263.

Eglinton, G., & Hamilton, R. J. (1967*). Leaf Epicuticular Waxes*. Science, 156(3780), 1322–1335.

Eglinton, T. I., & Eglinton, G. (2008). *Molecular proxies for paleoclimatology.* Earth and Planetary Science Letters, 275(1–2), 1–16.

Falkowski, P., Scholes, R. J., Boyle, E., Canadell, J., Canfield, D., Elser, J., & Steffen, W. (2000). *The global carbon cycle: A test of our knowledge of Earth as a system*. Science's Compass, 290(5490), 291–296.

Ficken, K. J., Barber, K. E., & Eglinton, G. (1998). *Lipid biomarker , d 13 C and plant macrofossil stratigraphy of a Scottish montane peat bog over the last two millennia*, 28(3).

Ficken, K. J., Li, B., Swain, D. L., & Eglinton, G. (2000b). *An n -alkane proxy for the sedimentary input of submerged /Floating freshwater aquatic macrophytes*. Organic Geochemistry, 31, 745–749.

Freeman, C., Ostle, N., & Kang, H. (2001). *An enzymic "latch" on a global carbon store*. Nature, 409(6817), 149.

Gamarra, B., & Kahmen, A. (2015). *Concentrations and δ2H values of cuticular n-alkanes vary significantly among plant organs, species and habitats in grasses from an alpine and a temperate European grassland*. Oecologia, 178(4), 981–998.

Gerold, J. (1995). *The Growth Dynamics of Sphagnum Based on Field Measurements in a Temperate Bog and on Laboratory Cultures Author*. Journal of Ecology, 83(3), 431–437.

Gocke, M., Kuzyakov, Y., & Wiesenberg, G. L. B. (2013). *Differentiation of plant derived organic matter in soil , loess and rhizoliths based on n -alkane molecular proxies*. Biogeochemistry, 112, 23–40.

Gocke, M., Peth, S., & Wiesenberg, G. L. B. (2014). *Catena Lateral and depth variation of loess organic matter overprint related to rhizoliths — Revealed by lipid molecular proxies and X-ray tomography*. Catena, 112, 72–85

Gorte, R. W. (2009). *Carbon Sequestration in Forests*. Congressional Research Service, 4, 2–37.

Guifang, Y., Shucheng, X. I. E., Junhua, H., & Zhongyuan, C. (2008). *Microbial Characteristics and Vegetation Changes as Recorded in Lipid Biomarker of Tianmushan Peat Bog*. 15(4).

Gunnarsson, U., Granberg, G., & Nilsson, M. (2004). *Growth, production and interspecific competition in Sphagnum: Effects of temperature, nitrogen and sulphur treatments on a boreal mire*. New Phytologist, 163(2), 349–359.

Hautevelle, Y., Michels, R., Malartre, F., & Trouiller, A. (2006). *Vascular plant biomarkers as proxies for palaeoflora and palaeoclimatic changes at the Dogger/Malm transition of the Paris Basin (France*). Organic Geochemistry, 37(5), 610–625

Houghton RA, Goetz SJ, 2008: *New satellites help quantify carbon sources and sinks*, Eos Trans. AGU, 89(43), 417 – 418.

Huang X, Wang C., Zhang J., Wiesenberg L.B.G., Zhang Z., Xie S., (2011): *Comparison of free lipid compositions between roots and leaves of plants in the Dajiuhu Peatland, central China*. Geochemical Journal, 45(2010), 365–373.

Huguet, A., Wiesenberg, G. L. B., Gocke, M., Fosse, C., & Derenne, S. (2012). *Branched tetraether membrane lipids associated with rhizoliths in loess: Rhizomicrobial overprinting of initial biomarker record*. Organic Geochemistry, 43, 12–19.

IGBP-DIS: International Geosphere-Biosphere Programme, Data Information Service

IPCC report : https://www.ipcc.ch/ipccreports/tar/wg1/099.htm

IPCC. (2000). Land use, land-use change, and forestry. Cambridge University Press.

Iturraspe, R., & Roig, C. (2000). *Aspectos hidrológicos de turberas de Sphagnum de Tierra del Fuego-Argentina.* ResearchGate, 1(January), 85–93.

Jansen M., Martelanc M., Vovk, I., & Simonovska, B.(2006). *Determination of three major triterpenoids in epicuticular wax of cabbage (Brassica oleracea L.) by high-performance liquid chromatography with UV and mass spectrometric detection*. 1164, 145–152.

Jansen, B., & Wiesenberg, G. L. B. (2017). *Opportunities and limitations related to the application of plant-derived lipid molecular proxies in soil science*. Soil, 3(4), 211–234.

John McMurry (2008): *Organic Chemistry*, 7° ed., Cornell University.

Joosen, H., & Clarke, D. (2002). *Wise use of mires and peatlands- Background and priciples including framework for decision makin*. Saarijärvi, Finland: International Mire Conservation Group and International Peat Society.

Kahmen, A., Schefuß, E., & Sachse, D. (2013). *Leaf water deuter ium enrichment shapes leaf wax n - alkane d D values of angiosperm* plants I : Experimental evidence and mechanistic insights. Geochimica et Cosmochimica Acta, 111, 39–49.

Killops S. and Killops V (2008*). Introduction to organic geochemistry*. 2nd edition. Blackwell Ltd.

Klemm, D., Heublein, B., Fink, H., & Bohn, A. (2005). *Cellulose : Fascinating Biopolymer and Sustainable Raw Material*. Polymer Science, 44, 3358–3393.

Krull ES, Skjemstad JO (2003): d13C and d15N profiles in 14C-dated Oxisol and Vertisols as a function of soil chemistry and mineralogy, Geoderma 122(1):1-29.

Kuhn, T. K., Krull, E. S., Bowater, A., Grice, K., & Gleixner, G. (2010). *The occurrence of short chain n - alkanes with an even over odd predominance in higher plants and soils*. Organic Geochemistry, 41(2), 88–95.

Lal, R. (2005). *Forest soils and carbon sequestration*. Forest Ecology and Management, 220, 242–258.

Lavrieux, M., Bréheret, J., Disnar, J., & Jacob, J. (2012*). Organic Geochemistry Preservation of an ancient grassland biomarker signature in a forest soil from the French Massif Central*. Organic Geochemestry, 51, 1–10.

Li, Y., Yang, S., Wang, X., Hu, J., Cui, L., Huang, X., & Jiang, W. (2016). *Leaf wax n-alkane distributions in Chinese loess since the Last Glacial Maximum and implications for paleoclimate*. Quaternary International, 399, 190–197.

Loisel, J., & Garneau, M. (2010). *Late Holocene paleoecohydrology and carbon accumulation estimates from two boreal peat bogs in eastern Canada: Potential and limits of multi-proxy archive*s. Palaeogeography, Palaeoclimatology, Palaeoecology, 291(3–4), 493–533.

Maffei, M. (1996*). Chemotaxonomic significance of leaf wax n-alkanes in the umbelliferae, cruciferae and leguminosae (subf. Papilionoideae)*. Biochemical Systematics and Ecology, 24(6), 531–545.

Malhi, Y., Baldocchi, D. D., & Jarvis, P. G. (1999). *The carbon balance of tropical, temperate and boreal forests.* Plant, Cell and Environment, 22, 715–740.

Nichols, J. E., Booth, R. K., Jackson, S. T., Pendall, E. G., & Huang, Y. (2006). *Paleohydrologic reconstruction based on n -alkane distributions in ombrotrophic peat*, 37, 1505–1513.

Nichols, J., Booth, R. K., Jackson, S. T., Pendall, E. G., & Huang, Y. (2010). *Differential hydrogen isotopic ratios of Sphagnum and vascular plant biomarkers in ombrotrophic peatlands as a quantitative proxy for precipitation/evaporation balance*. Geochimica et Cosmochimica Acta, 74(4), 1407–1416.

Niedermeyer, E. M., Forrest, M., Beckmann, B., Sessions, A. L., Mulch, A., & Schefuß, E. (2016). *The stable hydrogen isotopic composition of sedimentary plant waxes as quantitative proxy for rainfall in the West African Sahel*. Geochimica et Cosmochimica Acta, 184, 55–70.

Nierop, K. G. J., Naafs, D. F. W., & Bergen, P. F. Van. (2005). *Origin, occurrence and fate of extractable lipids in Dutch coastal dune soils along a pH gradient.* Organic Geochemestry, 36, 555–566.

Pan, Y., Birdsey, R. A., Fang, J., Houghton, R., Kauppi, P. E., Kurz, W. A., … Hayes, D. (2011). *A Large and Persistent Carbon Sink in the World's Forests*. Science, 333(6045), 988–993.

Pancost, R. D., Baas, M., & Geel, B. Van. (2002). *Biomarkers as proxies for plant inputs to peats : an example from a sub-boreal ombrotrophic bog*. Organic Chemestry, 33, 675–690.

Parish, F., Sirin, A., Charman, D., Joosten, H., Minayeva, T., Silvius, M., & Stringer, L. (2008). *Assessment on Peatlands, Biodiversity and Climate Change: Main Report*. Wageningen, Nederlands: Global Environment Centre, Kuala Lumpur & Wetlands International,.

Paul EA, Follett RF, Leavitt SW, Halvorson A, Peterson GA, Lyon DJ (1997) *Radiocarbon dating for determination of soil organic matter pool sizes and dynamics*. Soil Sci Soc Am J 61:1058–1067).

Perez, C. A., Armesto, J. J., Torrealba, C., & Carmona, M. R. (2003). *Litterfall dynamics and nitrogen use ef ciency in two evergreen temperate rainforests of southern Chile*. Austral Ecology, 28(6), 591–600.

Perez-Quezada F, Pérez CA, Brito CE, Fuentes JP, Gaxiola A: *Carbon, nitrogen and phosphorous pools in a temperate rainforest in northern Patagonia.* Unpublished data.

Price, J. (1996). *Hydrology and microclimate of a partly restored cutover bog, Quebec*. Hydrological Processes, 10(10), 1263–1272.

Rao, Z., Zhu, Z., Wang, S., Jia, G., Qiang, M., & Wu, Y. (2009). *CPI values of terrestrial higher plant-derived long-chain n-alkanes: A potential paleoclimatic proxy. Frontiers of Earth Science in China,* 3(3), 266–272.

Rao, Z., Zhu, Z., Wang, S., Jia, G., Qiang, M., & Wu, Y. (2009). *CPI values of terrestrial higher plant-derived long-chain n-alkanes: A potential paleoclimatic proxy. Frontiers of Earth Science in China*, 3(3), 266–272.

Rasse, D. P., Rumpel, C., & Dignac, M. (2005). *Is soil carbon mostly root carbon? Mechanisms for a specific stabilisation.* Plant and Soil, 269, 341–356.

Rattan L, Lorenz K, 2012: *Carbon Sequestration in Temperate Forests. Recarbonization of the Biosphere:* Ecosystems 187and the Global Carbon Cycle, Ch. 9.

Rethemeyer, J., Kramer, C., Gleixner, G., John, B., Yamashita, T., Flessa, H., Grootes, P. M. (2005). *Transformation of organic matter in agricultural soils: Radiocarbon concentration versus soil depth.* Geoderma, 128(1–2), 94–105.

Rochefort, L. (2000). *Invited essay: New Frontiers in Bryology and Lichenology Sphagnum—A Keystone Genus in Habitat Restoration*. The Bryologist, 103(3), 503–508.

Ronkainen, T. (2015). *Plant Biomarkers As a Proxy To Study Highly Decomposed Fen Peat*. Helsinki: Hansaprint Helsinki.

Rumpel, C., & Kögel-Knabner, I. (2011). *Deep soil organic matter-a key but poorly understood component of terrestrial C cycle*. Plant and Soil, 338(1), 143–158.

Sachse, D., Radke, J., & Gleixner, G. (2006). *dD values of individual n -alkanes from terrestrial plants along a climatic gradient – Implications for the sedimentary biomarker record*. Organic Geochemistry, 37, 469–483.

Saliot, A., Tronczynski, J., Scribe, P., & Letolle, R. (1988*). The application of isotopic and biogeochemical markers to the study of the biochemistry of organic matter in a macrotidal estuary, the Loire, France. Estuarine*. Coastal and Shelf Science, 27(6), 645–669.

Scharpenseel HW, Becker-Heidmann P (1989). *Shifts in 14C patterns of soil profiles due to bomb carbon, including effects of morphogenetic and trubation proces*ses. Radiocarbon 31:627–636

Schulze, E. D., Mooney, H. A., Sala, O. E., Buchman, N., Jobbagy, E., Bauer, G., Ehleringer, J. R. (1996). *Rooting depth, water availability , and vegetation cover along an aridity gradient in Patagonia*. Oecologia, 108, 503–511.

Sriamornsak, P. (2003). *Chemistry of Pectin and Its Pharmaceutical Uses : A Review. ResearchGate*, (January 2003).

Tarasov, P. E., Müller, S., Zech, M., Andreeva, D., Diekmann, B., & Leipe, C. (2013). *Last glacial vegetation reconstructions in the extreme-continental eastern Asia: Potentials of pollen and n-alkane biomarker analyses*. Quaternary International, 290–291, 253–263.

Tissot, B. P. and Welte, D. H.: *Petroleum Formation and Occurrence*, 2nd Edn., Springer-Verlag, Berlin, Germany, 1984.

Tolonen, K., Vasander, H., Damman, A. W. H., & Clymo, C. R. . (1992). *Preliminary estimate of long term carbon accumulation and loss in 25 boreal peatlands. Helsinki*.

Trumbore, S. E., & Zheng, S. (1996). *Comparison of fractionation methods for soil organic matter 14C analysis.* Radiocarbon, 38(2), 219–229.

Trumbore, S.E., Druffel, E.R. (1995). *Carbon isotopes for characterizing sources and turnover of nonliving organic matter*. In: Zepp, R.G., Sonntag, C. (Eds.), The Role of Nonliving Organic Matter in the Earth's Carbon Cycle. John Wiley & Sons, Chichester, England, pp. 7–22

University of New Hampshire. (2014). *An introduction to the Global Carbon Cycle*. GLOBE Carbon Cycle, 12.

University of New Hampshire: Balancing the Global Carbon Budget. Annu. Rev. Earth Planet. Sci 007.35:313-347, Carbon Budjet Project 2009

Ussiri, D. A. N., & Lal, R. (2017). *Carbon Sequestration for Climate Change Mitigation and Adaptation*. Springer International Publishing.

Vikki Tropical Resource Institute (VITRI), University of Helsinki

Villagran C., (1988): *Expansion of Magelianic Moorland during the Late Pleistocene*: Palynological Evidence from Northern lsla de Chiloé, Chile, Quaternary Research 30, 30, 314.

Villagran C, 1990: *Glacial climates and their effects on the history of the vegetation of Chile: A synthesis based on palynological evidence from Isla de Chiloe*'. Review of Palaeobotany and Palynology 65: 17-24 .

Villagran C, Hinojosa LF, 1997: *Historia de los bosques del sur de Sudamérica, II: Análisis fitogeográfico*. Revista Chilena de Historia Natural, 70:241-267.

Villagran, C. (1985). *Análisis palinológico de los cambios vegetacionales durante el Tardiglacial y Postglacial en Chiloé , Chile*. 57–69.

Xie, S., Nott, C. J., Avsejs, L. A., Volders, F., Maddy, D., Chambers, F. M. & Evershed, R. P. (2000). *Palaeoclimate records in compound-speci ® c D values of a lipid biomarker in ombrotrophic pea*t, 31, 1053–1057.

Yapo, B. M. (2011). *Pectic substances : From simple pectic polysaccharides to complex pectins — A new hypothetical model*. Carbohydrate Polymers, 86(2), 373–385.

Zegers, G., Larraín, J., Díaz, M. F., & Armesto, J. (2006). *Impacto ecológico y social de la explotación de pomponales y turberas de Sphagnum en la Isla Grande de Chiloé. Revista Ambiente y Desarrollo de CIPMA*, 22(1), 28–34.

Zheng, Y., Zhou, W., Meyers, P. A., & Xie, S. (2007). *Lipid biomarkers in the Zoigê-Hongyuan peat deposit: Indicators of Holocene climate changes in West China*. Organic Geochemistry, 38(11), 1927–1940.

Zheng, Y., Zhou, W., Xie, S., & Yu, X. (2009). *A comparative study of n-alkane biomarker and pollen records: An example from southern China*. Chinese Science Bulletin, 54(6), 1065–1072.

Zhou, W., Xie, S., Meyers, P. A., & Zheng, Y. (2005). *Reconstruction of late glacial and Holocene climate evolution in southern China from geolipids and pollen in the Dingnan peat sequence*. Organic Geochemistry, 36(9), 1272–1284.

Zoli C.: *Report applicativo analisi di laboratorio TOC*, Hach Lange, United for Water Quality, Lab L.A.V. s.r.

12 Acknowledgments

At the end of this path I think it is important and essential to thank the people who have allowed me to reach this awaited goal.

I am infinitely grateful to my parents for the support, love, patience and energy that they have dedicated to me.

I thank Professor Pitacco for the availability and patience, and for following me and supporting me also from far away in all these months.

I thank Professor Malagoli for the help and assistance given to me for my internship experience in Santiago de Chile.

I would like to thank Professor Perez, who has been patient and available for the whole period abroad and during the whole process of drafting and correcting my thesis.

I thank Dr. Niedermeyer for having welcomed me in her research team in Frankfurt and for having followed and supported me during the realization of the laboratory analysis and during the correction of the thesis work.

I thank the guys of LECS in Chile, in the Senckenberg Institute team, all my classmates and all the people who have been close to me and who have shared with me this year full of beautiful and fundamental experiences for my work and personal growth.

13 Appendices

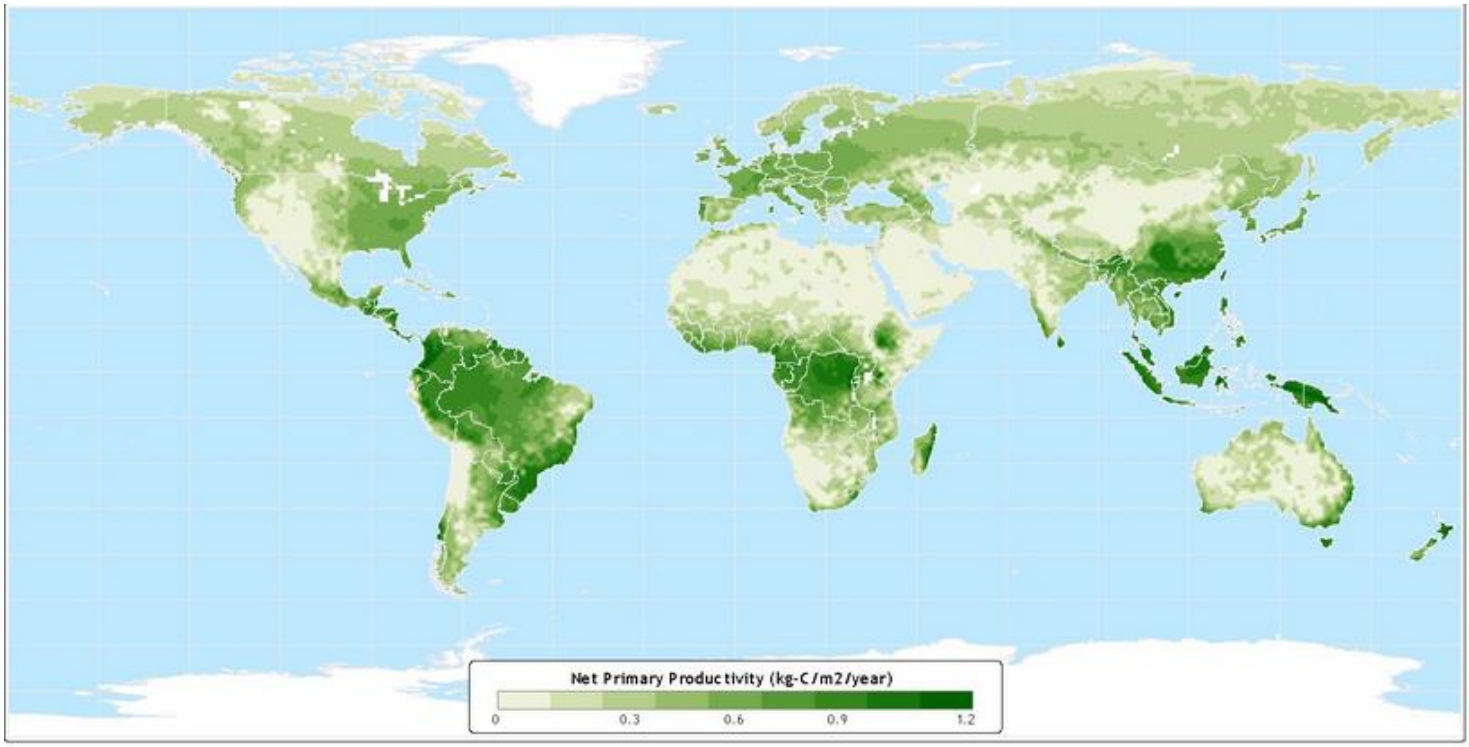

Data taken from: IBIS Simulation
(Kucharik, et al. 2000)
(Foley, et al. 1996)

Atlas of the Biosphere
Center for Sustainability and the Global Environment
University of Wisconsin - Madison

Appendix 1: *Net Primary Productivity: Global (above) and of South America (below)*

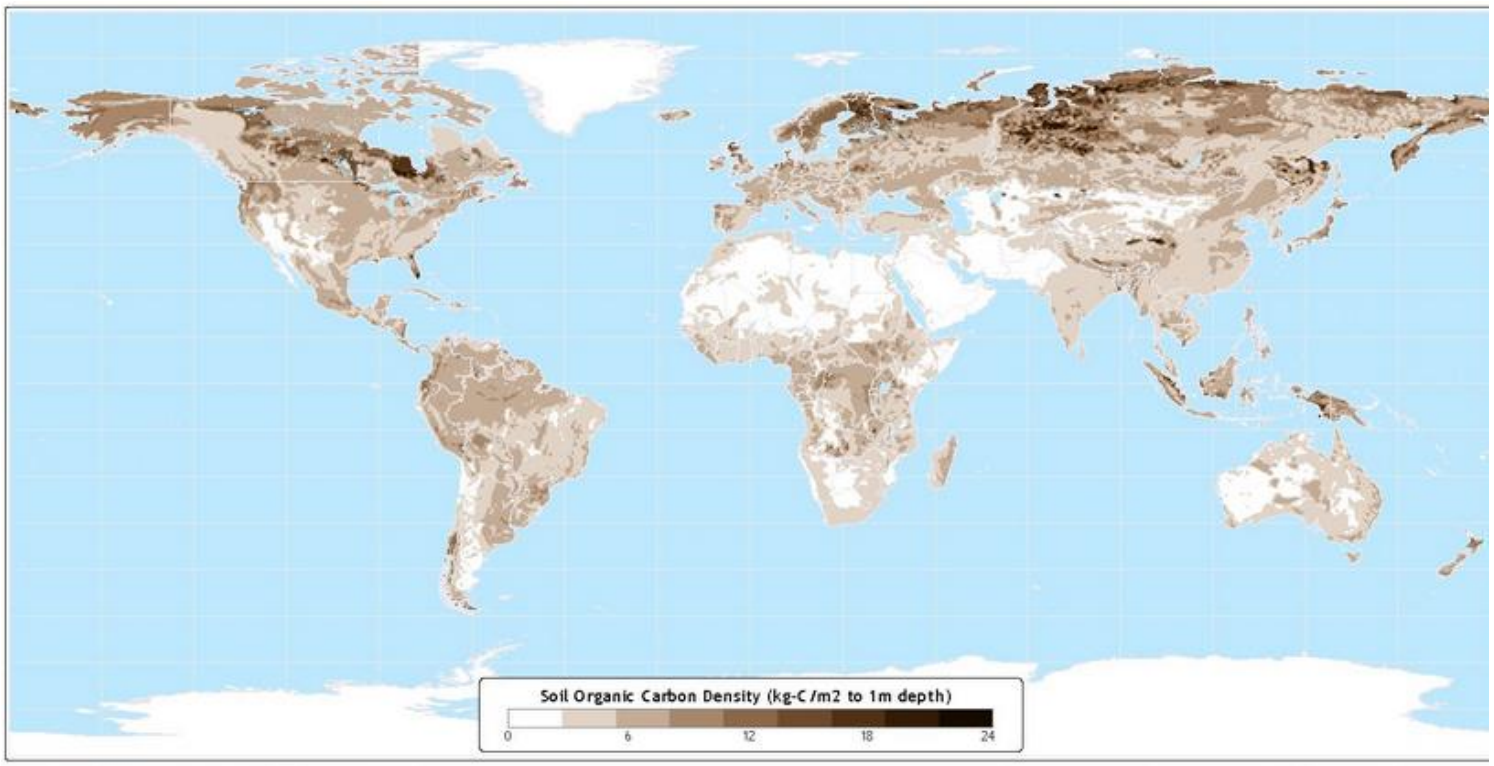

Data taken from: IGBP-DIS Global Soils Dataset (1998)

Atlas of the Biosphere

Center for Sustainability and the Global Environment
University of Wisconsin - Madison

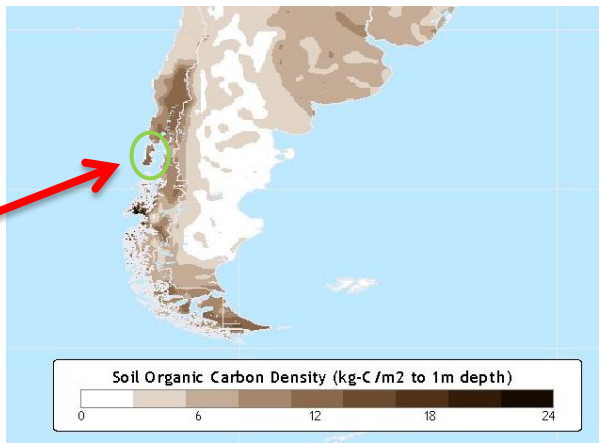

Appendix 2: *Soil Organic Carbon: Global (above) and of South America and* ***Chiloè Island*** *(below)*

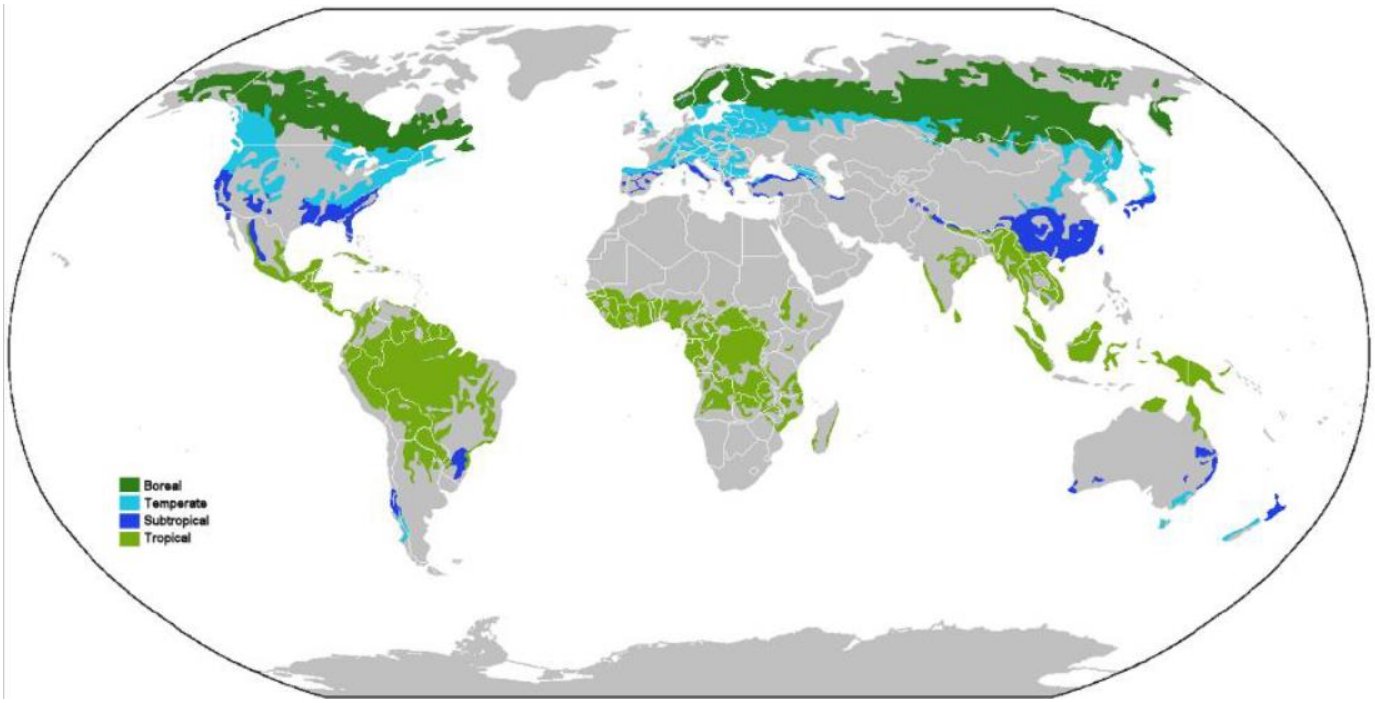

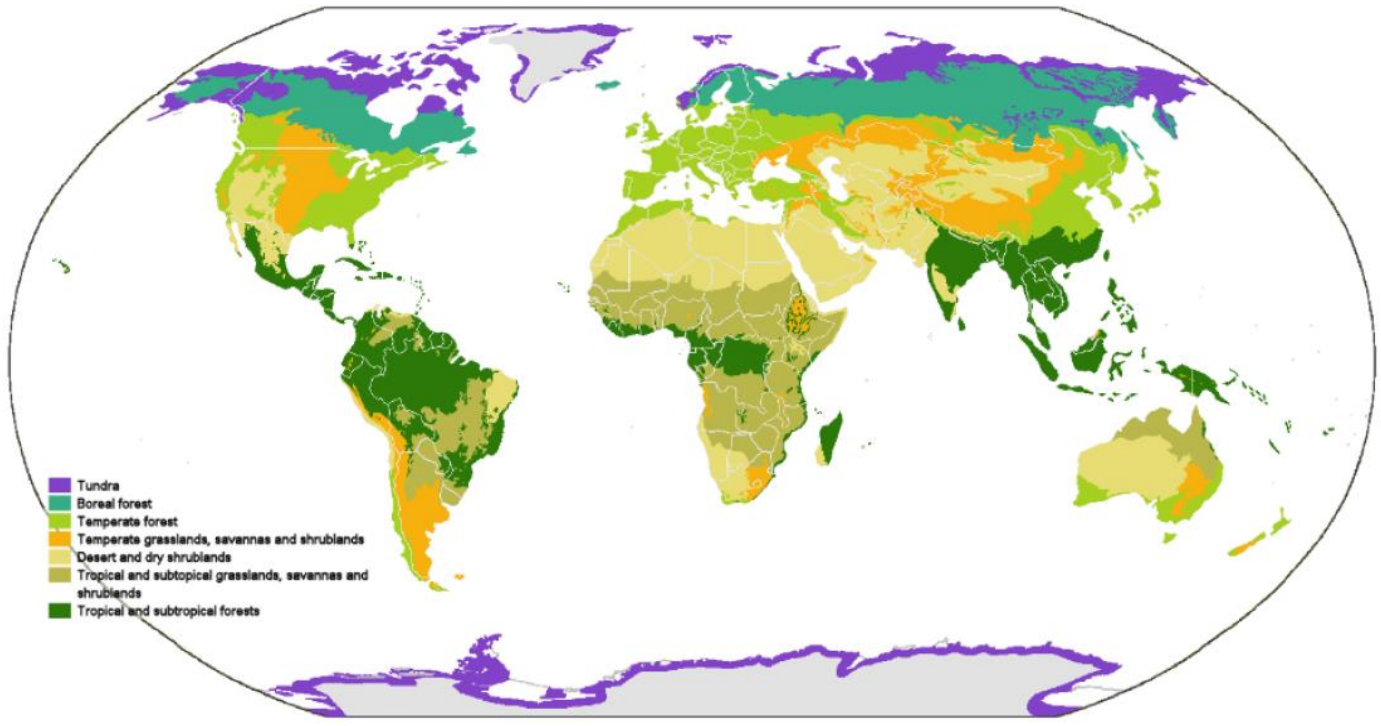

Appendix 3: *Global distribution of the different biome type*

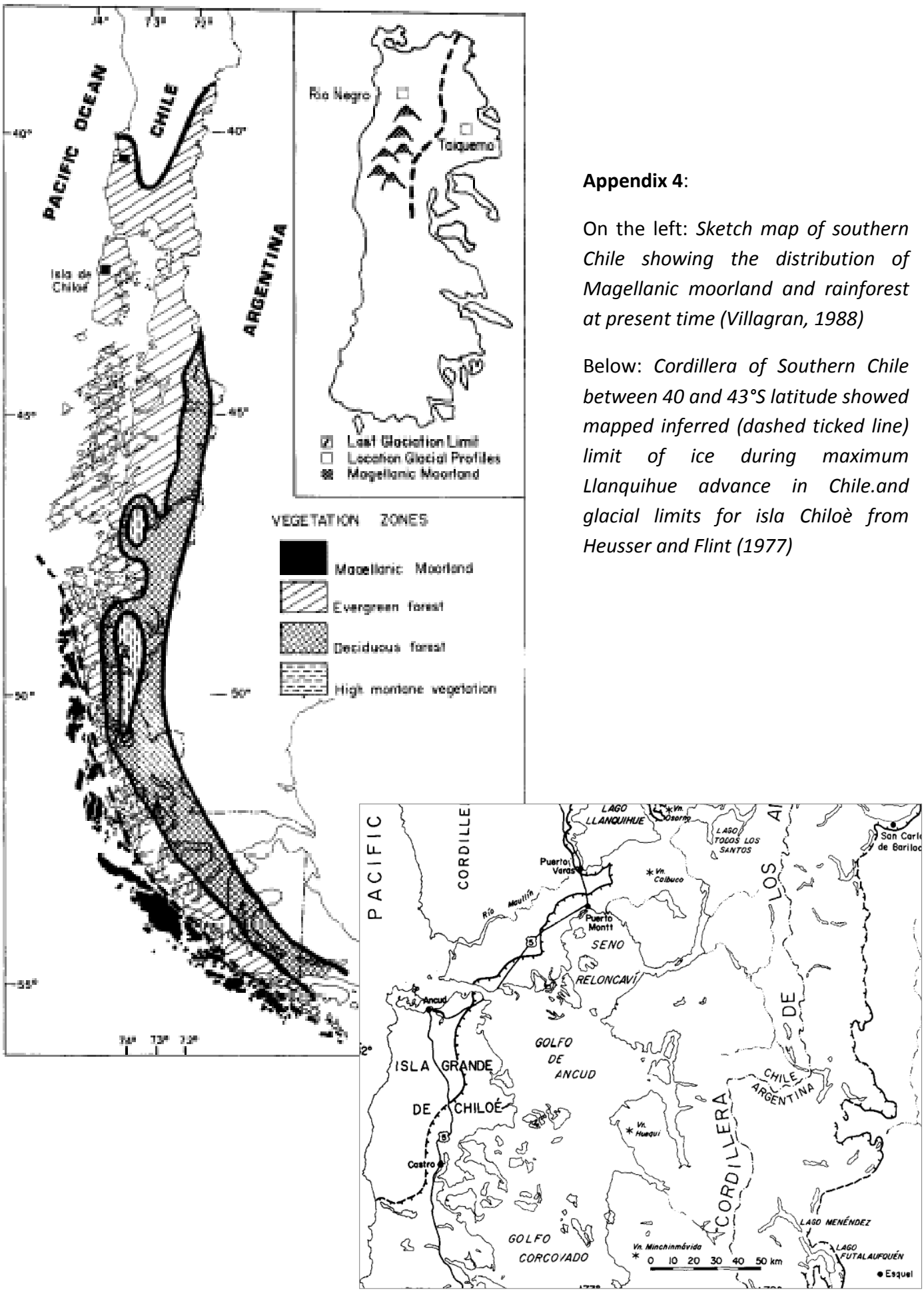

Appendix 4:

On the left: *Sketch map of southern Chile showing the distribution of Magellanic moorland and rainforest at present time (Villagran, 1988)*

Below: *Cordillera of Southern Chile between 40 and 43°S latitude showed mapped inferred (dashed ticked line) limit of ice during maximum Llanquihue advance in Chile.and glacial limits for isla Chiloè from Heusser and Flint (1977)*

NAME	DEPTH	GWW	T tube	WW	GDW	T box	DW	H20 CONTENT	Vol sampler	Vol sample	BD	Tot W sample	B fraction <0,063mm	TOC						EXTRACTION				BD	OC
	cm	g	g	g	g	g	g	g	cm3	cm3	g/cm3	g	g	%TOC ideal	µg ideal (+- 10/20%)	µg samples	C µg	Cc (kg)	TOC %	TOC fraction	Lab code	Weight (g)	Note	remained sample (g)	kg/m3	kg/m3
1A	0-5	7,73	1,67	6,06	5,37	4,15	1,22	4,84	3003,96	60,07	0,02	5,49	1,176	0,10	1200	1151,00	355,43	0,31	30,88	0,31	2AB	1,21	B+E fractions	/	20,31	3,14
1B	5-10	33,00	1,67	31,33	9,70	4,01	5,69	25,64	3003,96	60,07	0,09	6,00	1,154	0,09	2070	2102,00	487,54	0,23	23,19	0,23	2BB	1,18	B+E fractions	/	94,72	10,98
1C	10-15	59,58	1,67	57,91	16,75	4,17	12,58	45,33	3003,96	60,07	0,21	6,85	1,783	0,08	2940	2973,00	572,57	0,19	19,26	0,19	2CB	1,01	B+E fractions	/	209,41	20,17
1D	15-20	67,79	1,67	66,12	23,61	4,18	19,43	46,69	3003,96	60,07	0,32	7,99	2,225	0,07	3360	3503,00	608,00	0,17	17,36	0,17	2DB	1,00	B fraction	1,13	323,44	28,07
1E	20-25	77,95	1,67	76,28	29,65	4,11	25,54	50,74	3003,96	60,07	0,43	10,77	3,27	0,06	4680	4752,00	649,37	0,14	13,67	0,14	2EB	1,01	B fraction	1,31	425,14	29,05
1F	25-30	84,22	1,67	82,55	31,88	4,09	27,79	54,76	3003,96	60,07	0,46	11,37	3,626	0,05	6000	5961,00	729,09	0,12	12,23	0,12	2FB	1,00	B fraction	2,64	462,60	28,29
1G	30-35	98,85	1,67	97,18	41,73	4,08	37,65	59,53	3003,96	60,07	0,63	11,56	6,19	0,04	7500	7538,00	708,12	0,09	9,39	0,09	2GB	1,01	B fraction	5,24	626,73	29,44
1H	35-40	101,80	1,67	100,13	53,45	4,17	49,28	50,85	3003,96	60,07	0,82	12,01	6,295	0,03	9000	9075,00	678,10	0,07	7,47	0,07	2HB	1,00	B fraction	5,37	820,32	30,65
1I	40-45	103,38	1,67	101,71	66,81	4,15	62,66	39,05	3003,96	60,07	1,04	14,84	5,678	0,02	10500	10482,00	574,00	0,05	5,48	0,05	2IB	1,01	B fraction	4,72	1043,05	28,56
1J	45-50	108,79	1,67	107,12	77,75	4,33	73,42	33,70	3003,96	60,07	1,22	16,89	6,018	0,01	12000	12068,00	538,44	0,04	4,46	0,04	2JB	1,01	B fraction	5,01	1222,16	27,26
2A	0-5	44,27	1,67	42,60	14,85	5,70	9,15	33,45	3003,96	60,07	0,15	6,99	1,191	0,10	1200	1259,00	409,44	0,33	32,52	0,33	4AB	1,18	B+E fractions	/	152,31	24,77
2B	5-10.	53,30	1,67	51,63	18,00	6,16	11,84	39,79	3003,96	60,07	0,20	8,70	1,203	0,09	2070	2065,00	513,53	0,25	24,87	0,25	4BB	1,23	B+E fractions	/	197,09	24,51
2C	10-15.	65,32	1,67	63,65	22,48	6,26	16,22	47,43	3003,96	60,07	0,27	8,97	1,816	0,08	2940	2963,00	593,05	0,20	20,02	0,20	4CB	1,01	B fraction	0,83	270,00	27,02
2D	15-20	72,22	1,67	70,55	25,18	6,20	18,98	51,57	3003,96	60,07	0,32	10,09	2,283	0,07	3360	3324,00	612,13	0,18	18,42	0,18	4DB	1,01	B fraction	1,32	315,94	29,09
2E	20-25	76,09	1,67	74,42	26,59	6,17	20,42	54,00	3003,96	60,07	0,34	9,99	2,716	0,06	4680	4707,00	712,42	0,15	15,14	0,15	4EB	1,00	B fraction	1,73	339,92	25,72
2F	25-30	78,52	1,67	76,85	27,44	5,50	21,94	54,91	3003,96	60,07	0,37	11,15	3,079	0,05	6000	6056,00	795,89	0,13	13,14	0,13	4FB	1,00	B fraction	1,90	365,22	24,00
2G	30-35	82,80	1,67	81,13	34,63	6,12	28,51	52,62	3003,96	60,07	0,47	11,85	4,93	0,04	7500	7501,00	709,46	0,09	9,46	0,09	4GB	1,00	B fraction	3,93	474,58	22,44
2H	35-40	87,48	1,67	85,81	45,26	6,20	39,06	46,75	3003,96	60,07	0,65	11,17	5,587	0,03	9000	9027,00	631,68	0,07	7,00	0,07	4HB	1,01	B fraction	4,58	650,20	22,75
2I	40-45	85,82	1,67	84,15	39,38	6,18	33,20	50,95	3003,96	60,07	0,55	13,24	5,76	0,02	10500	10535,00	680,58	0,06	6,46	0,06	4IB	1,00	B fraction	4,76	552,65	17,85
2J	45-50	73,47	1,67	71,80	30,74	6,19	24,55	47,25	3003,96	60,07	0,41	12,90	3,97	0,01	12000	11990,00	847,24	0,07	7,07	0,07	4JB	1,00	B fraction	2,97	408,66	14,44
3A	0-5	32,62	1,67	30,95	10,80	5,49	5,31	25,64	3003,96	60,07	0,09	5,04		0,10	1200	/	/	/	/	/	/	/	just roots		88,39	/
3B	5-10	36,07	1,67	34,40	12,22	5,68	6,54	27,86	3003,96	60,07	0,11	4,95	0,23	0,09	2070	2061,00	605,07	0,29	29,36	0,29	5BB	0,47	B+E fractions	/	108,87	15,98
3C	10-15	32,36	1,67	30,69	10,66	5,65	5,01	25,68	3003,96	60,07	0,08	5,70	0,26	0,08	2940	2948,00	721,59	0,24	24,48	0,24	5CB	0,38	B+E fractions	/	83,40	10,21
3D	15-20	52,53	1,67	50,86	15,63	5,62	10,01	40,85	3003,96	60,07	0,17	6,90	0,39	0,07	3360	3360,00	771,46	0,23	22,96	0,23	5DB	0,63	B+E fractions	/	166,63	19,13
3E	20-25	53,93	1,67	52,26	17,58	5,62	11,96	40,30	3003,96	60,07	0,20	7,92	0,49	0,06	4680	4666,00	879,60	0,19	18,85	0,19	5EB	0,76	B+E fractions	/	199,09	18,77
3F	25-30	55,63	1,67	53,96	18,18	5,80	12,38	41,58	3003,96	60,07	0,21	7,46	0,38	0,05	6000	6007,00	1001,89	0,17	16,68	0,17	5FB	0,79	B+E fractions	/	206,08	17,19
3G	30-35	72,29	1,67	70,62	22,94	5,60	17,34	53,28	3003,96	60,07	0,29	8,64	1,829	0,04	7500	7528,00	1146,27	0,15	15,23	0,15	5GB	1,22	B+E fractions	0,61	288,64	21,98
3H	35-40	62,61	1,67	60,94	22,26	5,62	16,64	44,30	3003,96	60,07	0,28	9,29	3,361	0,03	9000	9053,00	1229,19	0,14	13,58	0,14	5HB	1,00	B+E fraction	2,36	276,99	18,80
3I	40-45	66,38	1,67	64,71	24,30	5,52	18,78	45,93	3003,96	60,07	0,31	10,09	4,333	0,02	10500	10516,00	1261,81	0,12	12,00	0,12	5IB	1,00	B fraction	3,34	312,62	18,76
3J	45-50	75,66	1,67	73,99	31,36	5,76	25,60	48,39	3003,96	60,07	0,43	10,41	4,829	0,01	12000	12001,00	1100,19	0,09	9,17	0,09	5JB	1,01	B fraction	3,82	426,14	19,53

Appendix 5: *Collection of data: physical analyses, TOC measurements, extraction analyses, calculation of bulk density and organic carbon content*

LAB CODE	WEIGHT(g)	Cell (ml)	Vial (ml)	Program
1A	1,206	20ml	240ml	DCM:MeOH (9:1)
1B	1,178	20ml	240ml	DCM:MeOH (9:1)
1C	1,013	20ml	240ml	DCM:MeOH (9:1)
1D	1,003	20ml	240ml	DCM:MeOH (9:1)
1E	1,01	20ml	240ml	DCM:MeOH (9:1)
1F	1,003	20ml	240ml	DCM:MeOH (9:1)
1G	1,006	20ml	240ml	DCM:MeOH (9:1)
1H	1,003	20ml	240ml	DCM:MeOH (9:1)
1I	1,007	20ml	240ml	DCM:MeOH (9:1)
1J	1,01	20ml	240ml	DCM:MeOH (9:1)
2A	1,178	20ml	240ml	DCM:MeOH (9:1)
2B	1,234	20ml	240ml	DCM:MeOH (9:1)
2C	1,014	20ml	240ml	DCM:MeOH (9:1)
2D	1,011	20ml	240ml	DCM:MeOH (9:1)
2E	1,004	20ml	240ml	DCM:MeOH (9:1)
2F	1,004	20ml	240ml	DCM:MeOH (9:1)
2G	1,004	20ml	240ml	DCM:MeOH (9:1)
2H	1,01	20ml	240ml	DCM:MeOH (9:1)
2I	1,004	20ml	240ml	DCM:MeOH (9:1)
2J	1,002	20ml	240ml	DCM:MeOH (9:1)
3A		20ml	240ml	DCM:MeOH (9:1)
3B	0,47	20ml	240ml	DCM:MeOH (9:1)
3C	0,38	20ml	240ml	DCM:MeOH (9:1)
3D	0,626	20ml	240ml	DCM:MeOH (9:1)
3E	0,76	20ml	240ml	DCM:MeOH (9:1)
3F	0,786	20ml	240ml	DCM:MeOH (9:1)
3G	1,222	20ml	240ml	DCM:MeOH (9:1)
3H	1,003	20ml	240ml	DCM:MeOH (9:1)
3I	1,002	20ml	240ml	DCM:MeOH (9:1)
3J	1,006	20ml	240ml	DCM:MeOH (9:1)

Appendix 6: *Procedure program for the organic extraction*

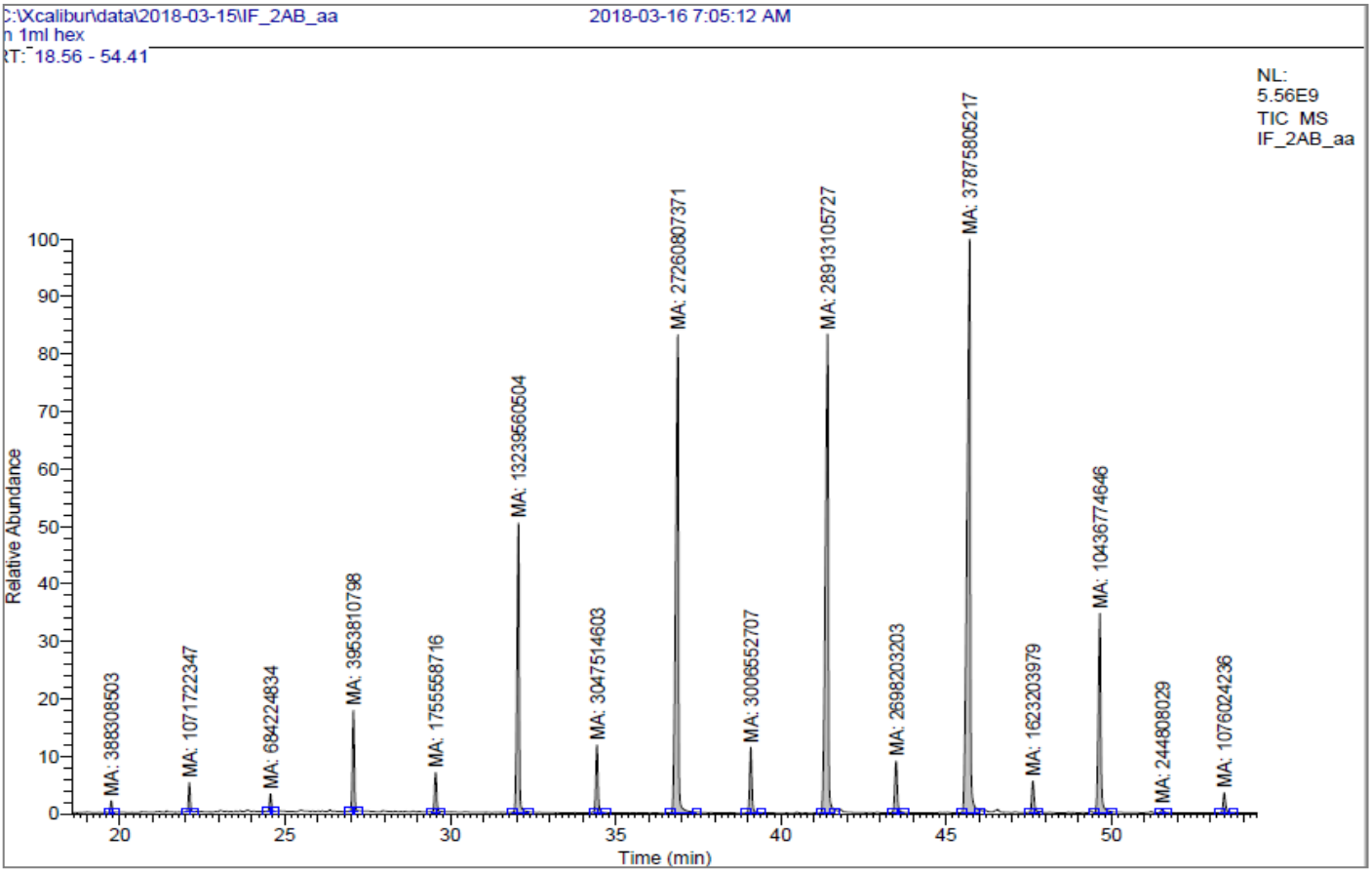

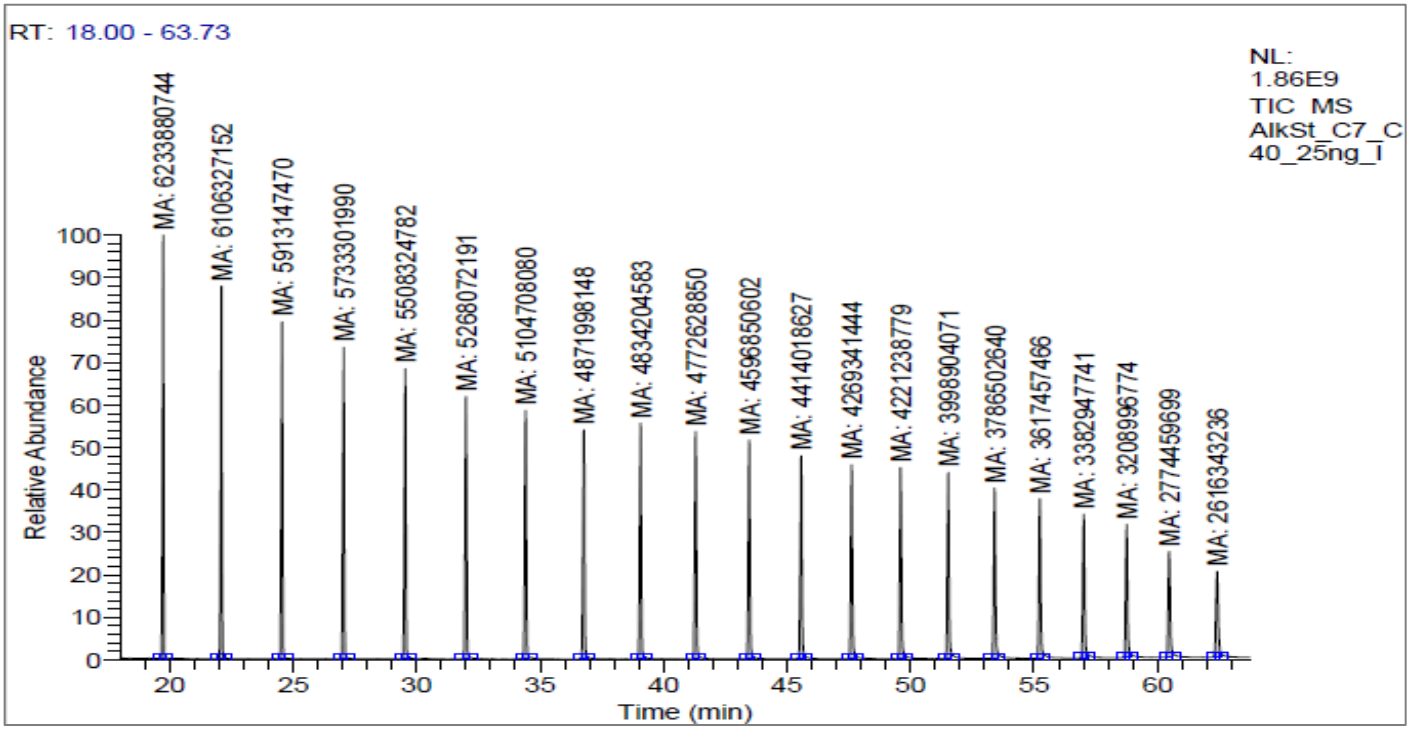

Appendix 7: *Example of n-alkane concentration peaks of sample(above) and standards (below)*

retention time (m)	depth / n alcan	0-5.0 1A	5.0-10.0 1B	10.0-15.0 1C	15-20 1D	20-25 1E	25-30 1F	30-35 1G	35-40 1H	40-45 1I	45-50 1J
		Peak area n-alkanes									
19,76	C20	388308503	296095383	232837297	88062318	54438507	95527154	69703349	47341176	45245454	20397174
22,12	C21	1071722347	911333115	777011869	389014561	229792940	402585795	279481494	185553260	127570659	78701862
24,57	C22	684224834	609569540	559913826	298088471	186527884	383413569	258885078	188825663	107885846	80568602
27,07	C23	3953810798	3666728916	3158833219	1645617263	974832630	2060936320	1399618278	877436323	333816235	240524638
29,56	C24	1755558716	1659637291	1561271650	797067668	436486863	1110062215	752139234	470836377	157214537	151025123
32,03	C25	13239560504	12616893851	11426951181	5291156232	2818640557	7407765550	5114122441	2667256056	602681846	623997004
34,44	C26	3047514603	2971489240	2722785162	1096060862	523838265	1675157490	1186411940	674501145	172955032	186510039
36,79	C27	27260807371	25451340587	23272650587	8908238743	4271443136	12808611072	9901400335	5600233931	1335791771	1383893851
39,08	C28	3006552707	2737946164	2420967399	800219697	329714410	1236264739	958320702	521187931	109442592	138100318
41,32	C29	28913105727	25889399266	22963580938	7199881126	3140799855	10559213077	8723075652	4634959005	914003545	1222196579
43,48	C30	2698203203	2315432789	1894292238	476667094	171579190	765578923	597878184	287178924	43040875	80881522
45,58	C31	37875805217	32895183312	28211906361	7701275558	3168297232	11405203293	9778784566	4961235179	941255449	1609901098
47,62	C32	1623203979	1349215206	1113980660	238771923	66439431	324496086	304083785	114598011	16781320	34936164
49,6	C33	10436774646	8839819089	6896214758	1469641352	505700256	2186236474	1977064130	964352452	143825408	402085340

W sample										
g	1,21	1,18	1,01	1,00	1,01	1,00	1,01	1,00	1,01	1,01

C sample in ng/ul									
1A	1B	1C	1D	1E	1F	1G	1H	1I	1J
1,69	1,29	1,01	0,38	0,24	0,42	0,30	0,21	0,20	0,09
4,73	4,02	3,43	1,72	1,01	1,78	1,23	0,82	0,56	0,35
3,08	2,74	2,52	1,34	0,84	1,72	1,16	0,85	0,49	0,36
18,07	16,76	14,44	7,52	4,46	9,42	6,40	4,01	1,53	1,10
8,19	7,74	7,29	3,72	2,04	5,18	3,51	2,20	0,73	0,70
64,33	61,31	55,52	25,71	13,70	35,99	24,85	12,96	2,93	3,03
15,18	14,80	13,56	5,46	2,61	8,34	5,91	3,36	0,86	0,93
142,42	132,96	121,58	46,54	22,32	66,92	51,73	29,26	6,98	7,23
15,89	14,47	12,80	4,23	1,74	6,53	5,07	2,75	0,58	0,73
154,80	138,61	122,95	38,55	16,82	56,54	46,70	24,82	4,89	6,54
15,04	12,91	10,56	2,66	0,96	4,27	3,33	1,60	0,24	0,45
219,45	190,59	163,46	44,62	18,36	66,08	56,66	28,75	5,45	9,33
9,67	8,04	6,64	1,42	0,40	1,93	1,81	0,68	0,10	0,21
63,44	53,73	41,92	8,93	3,07	13,29	12,02	5,86	0,87	2,44

	weight n alc (ug/g DW)									
C20	1,40	1,09	1,00	0,38	0,23	0,41	0,30	0,21	0,20	0,09
C21	3,92	3,42	3,39	1,71	1,00	1,77	1,23	0,82	0,56	0,34
C22	2,55	2,33	2,49	1,34	0,83	1,72	1,16	0,85	0,48	0,36
C23	14,98	14,23	14,25	7,50	4,41	9,39	6,36	4,00	1,52	1,09
C24	6,79	6,57	7,19	3,71	2,02	5,16	3,49	2,19	0,73	0,70
C25	53,34	52,04	54,81	25,63	13,56	35,89	24,70	12,92	2,91	3,00
C26	12,59	12,56	13,39	5,44	2,58	8,32	5,87	3,35	0,86	0,92
C27	118,09	112,87	120,02	46,40	22,09	66,72	51,42	29,17	6,93	7,16
C28	13,18	12,29	12,63	4,22	1,73	6,51	5,04	2,75	0,57	0,72
C29	128,36	117,67	121,37	38,43	16,65	56,37	46,43	24,74	4,86	6,48
C30	12,47	10,96	10,42	2,65	0,95	4,25	3,31	1,60	0,24	0,45
C31	181,97	161,79	161,36	44,49	18,18	65,88	56,32	28,66	5,42	9,24
C32	8,02	6,82	6,55	1,42	0,39	1,93	1,80	0,68	0,10	0,21
C33	52,60	45,61	41,38	8,91	3,04	13,25	11,95	5,84	0,87	2,42

Paq	0,20	0,22	0,22	0,32	0,38	0,30	0,26	0,27	0,34	0,23
Pwax	0.85	0,84	0,84	0,77	0,74	0,79	0,81	0,81	0,77	0,83
CPI	9,61	9,50	9,48	8,94	9,08	8,66	9,31	9,10	7,88	8,86
ACL	29,21	29,16	29,12	28,89	28,79	28,91	28,98	28,91	28,74	29,09
MT	0,04	0,04	0,04	0,07	0,09	0,06	0,05	0,06	0,10	0,06

Appendix 8 – *Table results CORE 1*

retention time (m)	depth n alcan	0-5.0 2A	5.0-10.0 2B	10.0-15.0 2C	15-20 2D	20-25 2E	25-30 2F	30-35 2G	35-40 2H	40-45 2I	45-50 2J
		Peak area n-Alkanes									
22,12	C20	141681490	133850179	94504864	5890304	56855107	8631621	4692713	3174122	5438629	8445746
24,57	C21	610320018	556130811	366495520	19593599	249176690	27568079	26881063	14679018	34148839	43740988
27,07	C22	393579303	389768290	267293650	14137535	219850849	21294511	22203372	9888214	19869300	26330088
29,56	C23	1932311771	1904403884	1264402962	62152647	1054729044	81619905	84434559	35248829	55376618	67317776
32,03	C24	1034887981	1119554598	634255019	28796179	514671807	36815187	40316419	16854226	24262578	33576976
34,44	C25	6917807295	7229648240	3591640596	192448822	3078629003	198955891	215415313	82131969	87119397	100937105
36,79	C26	2198779441	2342022307	845706607	38934026	677394406	41559929	52807336	24906131	25343534	26107568
39,08	C27	23189654629	23373831269	7719576673	407818447	5935598821	341507174	476253308	258035658	221361829	191366229
41,32	C28	3080328436	3148503772	762128095	23359406	463112400	24847566	37802768	21289604	16115038	11453740
43,48	C29	30680451319	29632616811	7066509849	286073303	4570557021	215371871	313063216	182784606	123330478	70597943
45,58	C30	2450903161	2440492057	418035200	9901167	233451724	11150791	17512533	8704001	5792403	2920291
47,62	C31	42831841026	39788881976	8116696755	242139522	4537059612	138516399	229947543	118871502	71755805	23367499
49,6	C32	1591887252	1504167129	189190275	3792005	78128294	3185754	4385187	1632362	2875657	2516700
51,53	C33	8005024247	7455457061	1060836017	19591727	534006974	6215533	11046646	4188885	0	0

W sample g	1,18	1,23	1,01	1,01	1,00	1,00	1,00	1,01	1,00	1,00

C sample in ng/ul									
2A	2B	2C	2D	2E	2F	2G	2H	2I	2J
0,62	0,58	0,41	0,03	0,25	0,04	0,02	0,01	0,02	0,04
2,69	2,46	1,62	0,09	1,10	0,12	0,12	0,06	0,15	0,19
1,77	1,75	1,20	0,06	0,99	0,10	0,10	0,04	0,09	0,12
8,83	8,70	5,78	0,28	4,82	0,37	0,39	0,16	0,25	0,31
4,83	5,22	2,96	0,13	2,40	0,17	0,19	0,08	0,11	0,16
33,61	35,13	17,45	0,94	14,96	0,97	1,05	0,40	0,42	0,49
10,95	11,66	4,21	0,19	3,37	0,21	0,26	0,12	0,13	0,13
121,15	122,11	40,33	2,13	31,01	1,78	2,49	1,35	1,16	1,00
16,28	16,64	4,03	0,12	2,45	0,13	0,20	0,11	0,09	0,06
164,27	158,66	37,83	1,53	24,47	1,15	1,68	0,98	0,66	0,38
13,66	13,60	2,33	0,06	1,30	0,06	0,10	0,05	0,03	0,02
248,17	230,54	47,03	1,40	26,29	0,80	1,33	0,69	0,42	0,14
9,48	8,96	1,13	0,02	0,47	0,02	0,03	0,01	0,02	0,01
48,66	45,32	6,45	0,12	3,25	0,04	0,07	0,03	0,00	0,00

	weight n alc (ug/g DW)									
C20	0,523	0,471	0,405	0,025	0,246	0,037	0,020	0,014	0,024	0,037
C21	2,287	1,990	1,596	0,086	1,096	0,121	0,118	0,064	0,150	0,193
C22	1,503	1,421	1,186	0,063	0,985	0,095	0,099	0,044	0,089	0,118
C23	7,497	7,053	5,699	0,281	4,801	0,372	0,384	0,160	0,252	0,307
C24	4,100	4,234	2,919	0,133	2,392	0,171	0,187	0,078	0,113	0,156
C25	28,535	28,468	17,211	0,925	14,899	0,963	1,043	0,395	0,422	0,489
C26	9,297	9,453	4,154	0,192	3,360	0,206	0,262	0,123	0,126	0,130
C27	102,843	98,956	39,772	2,107	30,886	1,777	2,478	1,335	1,152	0,998
C28	13,821	13,486	3,973	0,122	2,438	0,131	0,199	0,111	0,085	0,060
C29	139,445	128,570	37,312	1,515	24,374	1,149	1,669	0,969	0,658	0,377
C30	11,598	11,024	2,298	0,055	1,296	0,062	0,097	0,048	0,032	0,016
C31	210,668	186,820	46,379	1,388	26,183	0,799	1,327	0,682	0,414	0,135
C32	8,050	7,261	1,111	0,022	0,464	0,019	0,026	0,010	0,017	0,015
C33	41,304	36,722	6,359	0,118	3,233	0,038	0,067	0,025	0,000	0,000

Paq	0,1	0,1	0,2	0,3	0,3	0,4	0,4	0,3	0,4	0,6
Pwax	0,92	0,91	0,83	0,79	0,78	0,71	0,77	0,83	0,75	0,63
CPI	10,78	10,18	9,67	10,96	9,49	7,45	8,15	8,80	6,77	5,04
ACL	29,38	29,33	29,02	28,64	28,81	28,43	28,52	28,51	28,29	27,85
MT	0,02	0,02	0,06	0,07	0,07	0,12	0,08	0,06	0,13	0,24

Appendix 9 – *Table results CORE* 2

retention	depth	5.0-10.0	10.0-15.0	15-20	20-25	25-30	30-35	35-40	40-45	45-50
time (m)	n-alcane	3B	3C	3D	3E	3F	3G	3H	3I	3J
		Peak area n-alkanes								
19,76	C20	62251535	17848394	7797011	54109042	75257260	86398649	140914414	72471191	48309811
22,12	C21	395478692	82951525	36534676	289091570	474631201	647264261	1982708628	1041916981	632720478
24,57	C22	186817669	74655410	33748279	296897324	472028863	589667707	1002825878	410428663	254867821
27,07	C23	4895082263	594249120	245517677	2051995121	3450137018	3948703040	5075597402	1771594461	1138705822
29,56	C24	410964505	187726093	100272609	873871654	1258707227	1338670249	1432989964	405171480	265641657
32,03	C25	5522739465	1150852048	692226300	5895022285	8218428278	8185012857	8313696155	2310034032	1466401086
34,44	C26	656976371	264719427	234224350	1924701386	2657982173	2821651325	3246951456	704887284	462080132
36,79	C27	5573944691	2154339226	2016122173	17115639017	22221039985	25116527720	30655137115	7152605250	4985319989
39,08	C28	504058523	97456453	159008778	1648818338	1998747675	2973536628	4302853601	720868269	488705094
41,32	C29	5562767548	985816869	1564256734	15049725288	19010559580	27413727229	35523830396	7105666639	5256773135
43,48	C30	496244389	48674363	127226210	1351466087	1635071214	2755414804	3521472705	514314263	347725364
45,58	C31	6954427060	875153536	2045711409	21151881736	24639291359	39452126333	46969644599	8372599776	5875579052
47,62	C32	258374005	22041653	82787990	1016927152	1151182208	2165890969	2472238765	305100962	196840263
49,60	C33	1844470289	179548863	682685968	8298742879	9272669144	16632337568	19259167135	2870048834	1954967955
51,53	C34	28391100	15684622	43007914	201044431	229717012	530734699	714768283	73716936	41460207
53,41	C35	104731780	10754133		1042998668	1202684982	2653095556	3226854821	380371899	220319143

W sample									
g	0,47	0,38	0,63	0,76	0,79	1,22	1,00	1,00	1,01

C sample in ng/ul								
3B	3C	3D	3E	3F	3G	3H	3I	3J
0,27	0,08	0,03	0,24	0,33	0,38	0,61	0,31	0,21
1,75	0,37	0,16	1,28	2,10	2,86	8,75	4,60	2,79
0,84	0,34	0,15	1,34	2,12	2,65	4,51	1,85	1,15
22,37	2,72	1,15	9,38	15,77	18,05	23,20	8,10	5,20
1,92	0,88	0,49	4,08	5,87	6,25	6,69	1,89	1,24
26,84	5,59	3,45	28,64	39,93	39,77	40,40	11,22	7,13
3,27	1,32	1,22	9,59	13,24	14,05	16,17	3,51	2,30
29,12	11,25	10,66	89,42	116,09	131,22	160,15	37,37	26,04
2,66	0,52	0,85	8,72	10,56	15,72	22,74	3,81	2,58
29,78	5,28	8,72	80,58	101,78	146,78	190,20	38,04	28,15
2,77	0,27	0,74	7,53	9,11	15,36	19,63	2,87	1,94
40,29	5,07	12,19	122,55	142,76	228,58	272,14	48,51	34,04
1,54	0,13	0,50	6,06	6,86	12,90	14,73	1,82	1,17
11,21	1,09	4,38	50,44	56,36	101,09	117,06	17,44	11,88
0,18	0,10	0,29	1,29	1,48	3,41	4,59	0,47	0,27
0,72	0,07	0,00	7,15	8,25	18,19	22,13	2,61	1,51

	Concn-alcane (µg/g DW)								
	3B	3C	3D	3E	3F	3G	3H	3I	3J
C21	3,71	0,96	0,26	1,68	2,67	2,34	8,73	4,59	2,78
C22	1,79	0,88	0,25	1,76	2,70	2,17	4,50	1,84	1,14
C23	47,60	7,15	1,83	12,34	20,06	14,77	23,13	8,08	5,17
C24	4,08	2,31	0,78	5,37	7,47	5,11	6,67	1,89	1,23
C25	57,10	14,72	5,51	37,69	50,81	32,55	40,28	11,20	7,08
C26	6,96	3,47	1,95	12,61	16,84	11,50	16,12	3,50	2,29
C27	61,96	29,62	17,02	117,65	147,70	107,38	159,67	37,29	25,89
C28	5,67	1,36	1,36	11,47	13,44	12,86	22,68	3,80	2,57
C29	63,37	13,89	13,93	106,02	129,50	120,11	189,63	37,97	27,98
C30	5,89	0,71	1,18	9,91	11,60	12,57	19,57	2,86	1,93
C31	85,73	13,34	19,47	161,25	181,63	187,06	271,33	48,41	33,84
C32	3,27	0,35	0,80	7,97	8,72	10,56	14,68	1,81	1,17
C33	23,85	2,87	7,00	66,37	71,71	82,73	116,71	17,41	11,81

Paq	0,45	0,48	0,21	0,18	0,21	0,15	0,14	0,21	0,19
Pwax	0,63	0,70	0,86	0,87	0,85	0,88	0,89	0,85	0,86
CPI	10,88	8,51	9,66	9,76	9,46	9,48	9,18	10,35	10,97
ACL	29,14	28,37	29,00	29,14	29,06	29,29	29,26	29,09	29,10
MT	0,27	0,15	0,04	0,04	0,05	0,04	0,04	0,08	0,07

Appendix 10 – Table results CORE 3

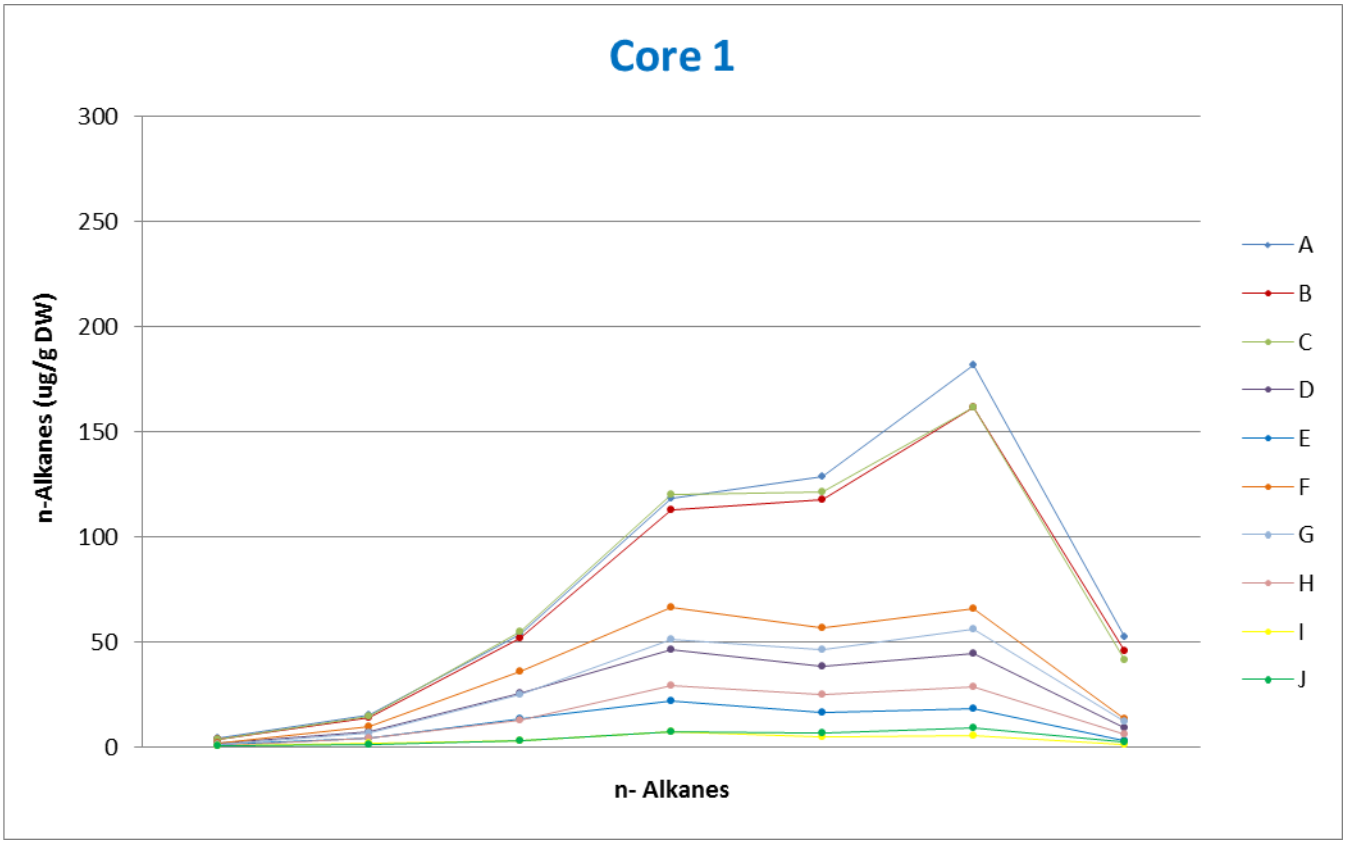

	A	B	C	D	E	F	G	H	I	J
C21	3,92	3,42	3,39	1,71	1,00	1,77	1,23	0,82	0,56	0,34
C23	14,98	14,23	14,25	7,50	4,41	9,39	6,36	4,00	1,52	1,09
C25	53,34	52,04	54,81	25,63	13,56	35,89	24,70	12,92	2,91	3,00
C27	118,09	112,87	120,02	46,40	22,09	66,72	51,42	29,17	6,93	7,16
C29	128,36	117,67	121,37	38,43	16,65	56,37	46,43	24,74	4,86	6,48
C31	181,97	161,79	161,36	44,49	18,18	65,88	56,32	28,66	5,42	9,24
C33	52,60	45,61	41,38	8,91	3,04	13,25	11,95	5,84	0,87	2,42
C35	6,12	5,17	4,51	0,58	0,16	0,66	0,72	0,00	0,07	0,22

Appendix 11: *odd n-Alkanes distribution and concentration of CORE 1*

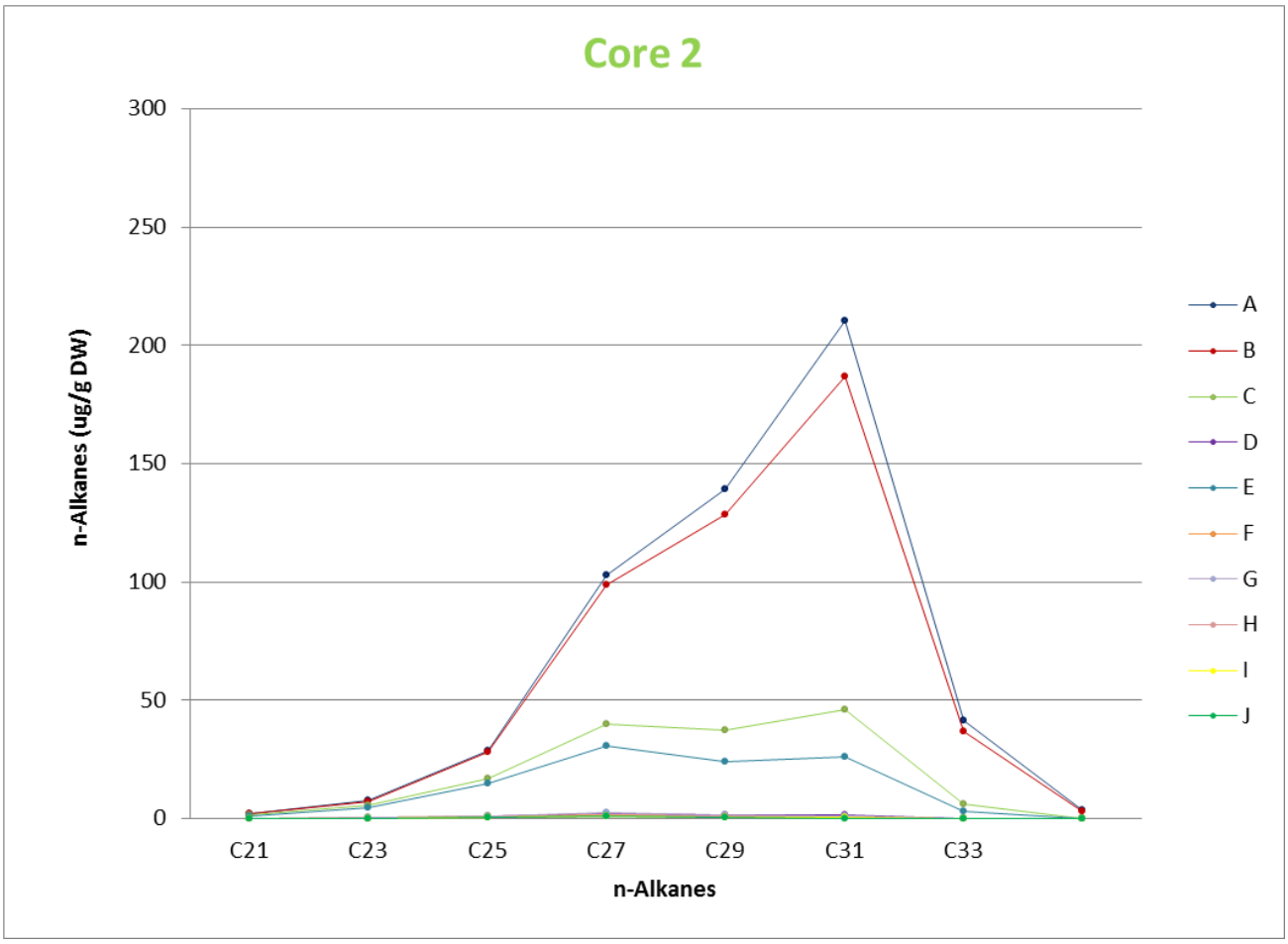

	A	B	C	D	E	F	G	H	I	J
C21	2,29	1,99	1,60	0,09	1,10	0,12	0,12	0,06	0,15	0,19
C23	7,50	7,05	5,70	0,28	4,80	0,37	0,38	0,16	0,25	0,31
C25	28,53	28,47	17,21	0,92	14,90	0,96	1,04	0,40	0,42	0,49
C27	102,84	98,96	39,77	2,11	30,89	1,78	2,48	1,33	1,15	1,00
C29	139,44	128,57	37,31	1,51	24,37	1,15	1,67	0,97	0,66	0,38
C31	210,67	186,82	46,38	1,39	26,18	0,80	1,33	0,68	0,41	0,14
C33	41,30	36,72	6,36	0,12	3,23	0,04	0,07	0,03	0,00	0,00
C35	3,55	3,23	0,00	0,00	0,14	0,00	0,00	0,00	0,00	0,00

Appendix 12: *odd n-Alkanes distribution and concentration of core 4*

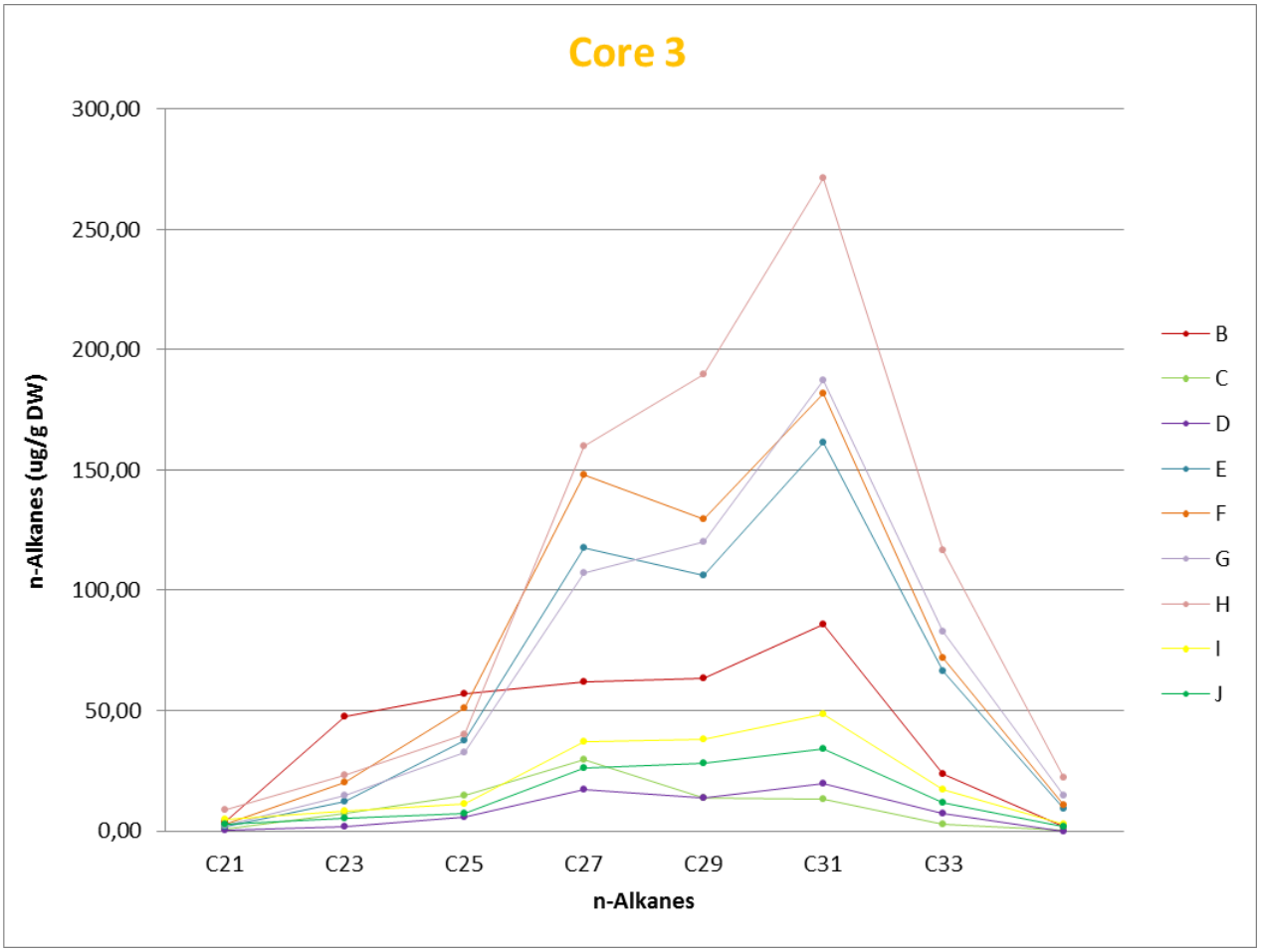

	B	C	D	E	F	G	H	I	J
C21	3,71	0,96	0,26	1,68	2,67	2,34	8,73	4,59	2,78
C23	47,60	7,15	1,83	12,34	20,06	14,77	23,13	8,08	5,17
C25	57,10	14,72	5,51	37,69	50,81	32,55	40,28	11,20	7,08
C27	61,96	29,62	17,02	117,65	147,70	107,38	159,67	37,29	25,89
C29	63,37	13,89	13,93	106,02	129,50	120,11	189,63	37,97	27,98
C31	85,73	13,34	19,47	161,25	181,63	187,06	271,33	48,41	33,84
C33	23,85	2,87	7,00	66,37	71,71	82,73	116,71	17,41	11,81
C35	1,53	0,19	0,00	9,41	10,49	14,89	22,06	2,60	1,50

Appendix 13: *odd n-Alkanes distribution and concentration of core 5*

depth	C content (kg(m3)	% TOC
5	3,14	30,88
10	10,98	23,19
15	20,17	19,26
20	28,07	17,36
25	29,05	13,67
30	28,29	12,23
35	29,44	9,39
40	30,65	7,47
45	28,56	5,48
50	27,26	4,46

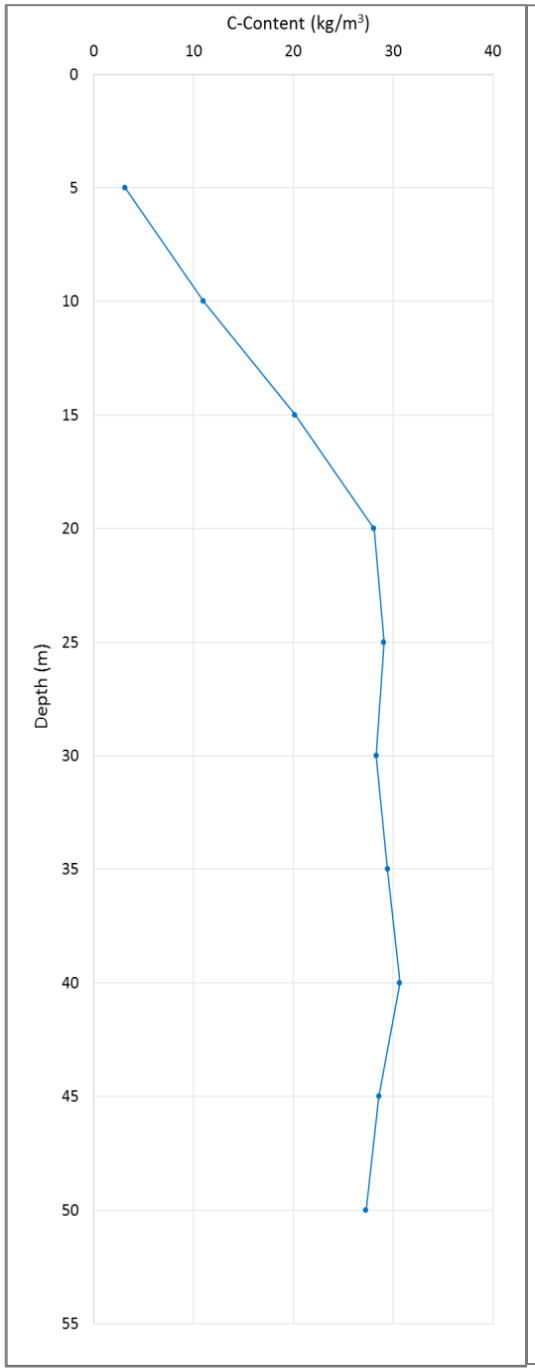

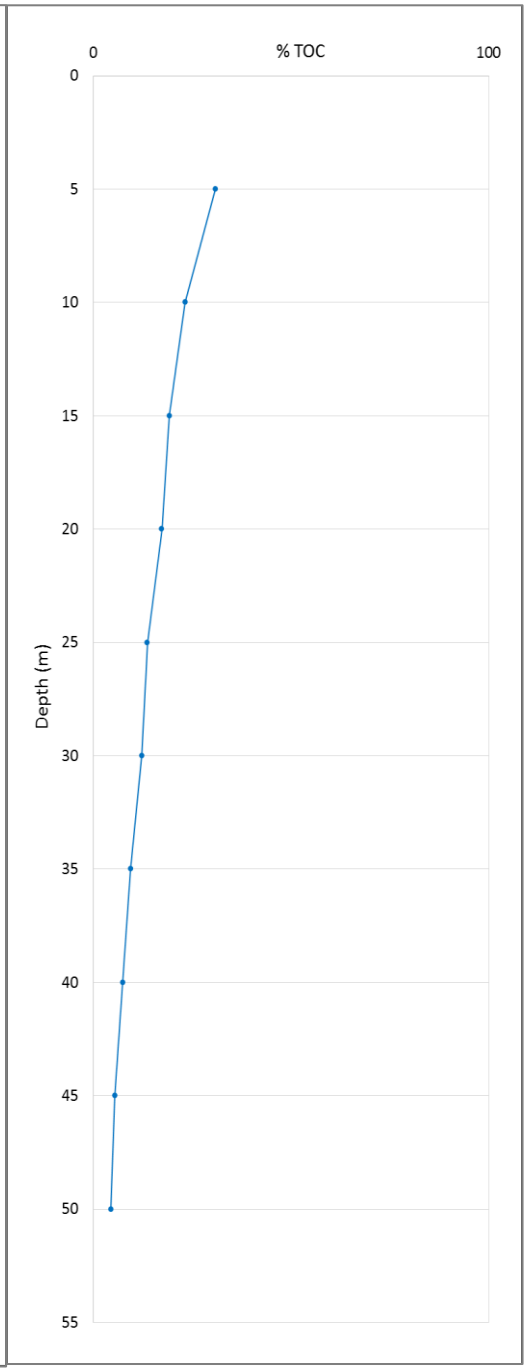

N-alkanes concentration

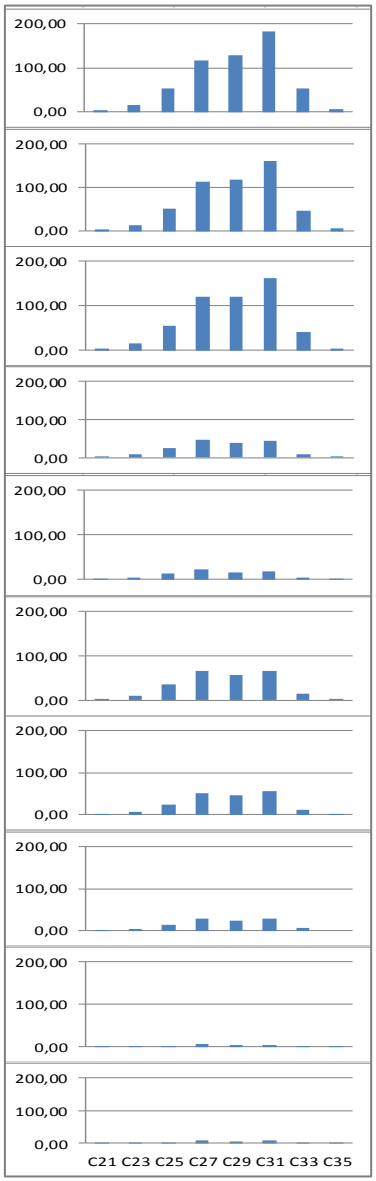

Appendix 14: *OC content, %TOC, n-alkanes concentration of CORE 1*

depth	C content (kg/m3)	% TOC
5	24,77	32,52
10	24,51	24,87
15	27,02	20,02
20	29,09	18,42
25	25,72	15,14
30	24,00	13,14
35	22,44	9,46
40	22,75	7,00
45	17,85	6,46
50	14,44	7,07

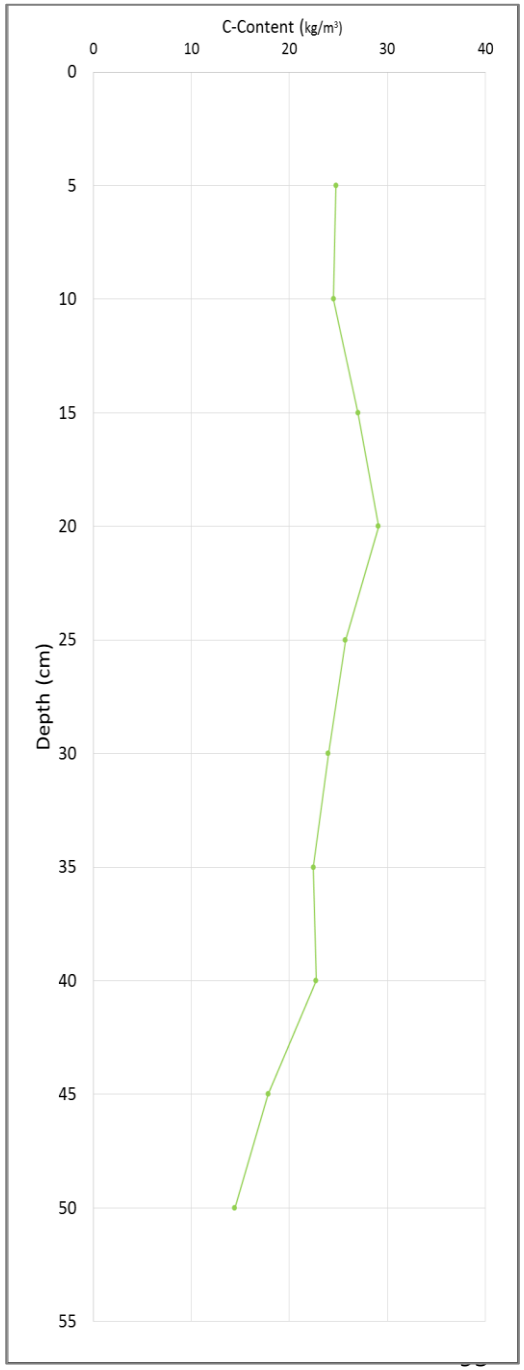

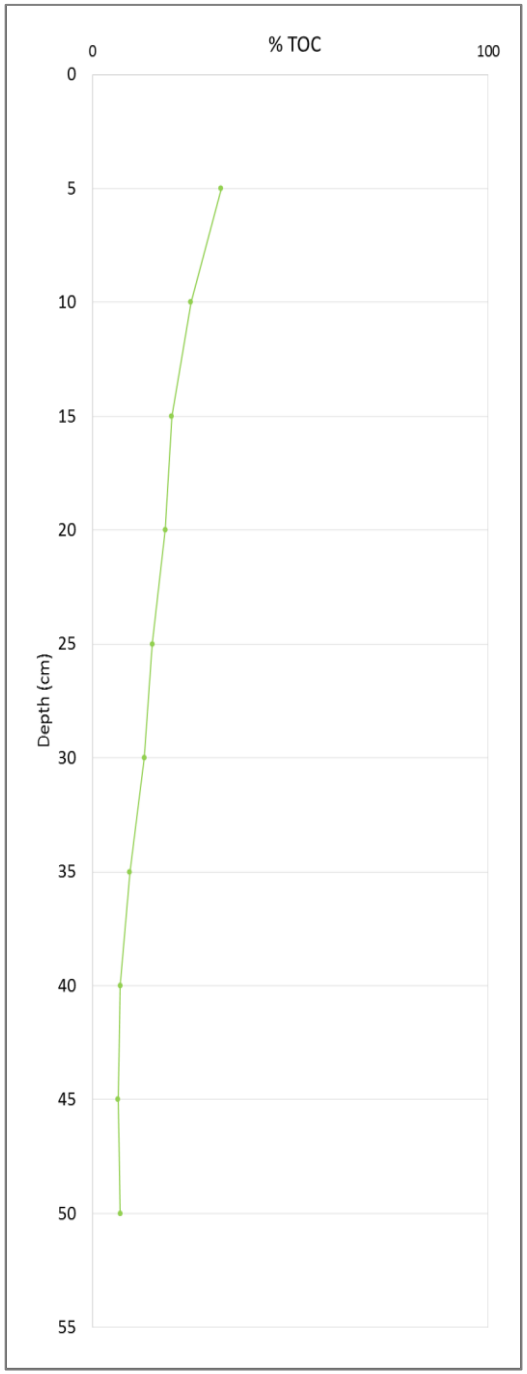

N-alkanes concentration

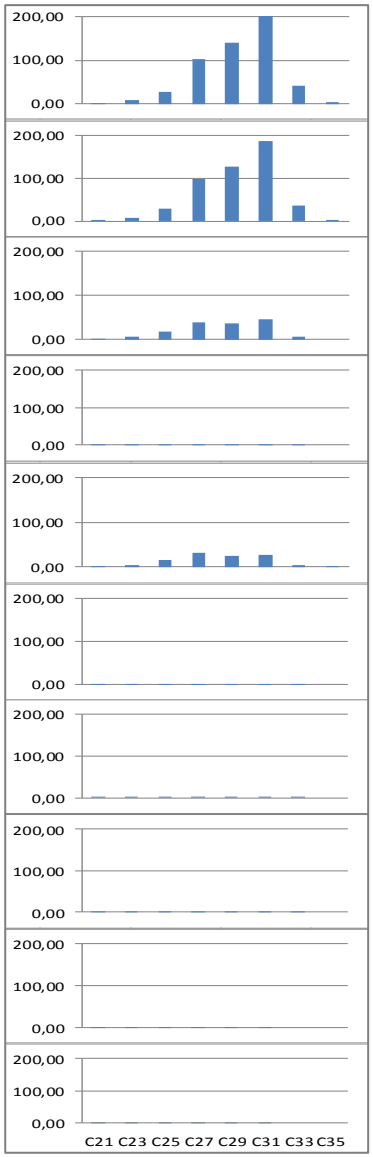

Appendix 15: *OC content, %TOC, n-alkanes concentration of CORE 2*

depth	C content (kg/m3)	% TOC
5	/	/
10	15,98	29,36
15	10,21	24,48
20	19,13	22,96
25	18,77	18,85
30	17,19	16,68
35	21,98	15,23
40	18,80	13,58
45	18,76	12,00
50	19,53	9,2

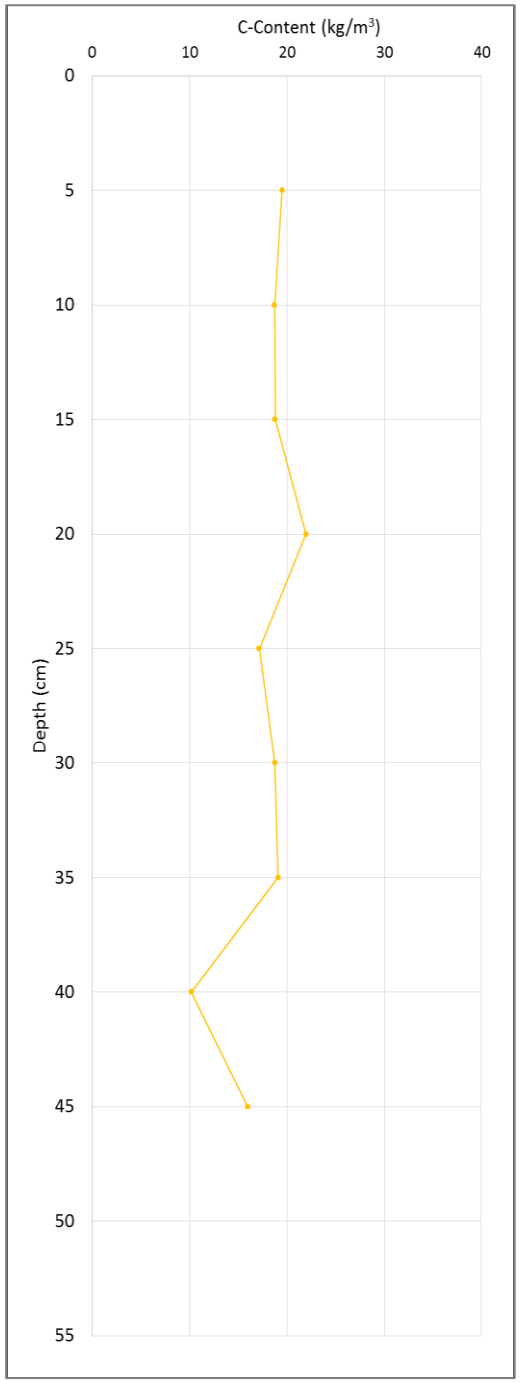

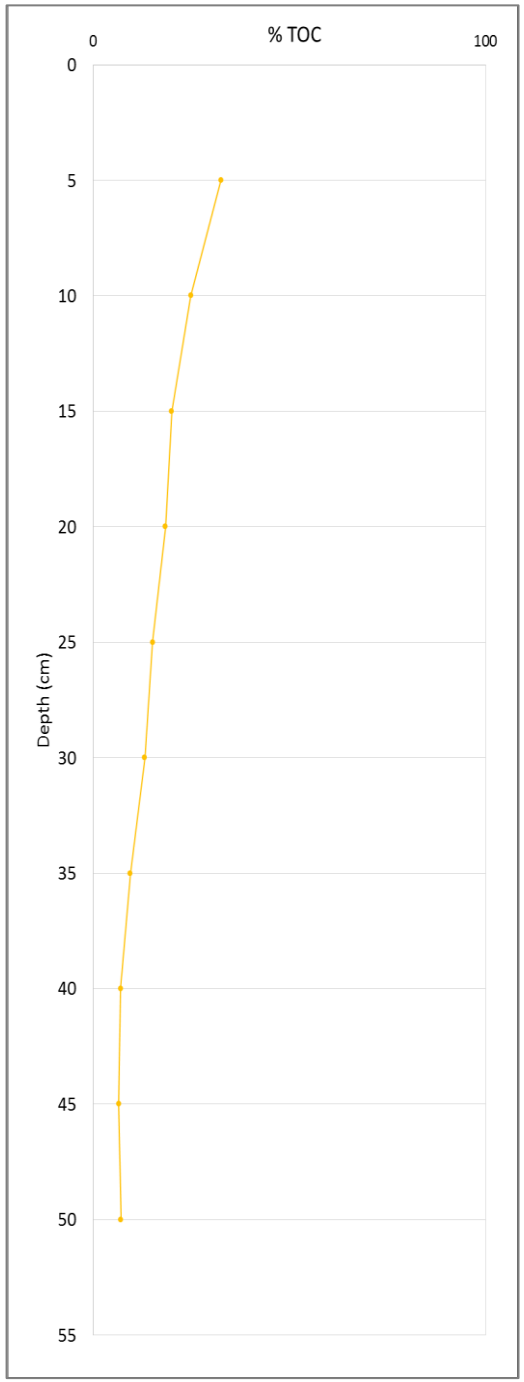

N-alkanes concentration

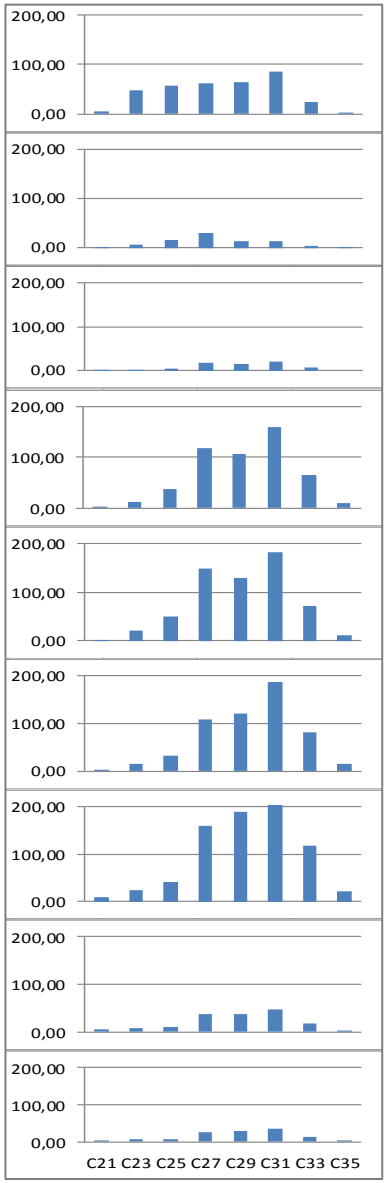

Appendix 16: *OC content, %TOC, n-alkanes concentration of CORE 3*

depth	5	10	15	20	25	30	35	40	45	50
sample	A	B	C	D	E	F	G	H	I	J
1	0,20	0,22	0,22	0,32	0,38	0,30	0,26	0,27	0,34	0,23
2	0,18	0,19	0,40	0,53	0,47	0,44	0,36	0,28	0,42	0,64
3		0,45	0,48	0,21	0,18	0,21	0,15	0,14	0,21	0,19

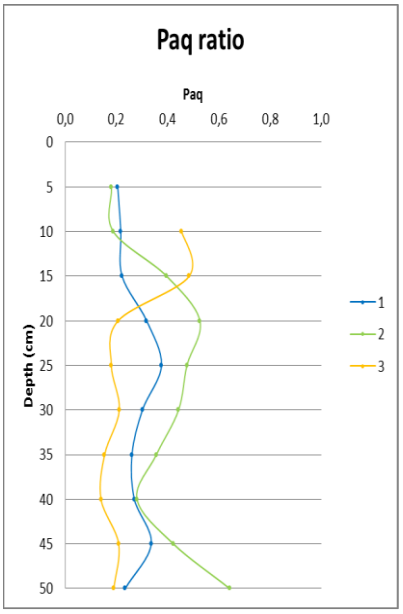

depth	5	10	15	20	25	30	35	40	45	50
sample	A	B	C	D	E	F	G	H	I	J
1	0,85	0,84	0,84	0,77	0,74	0,79	0,81	0,81	0,77	0,83
2	0,92	0,91	0,83	0,79	0,78	0,71	0,77	0,83	0,75	0,63
3		0,63	0,70	0,86	0,87	0,85	0,88	0,89	0,85	0,86

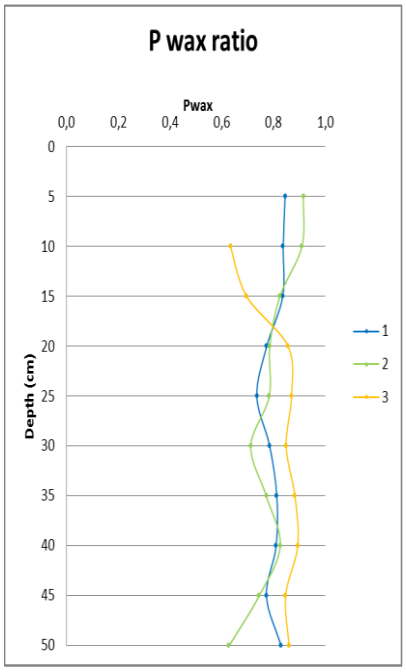

depth	5	10	15	20	25	30	35	40	45	50
sample	A	B	C	D	E	F	G	H	I	J
1	29,21	29,16	29,12	28,89	28,79	28,91	28,98	28,91	28,74	29,09
2	29,38	29,33	29,02	28,64	28,81	28,43	28,52	28,51	28,29	27,85
3		29,14	28,37	29,00	29,14	29,06	29,29	29,26	29,09	29,10

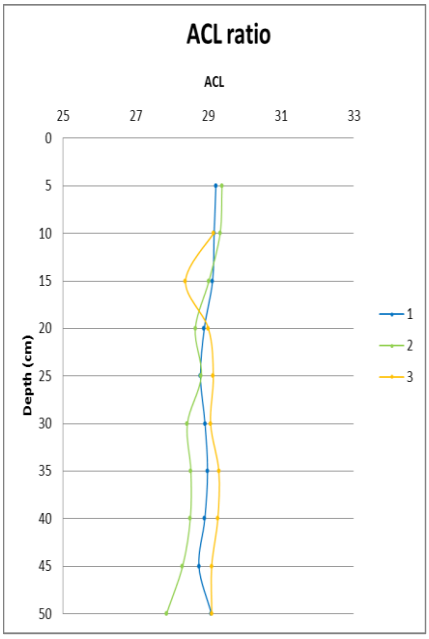

depth	5	10	15	20	25	30	35	40	45	50
sample	A	B	C	D	E	F	G	H	I	J
1	9,61	9,50	9,48	8,94	9,08	8,66	9,31	9,10	7,88	8,86
2	10,72	10,13	9,59	10,92	9,48	7,45	8,15	8,80	6,77	5,04
3		10,88	8,51	9,66	9,76	9,46	9,48	9,18	10,35	10,97

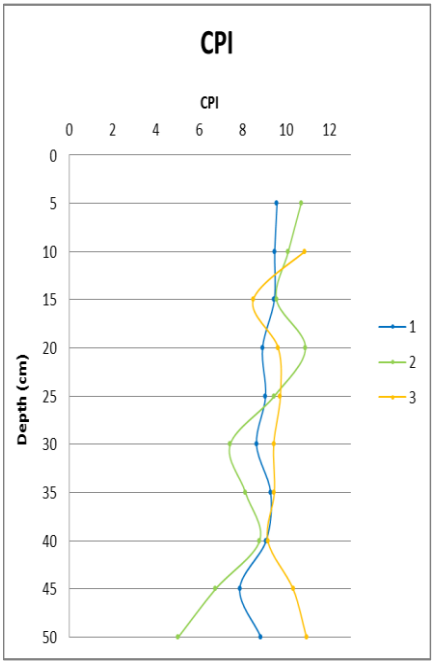

depth	5	10	15	20	25	30	35	40	45	50
sample	A	B	C	D	E	F	G	H	I	J
1	0,04	0,04	0,04	0,07	0,09	0,06	0,05	0,06	0,10	0,06
2	0,02	0,02	0,06	0,07	0,07	0,12	0,08	0,06	0,13	0,24
3		0,27	0,15	0,04	0,04	0,05	0,04	0,04	0,08	0,07

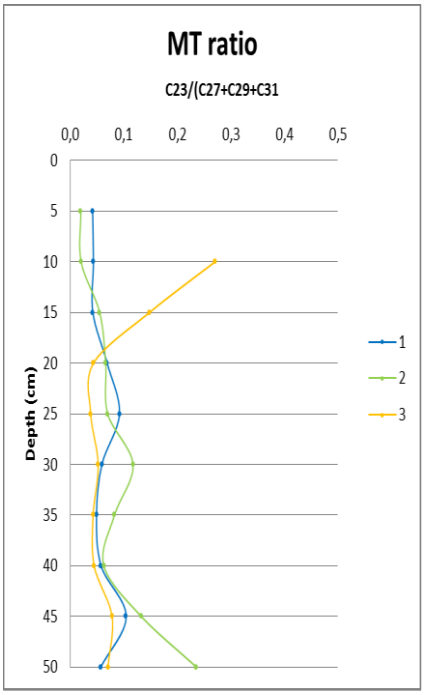

Appendix 17*: Tabs & graphs ratios*

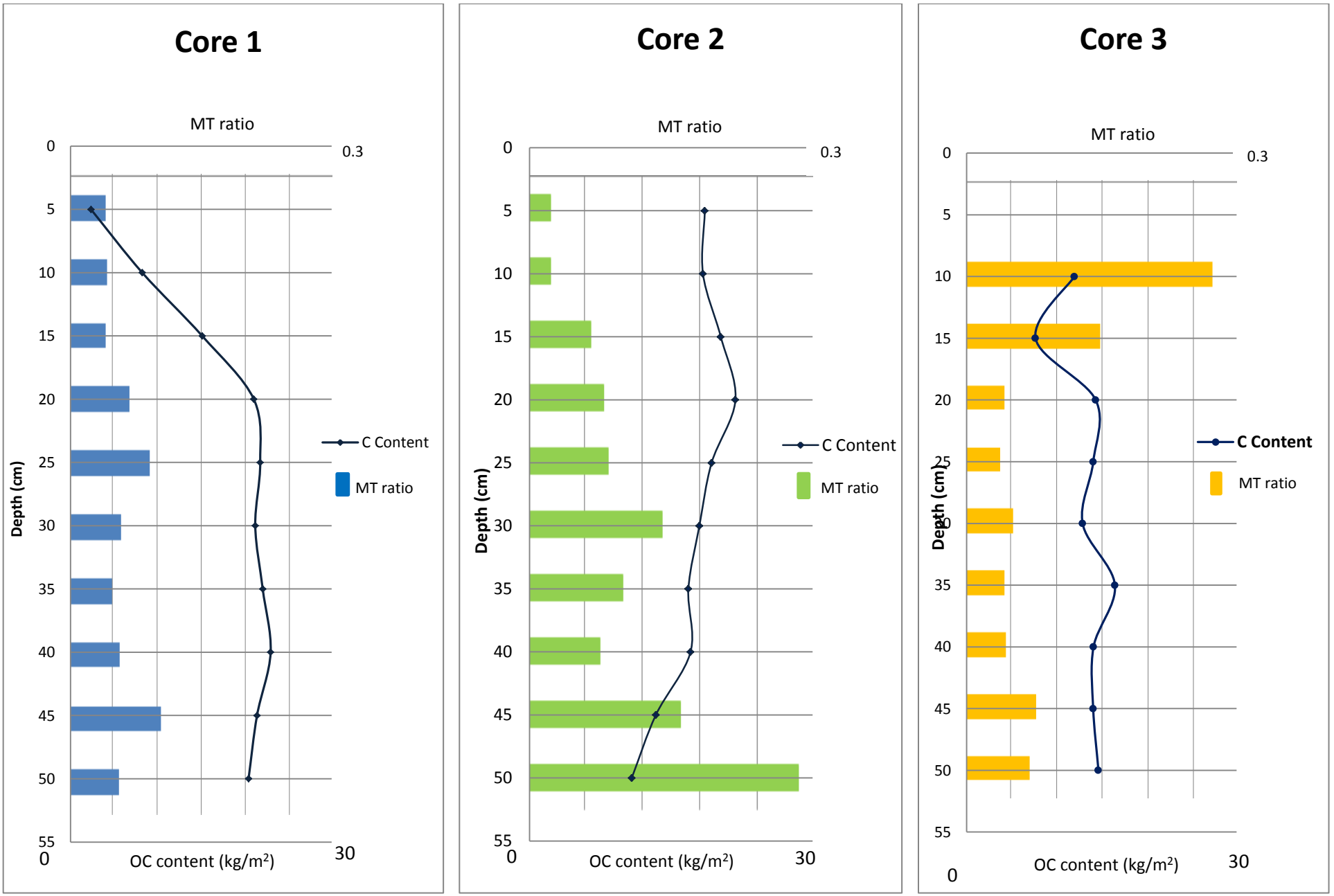

Appendix 18: *Comparison of MT ratio and OC content (kg/m^2) of the three profiles*